A THEORETICAL INVESTIGATION OF SOLVENT EFFECT ON THE CONFORMATIONAL EQUILIBRIA OF 2-SUBSTITUTED CYCLOHEXANONE KETAL DERIVATIVES

by

Safiye (Sağ) Erdem

B.S. in Chem., Boğaziçi University, 1985

M.S. in Chem., Villanova University, 1988

Submitted to the Institute for Graduate Studies in Science and Engineering in partial fulfillment of the requirements for the degree of

Doctor

of

Philosophy

Boğaziçi University

1995

to my family

ACKNOWLEDGMENT

ABSTRACT

The conformational equilibria of 6-substituted-1,4-dioxospiro-[4.5]decanes and 7-substituted-1,5-dioxospiro [5.5]undecanes, relatively complex polar systems, with substituents $X=-CH_3$, -F, -Cl, -CN, -OH, $-OCH_3$, $-NO_2$ have been studied. The complete geometry optimizations have been carried out sequentially in the gas phase and in solution to represent the effect of the solvent.

The methodology consists of the semiempirical PM3 hamiltonian and the self consistent reaction field computations. The effect of the solvent is implemented by the "cavity model". Ab initio calculations have also been performed on 1,1,2-trihydroxy ethane as a model for the hydroxy derivatives of the ketals studied.

The discussion of the results is focused on the solvent effects arising from structural aspects, steric and electrostatic interactions on the axial/equatorial relative stability. The role played by multipole moments is considered. Good agreement with available experimental data and with previous theoretical studies has been obtained in general. The semiempirical methods and the simple solvent models are useful to predict the main role of solute-solvent interactions in conformational equilibria of complex systems for which ab initio calculations cannot be performed.

ÖZET

6-Sübstitüe-1,4-diokzospiro[4,5]dekan ve 7-sübstitüe-1,5-diokzospiro [5,5]undekan'ların konformasyonel dengesi X=-CH$_3$, -F, -CI, -CN, -OH, -OCH$_3$, -NO$_2$ sübstitüentleri kullanılarak çalışıldı. Geometri optimizasyonları sırasıyla önce gaz fazında daha sonra da apolar ve polar çözücülerde yapıldı.

Metod olarak yarı-ampirik PM3 ve SCF hesapları kullanıldı. Çözücü etkisi "cavity model" yöntemi ile dikkate alındı. İlgili bileşiklerin X=-OH türevlerini modellemek amacı ile 1,1,2-trihidroksietan molekülü seçilerek ab initio hesapları da yapıldı.

Sonuçların tartışılıp yorumlanmasında çözücü etkisi esas alınmıştır. Multipol momentlerin önemi vurgulanmış, sterik ve elektrostatik etkileşimlerin sübstitüentlerin aksiyel veya ekvatoryel tercihleri üzerinde oynadıkları roller incelenmiştir. Bilinen deneysel ve teorik çalışmaların sonuçları ile uyum sağlanmış, ab initio uygulamalarının zor olduğu büyük moleküllerde, konformasyonel dengeye çözücü etkisinin incelenmesi için PM3 ve "cavity model"in kullanılabileceği görülmüştür.

TABLE OF CONTENTS

LIST OF FIGURES

LIST OF TABLES

1,1,2-trihydroxyethane for the models corresponding the conformers of 2-OH cyclohexanone **ethylene ketal**.

LIST OF ABBREVIATIONS

AM1	Austin Model 1
ax	Axial substituent
%ax	Total percentage of axial substituents (%Ia + %IIa)
CI	Configuration Interaction
CNDO	Complete Neglect of Differential Overlap
eq	Equatorial substituent
E_{solv}	Solvation Energy
E_{total}	Total Energy
GG	Gauche-Gauche Conformations
GTO	Gaussian-Type Orbital
HF	Hartree-Fock
INDO	Intermediate Neglect of Differential Overlap
LCAO	Linear Combination of Atomic Orbitals
MINDO	Modified INDO
MM	Molecular Mechanics
MNDO	Modified Neglect of Diatomic Overlap
MO	Molecular Orbital
MP	Moller-Plesset
MP2	Moller-Plesset at the 2nd order
NDDO	Neglect of Diatomic Differential Overlap
PM3	Parametric Method 3
PNDO	Partial Neglect of Differential Overlap

PPP	Pariser-Parr-Pople
RHF	Spin-Restricted Hartree-Fock
SCF	Self Consistent Field
SCRF	Self Consistent Reaction Field
STO	Slater-Type Orbital
TG	Trans-Gauche Conformations
UHF	Spin-Unrestricted Hartree-Fock
Ia	Anti-axial conformation
Ib	Anti-equatorial conformation
IIa	Syn-axial conformation
IIb	Syn-equatorial conformation

LIST OF SYMBOLS

ψ	Wave function
ΔE	Relative energy
μ	Dipole moment
ε	Dielectric constant
E	Energy
H	Hamiltonian operator
V	Potential energy

1. INTRODUCTION

Conformations are the arrangements formed by rotation about bonds and interconversion in cyclic systems. Conformational analysis is the analysis of chemical and physical properties of compounds in terms of the conformations. In 1890, Sachse (1) suggested that cyclohexane could exist in two arrangements, free from angle strain, which were later termed "chair" and "boat" conformations. Later Hassel and Barton(2) developed the principles of conformation and were jointly awarded the Nobel Prize in 1969. The interest given to the subject by these early workers has continued to expand from cyclohexane to a wide variety of other cyclic and acyclic systems.

A particularly well-understood aspect of conformational analysis is concerned with compounds containing six-membered rings. Aside from the importance of such compounds in many classes of natural products, they are easy to work with, since they are characterized by a small number of energy minima.

The cyclohexane ring may adopt "chair", "boat" and "twist-boat" conformations. These three conformations are free of angle strain since all carbons maintain tetrahedral bond angles 109°; however, the chair conformation also avoids repulsive van der Waals interactions. As a result, the energy of the chair conformation is lower than that of the boat or twist-boat conformations (Figure 1.1.) The two chair conformations of cyclohexane interconvert rapidly at room temperature via rotation around C-C bonds. In

this process the chair form deforms to flexible conformations (boat and twist-boat) and then to the new chair. Simultaneously, axial substituents pass to occupy equatorial positions, and vice versa.

The energy of activation for chair to boat interconversion is equal to 10.5 kcal/mol and the speed of chair-to-chair interconversion is of the

H_{ax}^1

—H_{eq}^2 ⇌ Boat, twist-boat ⇌ —H_{eq}^1

H_{ax}^2

Enthalpy (kcal/mol)

10.5

1.5

5.5

reaction coordinate
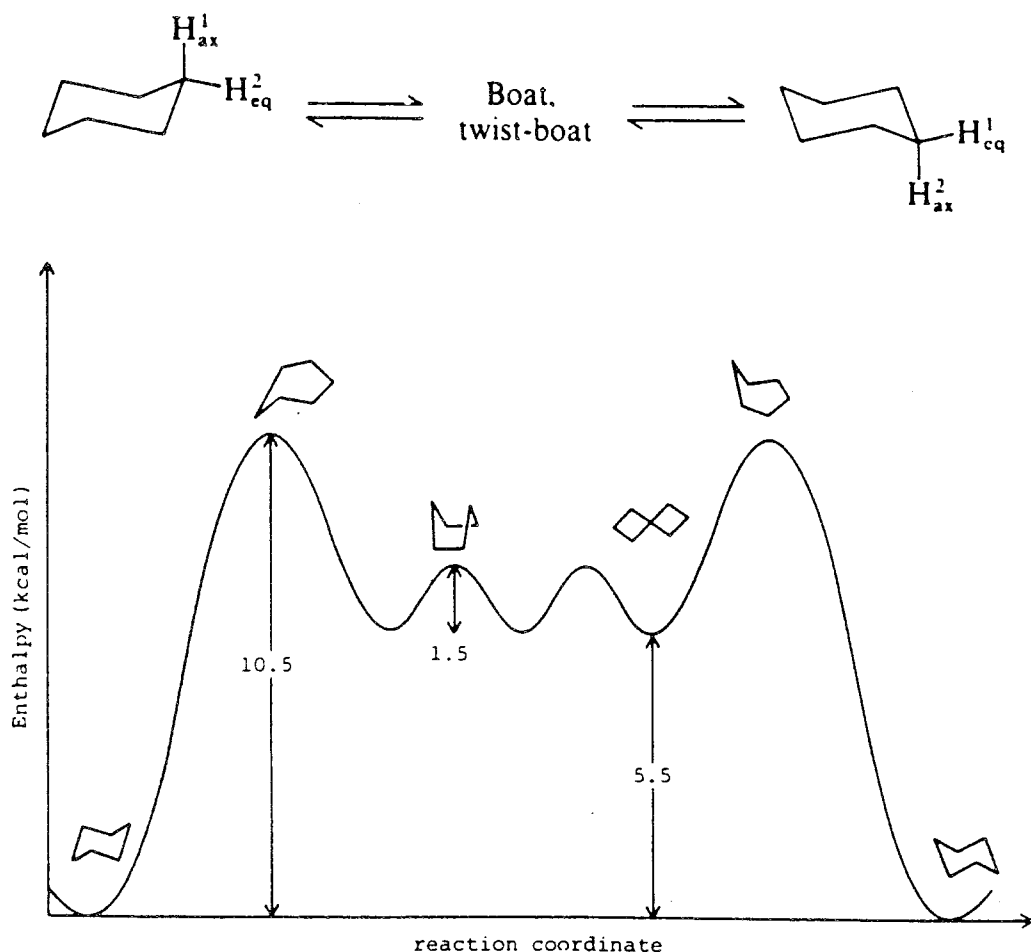
Figure 1.1. Chair-chair inversion and energy profile in cyclohexane(3).

order of magnitude 10^5 s^{-1}. Therefore, for many years chemists were unable to observe axial chlorocyclohexane and equatorial chlorocyclohexane. Nevertheless, the interconversion is sufficiently slow at low temperatures (~150C°) to permit their observation. Spectroscopic quantification of the axial and equatorial conformers at low temperature showed that most substituents exhibit a preference to adopt equatorial orientation(4). This is

rationalized in terms of the repulsive interactions present in the axial conformation between the substituent and the syn-axial hydrogens at the 3 and 5 positions of the cyclohexane ring. In general, the bulkier the substituent, the larger the preference for the equatorial position (4).

In 5-membered rings, there exist two conformations: the "half chair" and the "envelope" which prevent some of the eclipsing among C-H bonds that would be present in a planar ring. As illustrated in Figure 1.2, the envelope conformers of cyclopentane establish a dynamic equilibrium in which all methylene groups alternate to the out-of-plane position. This up-and-down movement of the five methylenes is called *pseudorotation.*
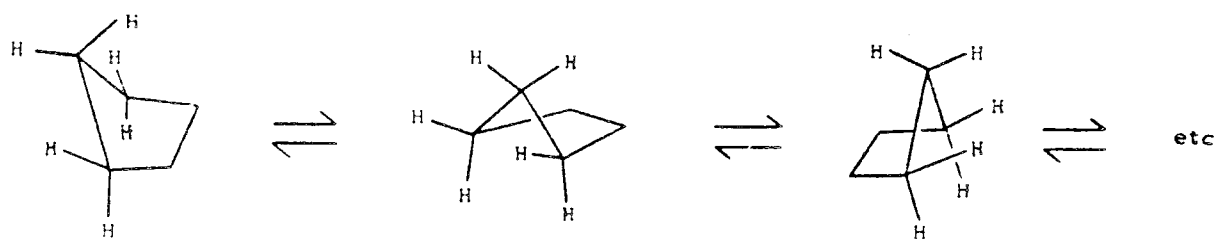
Figure 1.2. Pseudorotation in cyclopentane(5).

There is an apparent similarity between cyclohexane and six-membered heterocycles. Both systems adopt preferentially chair conformations, with comparable inversion barriers. However, the incorporation of heteroatoms into cyclic molecules produces changes in many of the structural parameters, and consequently effects the conformational characteristics of the molecule(6):

1. The carbon-heteroatom(C-X) bond lengths are smaller than C-C bond for C-O, and C-N, but longer than C-C bond for C-S Similarly, C-S-C bond angle (about 100°) deviates significantly from the ideal tetrahedral 109° angle.

2. The presence of heteroatoms in a molecule produces dipole moments.

With the incorporation of more than one heteroatom in the ring, electrostatic interactions (i.e: dipole-dipole interactions) modify molecular conformation. In addition, such electrostatic interactions are influenced by the solvent, so that conformation may change depending on the solvent.

3. Van der Waals radii for oxygen, nitrogen, and sulfur are different than that of carbon. Furthermore, carbon has four ligands, whereas nitrogen has only three; on the other hand, oxygen and sulfur have normally only two ligands. Therefore, steric interactions around the heteroatoms are smaller, since an electron pair is sterically less repulsive than, for instance, a hydrogen atom.

4. Other factors may be influential in heterocycles. For example, in a heterocyclic compound containing a hydroxyl group, the formation of intramolecular hydrogen bond may alter its conformation. On the other hand, nitrogen inversion plays an important role in conformational studies of nitrogen-containing heterocycles.

Five- and six-membered homo- and heterocyclic molecules have been subject of intense study for years (7-15) because they play important roles in the building of various biologically interesting compounds such as proteins, sugars, nucleic acids etc. Among them, 1,3 dioxanes have been studied in detail. The 1,3-dioxane ring also adopts a chair conformation, and the barrier for ring inversion (9.5 kcal/mol) is smaller than that for cyclohexane (16). The twist-boat conformer in the 1,3-dioxane ring is 7.1 kcal/mol less stable than the chair form (16). The conformational behaviour of 3- and 5-substituted 1,3-dioxanes have been investigated both experimentally (17-19) and by computational methods (20).

The dioxolane ring which contains one less carbon atom than the dioxane, pseudorotates essentially freely in the vapor phase (21-23) as in cyclopentane. Dioxolane is nonplanar, with the two most easily described geometries being the envelope (C_s symmetry) and the half-chair (C_2 symmetry) (Figure 1.3.) (24-25).
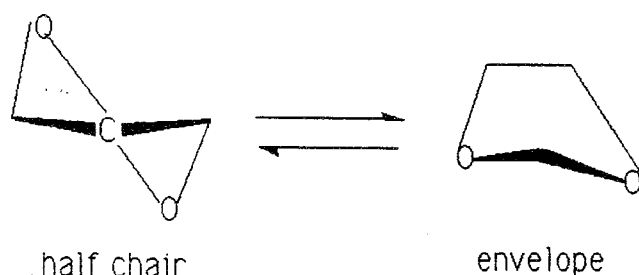
Figure 1.3. Envelope and half-chair forms of 1,3 dioxolane

In the envelope conformation, one C atom is displaced from the plane of the other four atoms. In the half-chair conformation three atoms are coplanar, while one atom is displaced above and another below the plane. The energy differences between conformers are small, and dioxolane exists in a shallow potential well in which rapid interconversion of conformers occurs. Substituted dioxolanes also adopt nonplanar geometries, which may be either envelope or half-chair, depending on the nature of the substitution (6).

The main tool in conformational analysis is generally the concept of steric bulk or size. A simple accounting of steric repulsion permits us to predict correctly various facts concerning the relative stabilities of conformers, their reactivities, the stereochemistry of products, etc.. However, quite a large number of cases have now accumulated in the literature in which the stability of the conformations actually observed cannot be explained only by steric factors. In most cases this is especially true for systems containing heteroatoms, electron pairs, or polar bonds. These cases are sometimes treated as special "conformational effects" and have special names, e.g. "gauche" (17, 26-30), "rabbit-ears" (17, 29), "hockey-sticks" (8, 29), "anomeric" (17, 29, 31) effects. Some of the well known and most important conformational effects within the scope of this work are briefly explained:

GAUCHE-EFFECT: This effect has been postulated to explain a tendency of 1,2-disubstituted ethane fragment to adopt the conformation which has a maximum number of gauche interactions between the adjacent electron pairs

and/or polar bonds (figure 1.4).
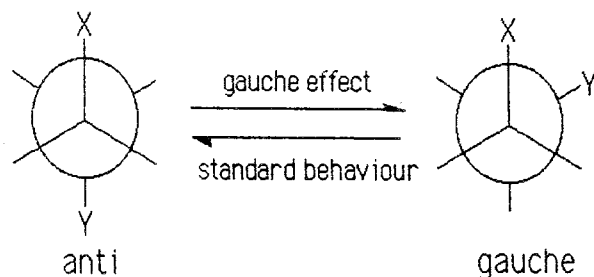
Figure 1.4. Gauche effect in 1,2-dibubstituted ethane

This effect has been usually observed in the case of highly electronegative substituents such as -F or -OR. There are many publications on the gauche effect: some of them are the examples of attractive gauche effect (32-38) and some others are the repulsive gauche effect (39).

ANOMERIC EFFECT: It was first recognized in sugars, but now is accepted as a general feature of tetrahydropyran chemistry. This effect is the preference of a polar 2-substituent e.g. halogen or methoxy group for the axial position in a tetrahydropyran ring due to the favourable dipolar interaction in which the dipole of the polar substituent and the dipole of the ring oxygen are less additive than that of the equatorial position (40, 41).

HYDROGEN BOND: An intramolecular H-bond often operates as a dominant factor, controlling conformational equilibrium. Therefore, the conformational energies are strongly effected by the extent of H-bonding. These examples are numerous and well studied (13, 14, 36-42).

SOLVENT EFFECT: It is the result of electrostatic interactions between the solvent and the conformers. In general, the conformation with the smaller dipole moment is favored in solvents of low dielectric constants. It has been observed experimentally and calculated theoretically (43) that the preferred conformation of 2-bromo- and 2-chloro cyclohexanones depends on the polarity of the medium. In solvents of low dielectric constant, the substituent is more stable in the axial orientation whereas the equilibrium

is reversed in the more polar solvents. The bond dipoles largely cancel in conformation with an axial chlorine but are additive for the equatorial chlorine.

In this research, a theoretical conformational analysis of 7-substituted 1,5 dioxospiro [5.5] undecanes (2-substituted cyclohexanone propylene ketals) and 6-substituted 1,4 dioxospiro [4.5] decanes (2-substituted cyclohexanone ethylene ketals), (Figure 1.5), has been performed using semiempirical SCF calculations with the PM3 method.
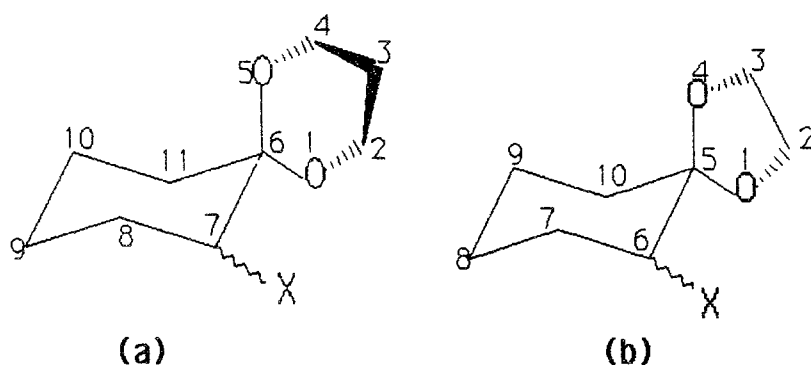
Figure 1.5. Numbering system for nomenclature of
(a) 7-substituted 1,5 dioxospiro [5.5] undecanes and
(b) 6-substituted 1,4 dioxospiro [4.5] decanes.
X= -F, -Cl, -CN, -CH$_3$, -NO$_2$, -OCH$_3$, -OH.

The spiroketals are the substructures of naturally occuring substances from many sources, including insects, microbes, plants, fungi, and marine organisms. The chemistry of spiroketals, their natural occurance and the conformational aspects are reviewed by Perron and Albizati (44).

Experimental studies on conformational equilibria of 1,1,2 tri-substituted cyclohexanes (45). provide ΔG values that give direct information on the most stable conformations. In particular, 1-(OR), 1-(OR'), 2-(R'') derivatives have attracted much attention because they are suitable to investigate different interactions.

The conformational analysis of spiro[5.5]undecane and its oxo analogues by low temperature NMR and force-field methods have been reported by H. Dodziuk. In ^{1}H and ^{13}C NMR, two dynamical processes have been detected upon temperature lowering: cyclohexane and dioxane ring inversion (46). On the basis of molecular mechanics calculations, chirality of spiro [5.5]undecanes has been discussed (47) and calculated heat of formation values have revealed an agreement with experimental values (48).

Molecular mechanics calculations on the conformational dynamics of 9,9-dimethyl-1,5-dihetero-spiro[5.5]undecanes have been published (49). A topological approach has led to a model consistent with available nmr data.

Deslongchamps et al. reported ^{13}C NMR data on 1,7-dioxaspiro[5.5]undecanes and related compounds. They also investigated the stereoelectronic effects in the same compunds and also in their dithia analogues. The results have been discussed concerning the importance of anomeric effect and the steric interactions (50-52).

Wolff et al. investigated the conformational behaviour of 10-substituted 1,4-dioxa and 1,4,6-trioxaspiro[4.5]decanes by NMR spectroscopy and by molecular mechanics calculations (53). An increase in the content of axial conformer has been observed when going from glycol compounds to pinacol compound, which is parallel to the increase in polarity of the substituent.

Varnali studied 2-CN, 2-NO_2, and 2-N_3 cyclohexanone ethylene and propylene ketals with ^{1}H NMR (54) and also with molecular mechanics (55). According to the results of ^{1}H NMR in $CDCl_3$, -CN and -N_3 groups display an equatorial preference with ethylene ketals and axial dominance with propylene ketals whereas -NO_2 group shows equatorial preference in both ketals. The molecular mechanics results show qualitative accordance with experimental data.

In spite of accumulated literature on the similar structures, the compounds under consideration have not been investigated extensively.

Obtaining accurate experimental data for the free energy change in these equilibria is far from being easy and NMR measurments are limited (56). Only qualitative or semiquantitative results are obtained in general. Zefirov and co-workers studied the conformational equilibria of ketals of 2-substituted cyclohexanones in variety of solvents using ^{1}H, ^{13}C, and ^{19}F NMR (28, 56, 57).They showed that 2-substituted propylene ketals usually prefer axial orientation but this preference decreases as the polarity of the solvent increases. Ethylene ketals behave almost in opposite direction except for -OH and -OCH$_3$ derivatives. Experimental results found on the compounds of interest are given in Table 1.1.

Table 1.1. Experimental total axial conformer percentages for 2-substitued cyclohexanone ketal derivatives in CCl$_4$ and CD$_3$CN

X	propylene ketals		ethylene ketals	
	ax % in CCl$_4$	ax % in CD$_3$CN	ax % in CCl$_4$	ax % in CD$_3$CN
F	70.5,65.7(56)	64.8,59.0(56)	31.5(56)	38.9(56)
Cl	56.2(56)	38.1(56)	19.6(56)	21.6(56)
	57.1(28)	37.5(28)	28.4(28)	30.4(28)
CN	82.91*(54)	–	40*(54)	–
CH$_3$	–	–	–	–
NO$_2$	7.28(58)	–	3.6(58)	–
OCH$_3$	72.4(56)	61.9,78.1(56)	46.1(28)	42.2(28)
OH	76.5,64.7(28)	–	52.9(28)	38.2(28)

*Studied in CDCl$_3$.

Theoretical computations may be quite helpful to analyze the experimental data. Three well known theoretical methods are the molecular mechanics, ab initio and semiempirical computations. Molecular mechanics has been widely used and represents an interesting approach to deal with conformational problems in large systems. Its main limitation is due to the rather poor description of electronic effects, in particular in those cases in

which there are lone pairs. On the other hand, ab initio computations which are the most interesting ones for the experimentalists, are too expensive for large molecules. Hence, semiempirical methods appear as an intermediate approach. Though quantitative molecular properties are not always obtained with these methods, their trend in a chemical family, or their modification through an external perturbation, are correctly reproduced in general.

A common problem to tackle in conformational equilibrium analysis is the effect of electrostatic solute-solvent interactions. The majority of the theoretical calculations deal with isolated molecules which correspond to a low pressure gaseous state. On the other hand, many chemical and physical phenomena are experimentally studied in condensed phase.The liquid state is of great importance because most of the chemical reactions and many physical measurements, especially the spectroscopic ones, are performed in this phase. It is well known that the results of experiments may depend to a large extent on the nature of the liquid phase, especially on the solvent in which the species subject to investigations are disolved. As a result, there is a strong need for the computational methods which take into account the solvent so that a better comparison of experimental and theoretical results can be made.

In the present work, the aim is to investigate the solvent effect on the conformational equilibria of 2-substituted cyclohexanone ethylene and propylene ketals by semiempirical PM3 calculations. The effect of solvent is taken into account by means of a "cavity model" (see section 2.11). The comparison of the calculated results with the experimental data in Table 1.1. provides useful information about the applicability of the cavity model on the molecules studied and the similar ones.

The compounds under investigation are expected to exhibit a strong solvent effect due to their large dipole moments. The magnitude of the dipole moment depends on the orientation of the substituent with respect to the heterocyclic ring spiro to the cyclohexane fragment. In Figure 1.6 (a), the arrows represent the directions of ring dipole and the dipole of the
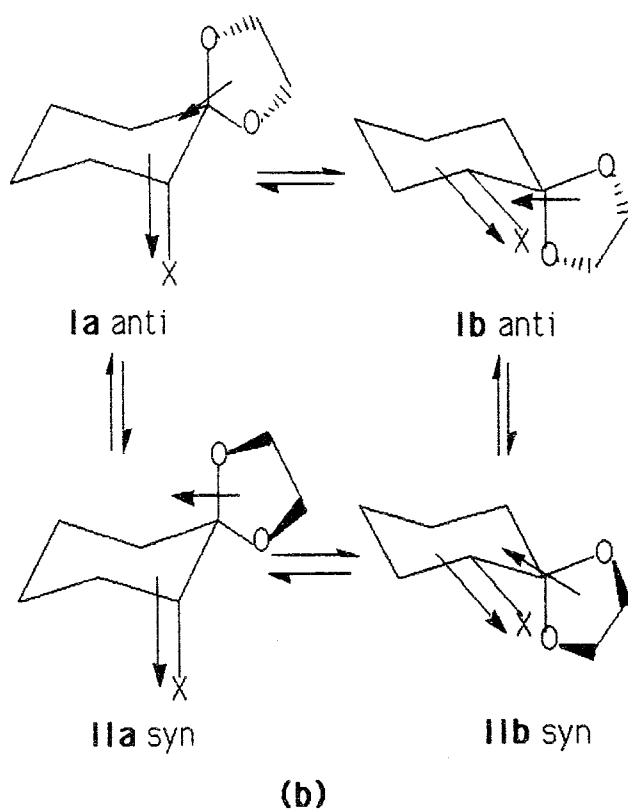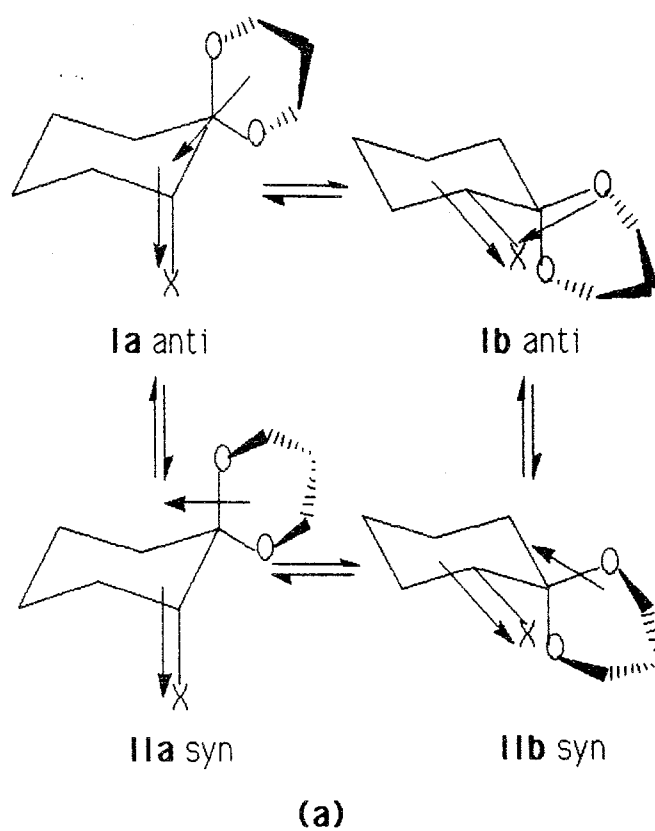
Figure 1.6. Conformational equilibria and the direction of dipoles in 2-substituted cyclohexanone **(a)** propylene ketals **(b)** ethylene ketals

substituent in 2-substituted cyclohexanone propylene ketals. The same figure also shows that the conformational equilibria of these compounds consist of four conformers. Two chair forms of cyclohexane ring and two chair forms of dioxane ring add up to four stable conformers. The name syn is reserved for those conformations with the dioxane ring extending towards the substituent whereas the name anti is reserved for the dioxane ring extending further away from the substituent.

A similar equilibrium can also be visualized in the case of 2-substituted cyclohexanone ethylene ketals. (Figure 1.6 (b)).

2-hydroxy cyclohexanone ethylene and propylene ketal systems are relevant to carbohydrate chemistry. 1,1,2-trihydroxy ethane is investigated as the simplest structure which incorporates functional groups found in large molecules of interest (Figure 1.7) at a high level of sophistication to ellucidate interactions that exist among these three functional groups.

Because of its small size, 1,1,2 trihydroxy ethane has allowed us to perform ab initio calculations which are extremely challenging to apply on large systems. In literature, there are many examples of applying ab initio calculations on small models of larger systems (37, 59, 60). As a result of more accurate ab initio calculations, we expect to obtain more reliable information. Our goal here is to highlight the abilities of semiempirical MO method PM3 to produce the structural and energetic properties associated with many interactions in our model molecule and thus 2-hydroxy cyclohexanone ketal systems.

2-HYDROXY CYCLOHEXANONE ETHYLENE KETAL (n=2)
2-HYDROXY CYCLOHEXANONE PROPYLENE KETAL (n=3)

axial ⇌ equatorial

1,1,2-TRIHYDROXYETHANE

Trans-Gauche   Gauche-Gauche
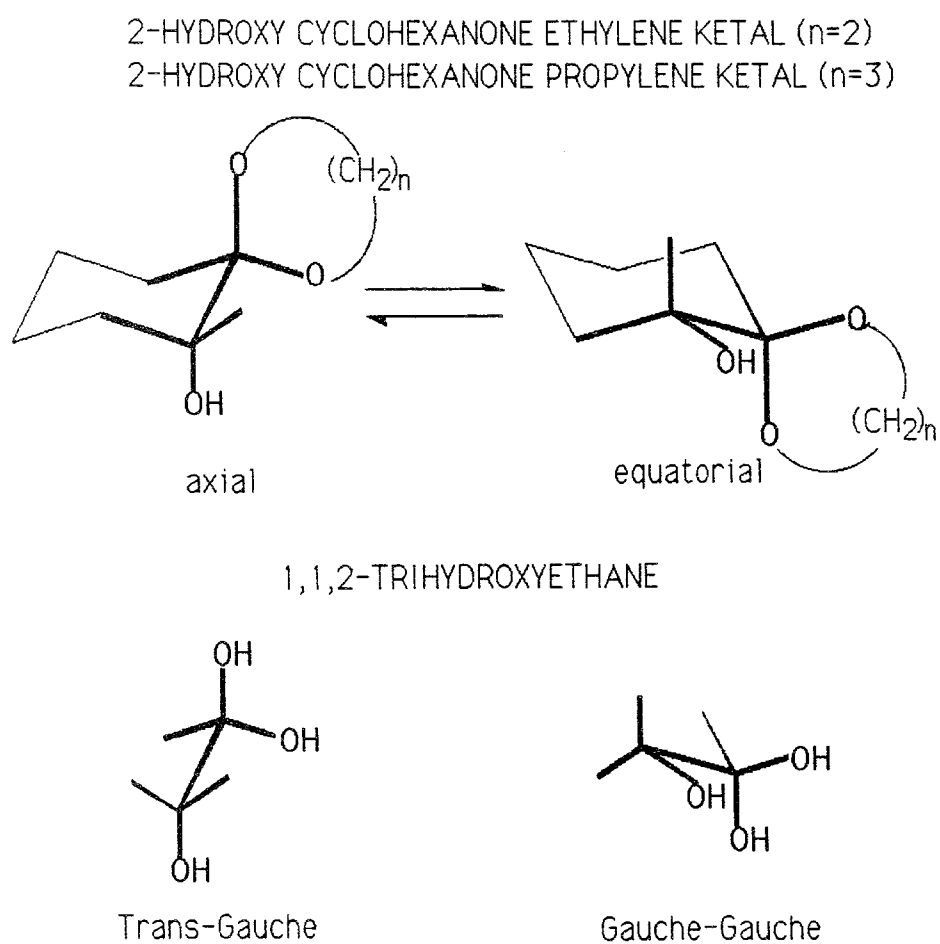
Figure 1.7. 1,1,2-Trihydroxyethane, a model molecule for 2-hydoxy cyclohexanone ketals.

2. THEORY

2.1. COMPUTATIONAL METHODS

Computational chemistry has become a very popular research area in recent years. Chemistry has been known as an experimental science which means no molecule could be investigated until it was synthesized or was found in nature. In contrast, computational chemistry requires no preparation, no separation techniques, and no physical measurements. There is a fundamental difference between calculations and all experimental techniques: calculations can be performed easily for compounds that have never been synthesized, or even cannot exist under normal conditions. Reaction intermediates with very short lifetimes present no more problems than do the stable products of the same reaction. There is no other method which can give the molecular structure, heat of formation, dipole moment, ionization potentials, charge densities, bond orders, spin densities in one experiment. However, the objection may arise about the reliability of the calculations, but the strengths and weaknesses of the common methods are well known. Therefore, realistic estimates about the probable accuracies of these methods can be made. In some cases, the results of calculations may be more reliable than those of experiments. For example, measuring the heat of formation of a polycyclic alkane requires a long and difficult procedure. There is no guarantee that the value obtained is correct even with the most careful experimental work. On the other hand, the calculated heat of

formation values for such alkanes using the most modern molecular mechanics methods differ from the "true" values by at most 2 kcal/mol.(61).

There are various computational methods that can predict the structures, energies and other properties of known and unknown molecules. These methods can be classified in two main classes as *force field* or *molecular mechanics* (MM) and *molecular orbital* (MO) calculations. See Figure 2.1

COMPUTATIONAL METHODS

Molecular Mechanics (Force Field)   Quantum Mechanics (Molecular Orbital)

Ab Initio   Semiempiric
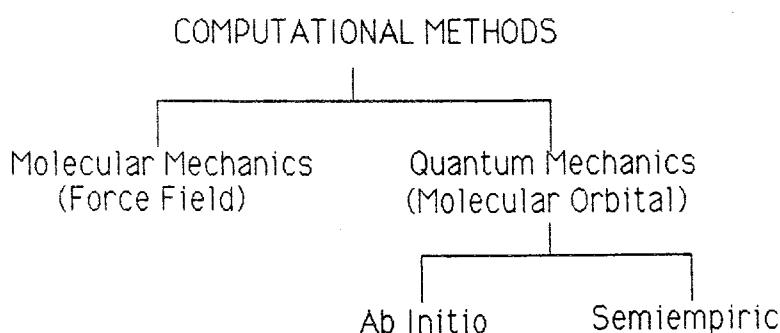
Figure 2.1. Classification of computational methods.

2.1.1. Molecular Mechanics Method (MM)

These calculations are based on a simple classical-mechanical model of molecular structure. The method starts out with a model of a molecule as composed of atoms held together by bonds; interactions between nonbonded atoms are also considered. It deals with the contributions to a molecule's electronic energy due to bond stretching, bond bending, van der Waals interactions and repulsions between nonbonded atoms, electrostatic interactions due to polar bonds, and energy changes accompanying internal rotation about single bonds. Summing these contributions, we have the potential energy V for motion of the nuclei within the molecule (62)

$$V = V_{str} + V_\theta + V_{vdW} + V_{es} + V_w \qquad (2.1)$$

where V_{str} is the contribution of bond stretching, V_θ is the contribution of

bond bending, V_{vdW} is due to the van der Waals interactions, V_{es} is the electrostatic term and V_w is present in molecules with internal rotation about single bonds.

The molecular mechanics method and its applications have been comprehensively reviewed by Burkert and Allinger (63).

2.1.2. Quantum Mechanics Methods (MO Calculations)

The object of molecular orbital (MO) programs is to build a set of molecular orbitals to be occupied by electrons assigned to the nuclei. In principle this can be achieved by combining any number of different types of electron probability functions. A far more convenient procedure is to build up the molecular orbitals from sets of orbitals centered on the constituent atoms. The MO calculation then simply involves finding the combination of these atomic orbitals that have the proper symmetries and that give the lowest (most negative) electronic energy. This is called *Linear Combination of Atomic Orbitals* (LCAO).

For a better explanation of MO type calculations, a short description of quantum mechanics is required.

2.2. QUANTUM MECHANICS

To understand the behaviour of individual atoms and molecules, and of the electrons, we need to know how particles move in response to the forces acting on them. Towards the end of nineteenth century, accumulated experimental evidence showed that classical mechanics failed when it was applied to very small particles. Later on, the appropriate concepts and equations were discovered to describe the motion of particles. This new approach is called quantum mechanics.

In quantum mechanics, it is supposed that the position of a particle is distributed through space like the amplitude of a wave. In order to describe

this distribution, we introduce the concept of *wave function* ψ is introduced in place of trajectory, and then set up a scheme for calculating and interpreting ψ. Since the state will, in general, change with time, ψ is also a function of time. The equation governing its change with time is known as *time dependent Schrödinger equation* which was discovered in 1926 by Erwin Schrödinger (65). The one particle , one dimensional Schrödinger equation is

$$H\Psi = i\hbar \frac{\partial \Psi}{\partial t}$$

(2.2)

where,

$$H = -\frac{\hbar^2}{2m}\frac{\partial^2}{\partial x^2} + V$$

(2.3)

V is the potential energy and $\hbar = \frac{h}{2\pi}$

For many applications of quantum mechanics to chemistry, it is not necessary to deal with this equation; instead, the simpler time-independent Schrödinger equation is used. This simpler form can be obtained by a method called separation of variables (66). A one dimentional time-independent Schrödinger equation is

$$-\frac{\hbar^2}{2m}\frac{d^2\Psi(x)}{dx^2} + V(x)\Psi(x) = E(x$$

(2.4)

or in more general expression:

$$H\Psi = E\Psi$$

(2.5)

H is an operator, operating on the function Ψ, and is called the Hamiltonian operator. See equation (2.3).

The solution of Schrödinger equation provides useful information related to the energy of an atom. Although there are an infinite number of different solutions of this equation, only some of the solutions are acceptable physically. In particular, these solutions exist only for certain values of E. That is, the interpretation of the wavefunction implies the *quantization* of energy which gives rise to the name of quantum mechanics.

2.3. MOLECULAR QUANTUM MECHANICS

For small systems consisting of a few particles, a very accurate solution for the Schrödinger equation can be found but, unfortunately, there is no simple way of obtaining exact solutions for many electron atoms and molecules. Therefore some assumptions have to be made. If we assume the nuclei and electrons to be point masses, and neglect spin-orbit and other relativistic interactions, then the nuclear Hamiltonian becomes

$$H=-\frac{h^2}{2}\sum_a\frac{1}{m_a}\nabla_a^2-\frac{h^2}{2m_e}\sum_i\nabla_i^2+\sum_a\sum_{b>a}\frac{Z_aZ_be^2}{r_{ab}}-\sum_a\sum_i\frac{Z_ae^2}{r_{ia}}+\sum_j\sum_{i>j}\frac{e^2}{r_{ij}} \qquad (2.6)$$

where a and b refer to nuclei and i and j refer to electrons. The first term is the operator for the kinetic energy of nuclei. The second term is the operator for the kinetic energy of the electrons. The third term is the energy of repulsions between the nuclei, r_{ab} being the distance between nuclei with atomic numbers Z_a and Z_b. The fourth term is the potential energy of the attractions between the electrons and the nuclei. The last term is the potential energy of repulsions between electrons(66).

Nuclei are much heavier than electrons. Hence the electrons move much faster than the nuclei, and to a good approximation, one can regard the nuclei as fixed while the electrons carry out their motion. Thus, we can omit the nuclear kinetic-energy terms from (2.6) to obtain the purely electronic Hamiltonian, H_{el}

$$H_{el}=-\frac{\hbar^2}{2m_e}\sum_i\nabla_i^2-\sum_a\sum_i\frac{Z_ae^2}{r_{ia}}+\sum_j\sum_{i>j}\frac{e^2}{r_{ij}} \qquad (2.7)$$

And the nuclear repulsion term V_{NN} is given by

$$V_{NN} = \sum_a \sum_{b>a} \frac{Z_a Z_b e^2}{r_{ab}}$$

(2.8)

Treating electronic and nuclear motions separately is called the *Born-Oppenheimer approximation* (66).

2.4. THE VARIATION METHOD

This method allows us to obtain an approximation to the ground state energy of a system without solving the Schrödinger equation, finding an upper bound for the system's ground state energy. Consider the ground state of some particular arbitrary system. The ground state wave function ψ_0 and energy E_0 satisfy the Shrödinger equation $H \psi_0 = E_0 \psi_0$. Multiply this equation from the left by ψ_0^* and integrate over all space to obtain:

$$E_0 = \frac{\int \psi_0^* H \psi_0 d\tau}{\int \psi_0^* \psi_0 d\tau}$$

(2.9)

where $d\tau$ represents the appropriate volume element. Variational theorem says that if we substitute any other function for ψ_0 in equation (2.9) and calculate

$$E_\phi = \frac{\int \phi^* H \phi d\tau}{\int \phi^* \phi d\tau}$$

(2.10)

then E_ϕ calculated through (2.10) will be greater than the ground state energy E_0. In an equation, we have the variational principle

$$E_\phi \geq E_0$$

(2.11)

The closer ϕ is to ψ_0 in some sense, the closer E_ϕ will be to E_0. To arrive at good approximation to the ground-state energy E_0, many trial functions are used and the one that gives the lowest value of the variational integral is found (67).

In practice, one can choose ϕ such that it depends on some arbitrary parameters. The energy E_ϕ also will depend on these variational parameters. Therefore, one can minimize E_ϕ with respect to each of the variational parameter and thus approach the exact ground-state energy.

There is a systematic way to handle a trial function which is a linear combination of functions. When E_ϕ is derived as a function of the variational parameters and is differentiated with respect to all the variational parameters, a pair of linear algebraic equations for the parameters can be obtained. This procedure gives rise to a secular determinant. If a linear combination of N functions is used, a secular determinant of NxN is obtained. The secular equations associated with this determinant is an Nth order polynomial in E. The smallest root of the Nth order secular equation is chosen as an approximation to the energy. The secular determinant simplifies if the trial function is a linear combination of orthonormal functions (68)

2.5. HARTREE-FOCK (HF) SELF-CONSISTENT-FIELD METHOD (SCF)

The main difficulty in solving the Schrödinger equation is the presence of the electron-electron interaction terms, the last term in equation (2.6). It is very difficult to find analytical solutions of a Schrödinger equation that has this as part of its potential energy term, but computational techniques are available that give very detailed and reliable numerical solutions for the wavefunctions and energies. The techniques were introduced by Douglas Hartree and modified by Vladimir Fock (69). In broad outline, Hartree-Fock procedure is as follows.

In the Na atom, for instance, the orbital approximation suggests the configuration $1s^2\ 2s^2\ 2p^6\ 3s^1$. Now consider the 3s electron. A Schrödinger equation can be written for this electron by ascribing to it a potential energy that arises from the nuclear attraction and the average electronic repulsion

from the other electrons in their approximate orbitals. The equation may be solved for ψ_{3s} and the solution obtained will be different from the solution guessed initially. The procedure is then repeated for another orbital, such as 2p. The Schrödinger equation is written again but with the improved 3s orbital used in setting up the electron-electron repulsion term. The equation is then solved, giving an improved version of 2p. This procedure is repeated for the 2s and 1s orbitals. Then the whole procedure is repeated using the improved orbitals. The recycling continues until the orbitals and energies obtained are insignificantly different from those used at the start of the latest cycle. The solutions are then *self-consistent* and accepted as solutions of the problem. This procedure uses the variational method to minimize the energy.

Hartree-Fock theory approximates the true many electron wavefunction as a single determinant of orthonormalized spin orbitals. A full many-electron molecular orbital wave function for the closed shell ground state of a molecule with n (even) electrons, doubly occupying n/2 orbitals can be written as

$$\Psi = (n!)^{-1/2} \begin{vmatrix} \psi_1(1)\alpha(1) & \psi_1(1)\beta(1) & \psi_2(1)\alpha(1)\ldots\psi_{n/2}(1)\beta(1) \\ \psi_1(2)\alpha(2) & \psi_1(2)\beta(2) & \psi_2(2)\alpha(2)\ldots\psi_{n/2}(2)\beta(2) \\ \cdot & & \cdot \\ \cdot & & \cdot \\ \cdot & & \cdot \\ \psi_1(n)\alpha(n) & \psi_1(n)\beta(n) & \psi_2(n)\alpha(n)\ldots\psi_{n/2}(n)\beta(n) \end{vmatrix}$$

$$(2.12)$$

where α and β are spin functions and $\psi_1, \psi_2, \psi_{n/2}$ are molecular orbitals. The determinantal wave function (2.12) may be normalized by multiplication by a factor of $(n)^{-1/2}$. This determinant is often reffered to as *Slater determinant* (70). Various levels of Hartree-Fock theory are possible depending on the kind of system to be investigated.

2.5.1. Closed-Shell Determinantal Wavefunctions

They are the most commonly used form of HF theory and are appropriate for the description of the ground states of most molecules with an even number of electrons. The determinantal wavefunction, (2.12), formed from the spin orbitals is precisely of singlet type, and therefore is classified as spin restricted Hartree-Fock (RHF). Its advantage is the ease of application. The disadvantage is that it does not always give the lowest possible energy

2.5.2. Open-Shell Determinantal Wavefunctions

They are appropriate for the descriptions of the systems with odd number of electrons. These systems can be treated either with RHF wavefunctions which represent a pure doublet, triplet, etc spin states. The alternative open-shell procedure is the spin-unrestricted Hartree-Fock (UHF) method in which the orbitals associated with different spin electrons are treated completely independently. The advantage of this method is that it generally gives a lower energy than the corresponding RHF treatment and that is generally computationally more efficient. The principle disadvantage is that the resulting wavefunction is no longer spin pure. Thus, a UHF calculation on a system with one extra electron might lead to a wave function that is a mixture of a doublet and quartet rather than a pure doublet (71)

2.6. BASIS FUNCTIONS

In 1951, Roothaan proposed representing the Hartree-Fock orbitals as linear combinations of a complete set of known functions, called *basis functions*. Thus for Li the Hartree-Fock 1s and 2s spatial orbital can be written as (69)

$$f = \sum_i b_i \chi_i \text{ and } g = \sum_i c_i \chi_i \tag{2.13}$$

where the χ_i's are some complete set of functions, and where the b_i's and c_i's are expansion coefficients that are found by the SCF iterative procedure. There are two types of set of basis functions for atomic Hartree-Fock calculations, *Slater-type* functions and *Gaussian-type* functions (70).

In the simplest Hartree-Fock model, the number of basis functions on each atom is as small as possible, that is only large enough to accomodate all the electrons and still maintain spherical symmetry. As a consequence, the molecular orbitals have only limited flexibility. If larger basis sets are used, the number of adjustable coefficients in the variational procedure increases, and an improved description of the molecular orbitals is obtained. Very large basis sets will result in nearly complete flexibility. The limit of such an approach, termed the Hartree-Fock limit, represents the best that can be done with a single electron configuration.

2.7. ELECTRON CORRELATION (CONFIGURATION INTERACTION, CI)

The main deficiency of Hartree-Fock theory is its incomplete description of the correlation between the motions of the electrons. Even with a large and completely flexible basis set, the full solution of the Schrödinger equation cannot be expressed in terms of a single electron configuration which is discussed above, that is a unique assignment of electrons to orbitals. To correct for such a deficiency, it is necessary to use wave functions that go beyond the Hartree-Fock level, that is, that represent more than a single electron configuration. If ψ_0 is the full Hartree-Fock many electron wavefunction, the extended approximate form for the more accurate wavefunction ψ is (72)

$$\psi = a_0 \psi_0 + a_1 \psi_1 + a_2 \psi_2 + \ldots \tag{2.14}$$

Here ψ_1, ψ_2,.... are wavefunctions for other configurations, and the linear

coefficients a_0, a_1,... are to be determined. Inclusion of wavefunctions for all possible alternative electron configuration (within the framework of a given basis set) is termed full configuration interaction. It represents the best that can be done using that basis set.

There are two kinds of correlation methods, one is variational, called limited configuration interaction and the other is Moller-Plesset Perturbation Treatment. Each method has its own levels such as CID, CISD and MP2, MP3, MP4, etc. (73)

The two directions, using more flexible basis sets and the improvement of electron correlation, in which theoretical models may be improved can be shown with a two-dimentional chart as in figure 2.2. The bottom right-hand corner of the diagram shows the best that can be done with both methods. Therefore it constitutes the exact solution of the nonrelativistic Schrödinger equation.
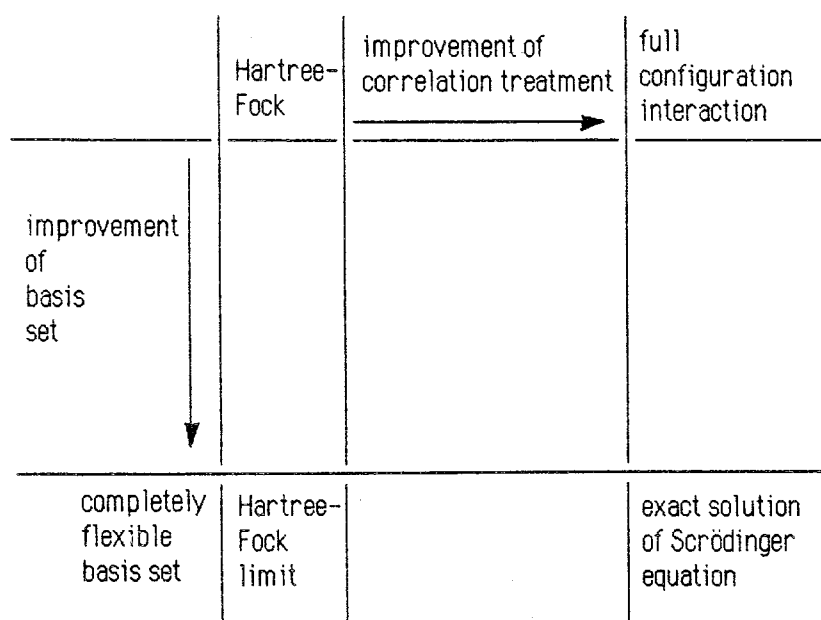
Figure 2.2. Schematic representation of theoretical models showing basis set improvement vertically and correlation improvement horizontally (72).

2.8. AB INITIO MO THEORY

The term ab initio implies a rigorous, nonparametrized molecular orbital treatment derived from its principles. This is not completely true. There are a number of simplifying assumptions in ab initio theory, but the calculations are more complete, and therefore more expensive, than those of the semiempirical methods discussed below. It is possible to obtain chemical accuracy via ab initio calculations, but the cost in computer time is enormous. In practice most calculations are performed at lower levels of theory. Like the semiempirical calculations, ab initio theory makes use of the Born-Oppenheimer approximation. Then, a Hartree-Fock SCF calculation seeks the antisymmetrized product ϕ of one-electron functions that minimizes

$$\int \phi^* H \phi d\tau$$

where H is the true Hamiltonian, and is thus an ab initio calculation.

The most widely used software for ab initio calculations is the GAUSSIAN (74) series of programs which deal exclusively with Gaussian-type orbitals (GTO's) and includes several optional GTO basis sets of varying size.

2.8.1. Basis Sets Used in Gaussian Programs

2.8.1.1. Minimal Basis Set (STO-nG)

These are the simplest of the optional basis sets. STO-nG is an abbreviation for Slater-Type-Orbitals simulated by n Gaussian functions each. This means that each atomic orbital consists of n Gaussian functions added together. In early tests on STO-nG bases, it was found that basis sets with n=3 and n>3 gave very similar results (71). So the smallest of these, STO-3G, was chosen for calculations extensively. It is a *minimal basis set* which means that it has only as many orbitals as are necessary to

accomodate the electrons of the neutral atom. It is very economical, having only one basis function per H atom (the 1s), five per atom from Li to Ne (1s, 2s, 2px, 2py, 2pz) and nine per atom for the second row elements Na-Ar (1s, 2s, 2px, 2py, 2pz, 3s, 3px, 3py, and 3pz). As it is seen a complete set of p orbitals are added to maintain spherical symmetry.

2.8.1.2. Split-Valence Basis Sets

Although STO-3G was the standard basis set for ab initio optimizations for several years, it was eventually replaced by small split-valence basis sets and is now rarely used. The greater problem of any minimal basis set is its inability to expand or contract its orbitals to fit the molecular environment. The lone-pair orbitals in water, for instance, need to be more diffused than the OH bonding orbitals. In minimal-basis-set calculations, however, the same atomic orbitals must be used for both type of molecular orbitals.

One solution to the problem is to use *split valence* or *double zeta* basis sets (75) In these bases the atomic orbitals are split into two parts, an inner, compact orbital and an outer, more diffuse one. Thus the size of the atomic orbital that contributes to the molecular orbital can be varied within the limits set by the inner and outer basis functions (Figure 2.3.).

range attainable by combination of inner and outer functions

outer *p*-function

inner *p*-function
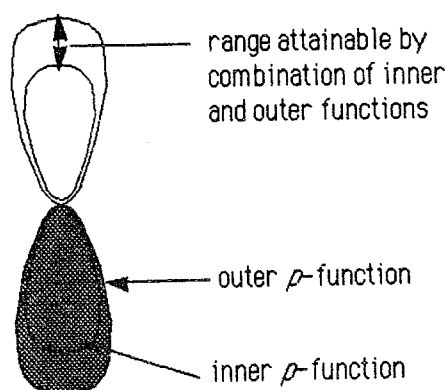
Figure 2.3. Schematic representation of the effect of split valence orbitals.

Split-valence basis set split only the valence orbitals in this way, whereas double zeta bases also have split core orbitals. There are various levels of these calculations (73). The split-valence basis set most widely used for the early calculations was 4-31G. This nomenclature means that the core orbitals consist of four and the inner and outer valence orbitals of three and one Gaussian functions, respectively. However, the basis set used most commonly for initial geometry optimizations is now 3-21G which has replaced STO-3G for all except the largest molecules. A closely related basis set which is widely used is 6-31G. It comprises core functions each written in terms of a linear combination of six gaussians, and two valence shells represented by three and one gaussian primitives, respectively. This representation has found its most important use as a starting point for the construction of the higher level calculations, 6-31G* and 6-31G**. 6-31G* and 6-31G** basis sets are explained in the following section.

2.8.1.3. Polarization Basis Set

The next step in improving a basis set is usually the addition of d-orbitals for all heavy (nonhydrogen) atoms. Mixing the d-orbital, which has lower symmetry, with the p-orbital results in a deformation of the resulting orbital to one side of the atom. This polarization is illustrated in figure 2.4.
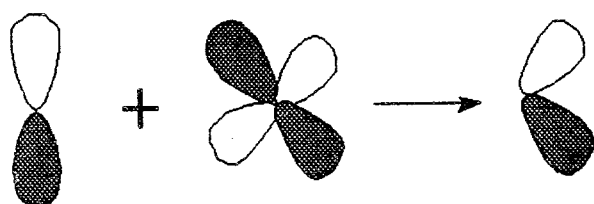
Figure 2.4. Polarization of a p-orbital by mixing with a d-function.

The most commonly used polarization basis sets are 6-31G* which includes a set of six d-functions (equivalent to five d- and one s-orbital) and

6-31G** in which a set of p-orbitals has been added to each hydrogen in 6-31G* basis set. These p-orbitals perform the same function for the s-valence orbital of hydrogen as the d-orbitals do for p-valence orbitals.

2.9. SEMIEMPIRICAL MO THEORY

Semiempirical methods use a simpler Hamiltonian than the correct molecular Hamiltonian and parameters whose values are adjusted to fit experimental data or the results of ab initio calculations. They are classified into two categories: those using a Hamiltonian that is the sum of one-electron terms, and those using a Hamiltonian that includes two-electron repulsion terms, as well as one-electron terms. The Hückel method is a one-electron theory, whereas the Pariser-Parr-Pople (PPP) method is a two-electron theory (76). Both of these theories were applied on planar molecules. The extended Hückel Method, one-electron theory, was later developed for nonplanar molecules. Similarly, several semiempirical two-electron MO generalizations of the PPP method have been developed for nonplanar molecules. Some of these methods are discussed below.

2.9.1. CNDO, INDO, and NDDO

CNDO, INDO, and NDDO methods were developed by J. A. Pople and his group (77) and were not intended to reproduce molecular geometries and heats of formation, but rather other electronic properties, such as the dipole moment. The simplest, CNDO (Complete Neglect of Differential Overlap), assumed the atomic orbitals to be spherically symmetrical when evaluating electron repulsion integrals. The next stage, the INDO (Intermediate Neglect of Differential Overlap) approximation, included one-center repulsion integrals between atomic orbitals on the same atom. The NDDO (Neglect of Diatomic Differential Overlap) approximation was the first in which the directionality of the atomic orbitals was considered in calculating the

repulsion integrals. These methods do pretty well on molecular geometry and do poorly on binding energies (77).

2.9.2. MINDO, MNDO, AM1, PM3

Dewar (77) and co-workers devised several semiempirical SCF MO theories that closely resemble the INDO and NDDO theories. Their aim was to have a theory that would give molecular binding energies with chemical accuracy and that would be applicable to large molecules without a lot of computation. In 1967 and 1969, Dewar published the PNDO (Partial Neglect of Differential Overlap) and MINDO/1 (first version of Modified INDO) theory (77) The parameters were chosen so as to have the predicted molecular heats of formation fit experimental data as well as possible. Although these theories worked well for heats of formation, they were quite poor for geometry. Later, the same researchers developed MNDO (Modified Neglect of Diatomic Overlap) which was based on the NDDO approximation and included also metallic elements. MNDO fails to reproduce intermolecular hydrogen bonds (77) and so is unsuitable for many biological problems. MNDO type methods were disscused by W. Thiel in more detail (78). In 1985, Dewar and co-workers published an improved version of MNDO called AM1 (Austin Model 1) (79) which partly corrects this failing. In 1989, Stewart reparametrized MNDO to give MNDO-PM3, also called simply PM3 (Parametric Method 3)(80), which substantially reduces the errors of MNDO and AM1 in calculating heats of formation without loss of accuracy in molecular geometry and dipole moments. PM3 method has been also found to predict successfully the intermolecular H-bonding between neutral molecules (81).

2.10. HOW THE PROGRAMS WORK

The basic steps involved in performing a typical ab initio or semiempirical calculation are very similar. The programs are usually

controlled by specific keywords, which request a given type of calculation. First, the keywords are converted to internal parameters. The next step is to read in a title for the job, the molecular charge, and the required multiplicity. The molecular geometry is then read in, usually in the form of a Z-matrix. The Z-matrix is only a geometrical means of defining the positions of the atoms in terms of atomic numbers, bond lengths, bond angles, and dihedral angles (82). The information from the Z-matrix is used to calculate the Cartesian (x, y, z) coordinates of the atoms, atomic numbers, and multiplicity, to work out the total number of electrons and the orbital occupancy. The atomic orbitals are then assigned to each nucleus. Semiempirical programs use a set of predetermined parameters to define the forms and energies of the atomic orbitals whereas ab initio programs may use the basis sets. Ab initio programs next calculate the various one- and two-electron integrals required later in the calculation. Figure 2.5 shows the flow chart for ab initio and semiempirical calculations. Both semiempirical and ab initio programs must then produce an initial guess, a trial set of molecular orbitals to be used as a starting point for the SCF calculations. There are several possibilities for the initial guess. Semiempirical programs generally divide the electrons evenly among the atomic orbitals and allow the SCF procedure to find more realistic molecular orbitals. For ab initio programs, the usual form of initial guess is obtained from an extended Hückel calculation on the molecule in question.

The program uses the initial guess as a starting point for an iterative SCF calculation. The solution to the SCF equations is improved cycle by cycle until the electronic energy is at minimum. At this stage the calculation is said to be converged, or to have reached self consistency.
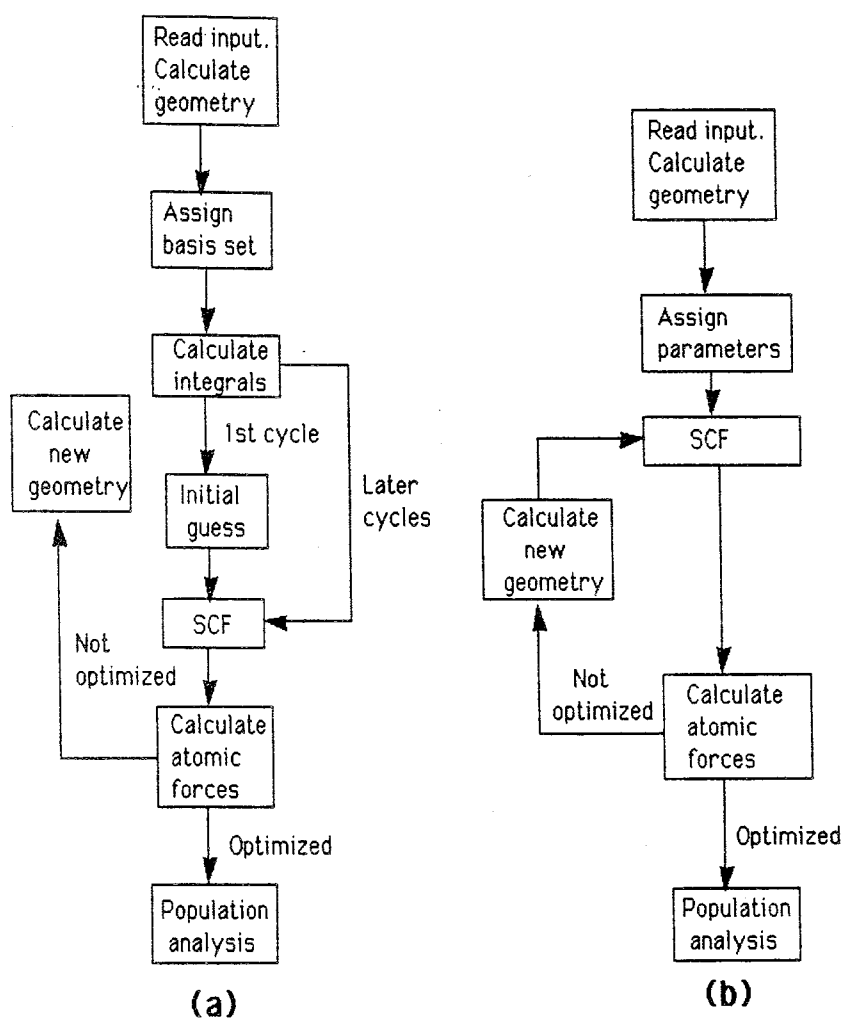
Figure 2.5. Flow chart of a typical **(a)** ab initio **(b)** semiempirical calculation method (82).

The next stage of the calculation depends on the type of job to be performed. The program may either perform some sort of post-SCF correlation energy calculation or move directly to the population analysis, which calculates the atomic charges, overlaps, dipole moment, etc. For a geometry optimization, the atomic forces are then determined analytically and used to estimate the minimum-energy geometry for the molecular species being calculated. The above process is repeated for each new geometry until the atomic forces are close to zero and the total energy does not change significantly from cycle to cycle. At this stage the optimization

is complete and the program moves on to a population analysis of the optimized species. ···

2.11. MODELING SOLVENT EFFECT
(SELF-CONSISTENT REACTION FIELD APPROACH, SCRF)

The necessity to develop computational methods which take into account the effect of solvent on the species studied has been discussed in section 1. Chemical problems related with the liquid state are very diverse and theoretical approaches vary according to the nature of the phenomenon under investigation (83-87). These problems are quite complicated and some simplifications are required. Depending on the type of simplification made, two main classes of approaches have been proposed:

1. Model Molecules in True Liquid: It uses a simplified representation of the molecules and of the intermolecular forces, which can be used in a simulation of the liquid by using the techniques such as Monte Carlo or Molecular Dynamics calculations (88-90).

2. True Molecules in Model Liquids: SCRF approach belongs to this class. It consists in performing a usual quantum chemical calculation for a molecule undergoing the influence of a simplified surroundings. It is therefore able to tell us more about the modifications of the electronic structure than the previous one, but the necessity of using a model of the liquid introduces many assumptions which need to be carefully examined. The way for a better understanding and therefore a better use of this kind of approach depends on obtaining a large number of results from the applications of the theory on various systems and by using various models. Examples of such applications are present in the literature (91-96). The ultimate goal of the present work is to check the applicability of SCRF approach on the molecules chosen.

The simplest model for the liquid which can be conceived for electrostatic interactions is to consider it as a *dielectric continuum*. The

historical background of this treatment goes back to Kirkwood (97) who proposed to consider the solute as a distribution of charges placed in a vacuum. The solute in this vacuum is separated from a continuum having the macroscopic dielectric properties of the solvent by a spherical surface. This spherical surface defines the molecular cavity. Then, Onsager (98) showed that the dipolar liquids can be fairly well described by a spherical cavity model in which the volume of the cavity is equal to the molecular volume in the liquid. On the other hand, simplifying the solvent by expressing it with only its dielectric constant brings some limitations on the application. For example, no specific interaction between the solute and the solvent is considered in the model. Therefore the solvents that are expected to make intermolecular H-bonding with the solute cannot be well described with this method.

This model has been extended to quantum chemical calculations (99, 100) on small molecules and proved to be useful in the prediction of solvent effects on molecules which do not depart too much from a spherical shape. However, this limitation is difficult to accept since a great variety of chemicaly interesting molecules cannot fit a spherical cavity. Rivail and his group also developed the ellipsoidal cavity model and showed that the electronic structures can be obtained with a good accuracy with this model (101). The key feature of the model is the shape of the cavity. The volume of the cavity is taken as the partial molecular volume of the solute. If one states that the cavity should include all the nuclei and as much as possible of the electron cloud, one is then led to limiting the cavity by an electronic density surface, called isodensity surface. Other cavity specifications have been also discussed such as isopotential surface and van der Waals surface (97). It is possible to generate a flow chart for quantum chemical calculations of solute molecules (Figure 2.6.).
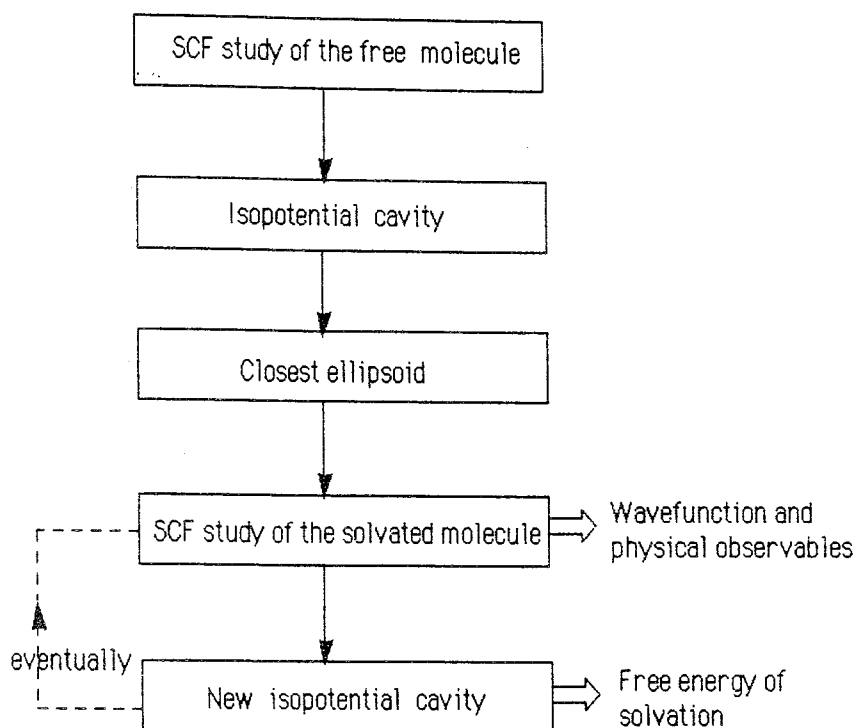
Figure 2.6. Flow chart of SCRF type calculation (97).

The Reaction Field The solute molecule can be imagined to be surrounded by an arbitrary large number of solvent molecules, **S** (Figure 2.7). The molecule is considered as a quantum system perturbed by its surroundings while the solvent is simplified as a dielectric continuum. To analyze the perturbation of the solute, one can imagine that the solute is removed without any modification either in the solvent or in the solute structure. The volume previously occupied by the solute is now empty and is called the solute's cavity (Figure 2.7)
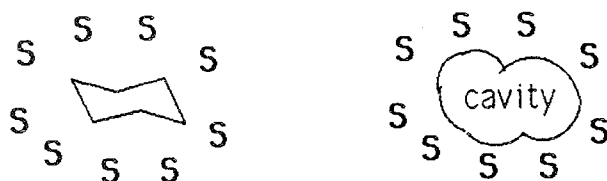
Figure 2.7. Representation of the cavity model. **S** is the solvent molecule.

In this cavity, the averaged electric potential is nonzero. It usually varies from one point to another giving rise to a non-uniform electric field which is called the *reaction field*. The overall effect is an electric polarization of the solvent around the solute which is at the origin of the electric field in the cavity. The bulk solvent and the solute can be considered separately. Then, the free energy of solvation, ΔA_S, is the sum of six terms that correspond to each step in solvation process:

$$\Delta A_S = \Delta A_c + \Delta A_p + \Delta A_i + \Delta A_e + \Delta A_d + \Delta A_t \qquad (2.15)$$

where,

ΔA_c is the corresponding free energy variation due to the creation of the cavity in the solvent (cavitation energy)

ΔA_p is the polarization of the solvent around the cavity.

ΔA_i is the induced polarization of the solute by the reaction field.

ΔA_e is the electrostatic interaction between the polarized solute and the reaction field.

ΔA_d is the contribution of the dispersion and repulsion forces between the solute and the neighbouring solvent molecules.

ΔA_t is the translational, rotational and vibrational partition functions of the solute.

In some special processes, some contributions can be considered as constant during the process and the number of terms that ought to be evaluated decrease.

The definition of the cavity shape is the crucial point of this model. Analytical formula for the interaction energy may be obtained for constant coordinate cavities such as the sphere (99) or the ellipsoid (101). Then the free energy of solvation is given by

$$\Delta A_S = -(1/2) M_l^m f_{ll'}^{mm'} M_{l'}^{m'} \qquad (2.16)$$

where M_l^m is a component of the multipole moment of order l and the

reaction field factors $f_{ll'}^{mm'}$ depend only on the dielectric properties of the medium and on the cavity shape. Repeated indices stand for a sum over all their possible values: l from 0 to ∞ (in practice, a good convergence is in generally obtained for l = 6 and m from $-l$ to $+l$) The induction energy may be computed by performing an SCF calculation in which one minimizes the energy of the molecule plus the free energy of solvation.

Although many molecules may be reasonably fitted by an ellipsoidal cavity, in some cases it may be necessary to use a more realistic cavity shape. The cavity defined by the isodensity surface, which encloses the largest fraction of particles belonging to the solute's molecule, appears to be the better choice (95). The solvation energy is computed numerically from the expression

$$\Delta A_S = (1/2) \sum V(r) \rho(r) d\tau \qquad (2.17)$$

where $V(r)$ is the electrostatic potential created in the cavity by the polirized continuum, $\rho(r)$ is the molecular charge density, where it is assumed that the electronic density outside the cavity is negligible. The potential $V(r)$ is computed by considering a fictitious surface charge density which is defined as being proportional to the normal component of the electric field (97).

Two other terms are lacking in this model: The cavitation and the dispersion energies. However, in conformational equilibria the variation of the cavitation term is expected to be small and can be neglected. The dispersion energy may be included in the model but its variation with the molecular conformation is slight. Therefore the main terms assumed to vary during the solvation process are essentially due to the electrostatic plus induction terms.

3. CALCULATIONS AND RESULTS

The energies for the conformers of 2-substituted cyclohexanone ethylene and propylene ketals are calculated for isolated and solvated species in order to investigate the effect of solvent on their conformational equilibria.

3.1. COMPUTATIONS

The calculations in this study can be divided into three main groups:

1. Calculations on 2-substituted cyclohexanone propylene ketals

2. Calculations on 2-substituted cyclohexanone ethylene ketals

3. Calculations on 1,1,2 trihydroxy ethane.

We performed semiempirical SCF calculations on the first two groups of compounds with the PM3 method. On the third one, 1,1,2 trihydroxy ethane, we performed ab initio calculations in addition to semiempirical SCF calculations. This molecule was first studied with PM3 and the optimized geometries were used as starting geometries in ab initio calculations.

We studied all the molecules both in isolated form (gas phase) and in solvated form. The solvents used are $CCl_4(\varepsilon=2.24)$, $CDCl_3(\varepsilon=4.81)$, and CD_3CN $(\varepsilon=37.50)$. The gas phase computations of all the molecules except $-F$, $-Cl$, and $-CH_3$ substituted ketals have been performed with MOPAC 5 (102) using the key words PRECISE and GNORM=0.1. The substituents $-F$, $-Cl$, and $-CH_3$ have been studied in gas phase using GEOMOS. All of the calculations in the

solvent have been done using the program GEOMOS (103). Both programs have been implemented for VAX/VMS and DS5500 ultrix operating system.

GEOMOS is a program that makes use of semi-empirical methods and to which the SCRF method and the cavity model has been implemented. An ellipsoidal surface is used to define the cavity (Section 2.11). Its characteristics (axis, volume) are determined as proposed in the literature (101). The volume of the cavity is equal to the molecular volume of the solute and the shape is simplified to an ellipsoid which allows an analytical expression of the perturbations. In this model, the solvation energy is computed through a multipole moment series which includes six non-zero terms of lowest order (i.e., the dipole, quadrupole, octupole and hexadecapole, etc. moments). For the first two groups of molecules, this term was calculated up to the fourth order. For 1,1,2-trihydroxyethane, it was calculated up to the sixth order.

The input Z-matrices have been prepared according to the numbering shown in Figure 3.1. Two dummy atoms, X1 and X2 are used to describe the cyclohexane ring as in reference 82. These dummy atoms are assumed to be at the centers of the triangles defined by C4-C5-C6 and C1-C2-C3. The Z-matrix of the substituted molecules at C3 have been prepared by substituting H9 or H14 with the substituents, which correspond to axial and equatorial orientations respectively. Examples of input data for MOPAC and GEOMOS are given in the appendix B. All the geometries have been fully optimized with respect to the internal coordinates unless otherwise indicated. The optimized geometries were further checked by force calculations and positive vibrational frequencies were obtained indicating that the resultant geometries correspond to local minima.

For -OH, -OCH$_3$, and -NO$_2$ substituted molecules rotation around the bond between the substituent and cyclohexane ring has been also considered both (Figure 3.2) in the isolated and in the solvated molecules, since several rotamers having close energies may be expected. Unless otherwise indicated, the results below are given for the rotamer of lowest energy The value of the

dihedral angles in Figure 3.2 has been varied from 0° to 360° (except $-NO_2$ derivatives in which 180°=360°) with 30° intervals. All the minima obtained from the potential curves have been fully optimized.
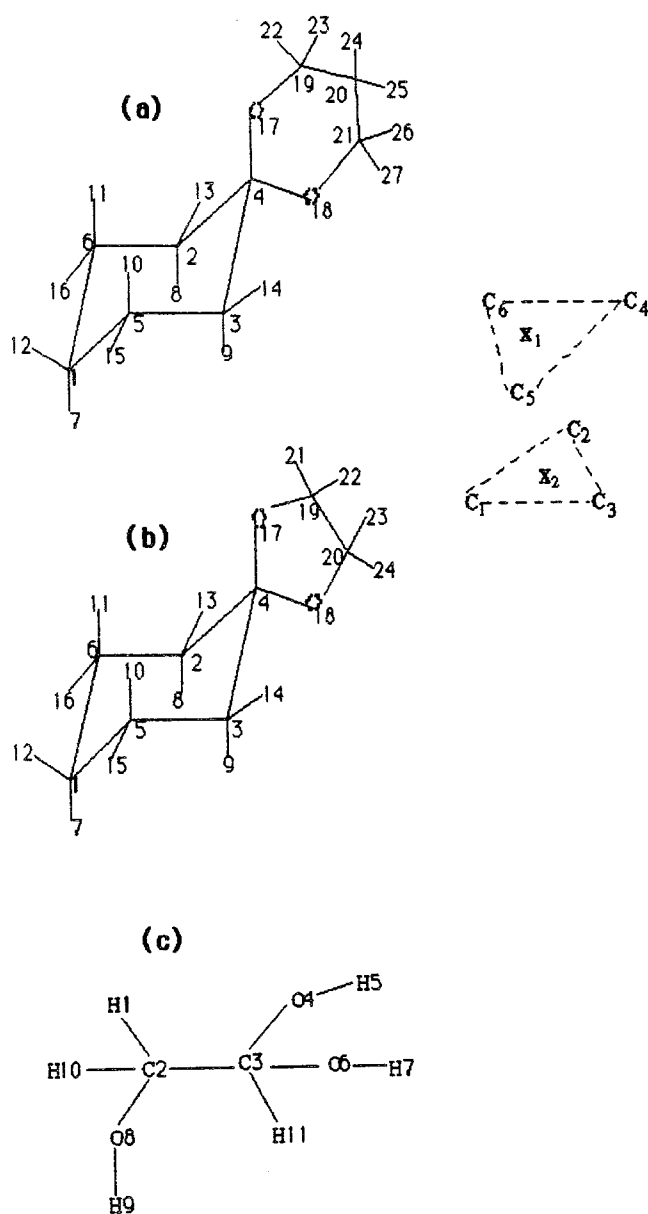
Figure 3.1. Z-matrix numbering system used for (a) propylene ketals (b) ethylene ketals (c) 1,1,2-trihydroxy ethane.
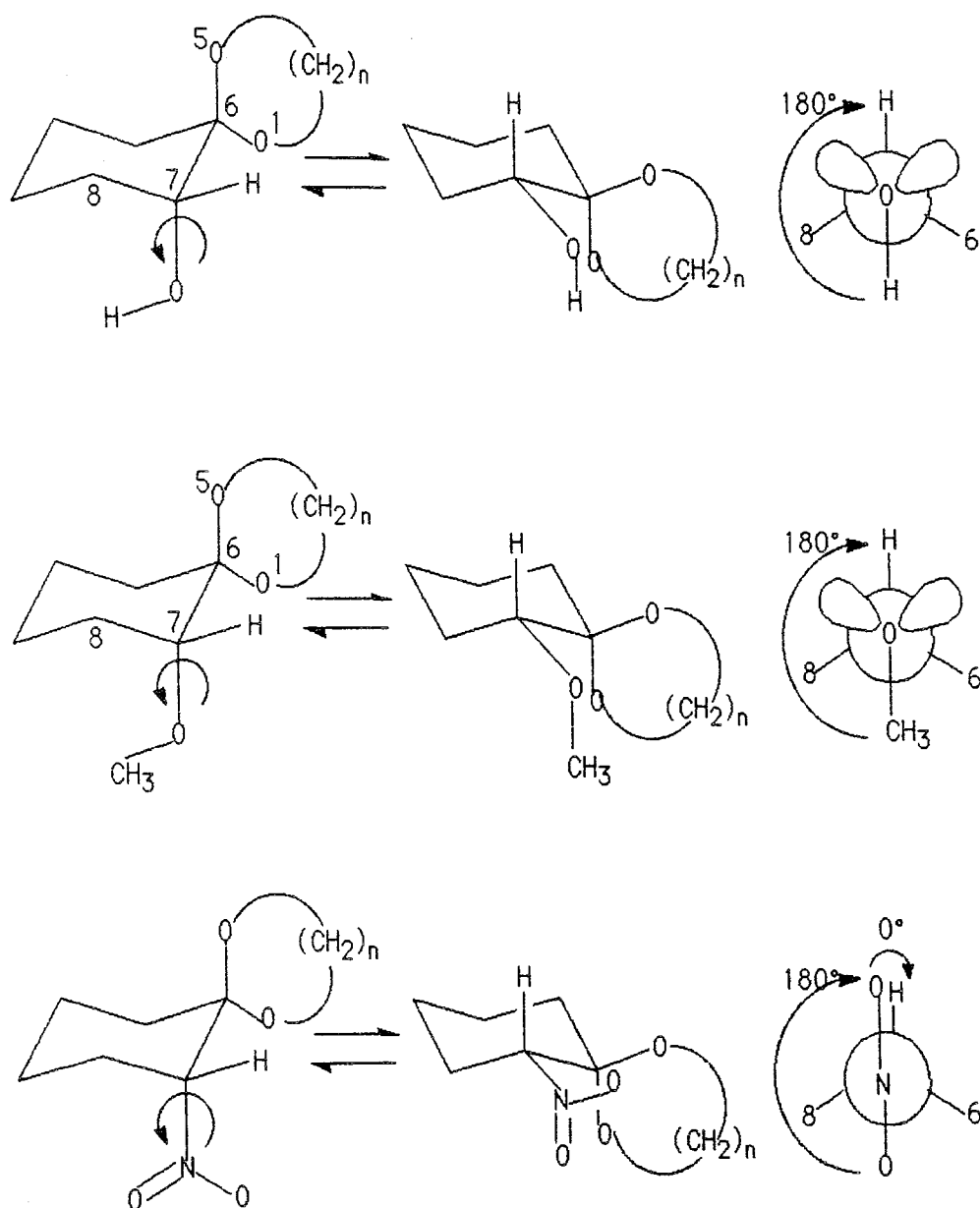
Figure 3.2. Representation of dihedral angles. (n=2, 3).
H-O-C-H angle for X=-OH, C-O-C-H angle for X=-OCH$_3$,
and O-N-C-H angle for X=-NO$_2$.
(Numbers are given for propylene ketals.)

3.2. RESULTS FOR 2-SUBSTITUTED CYCLOHEXANONE PROPYLENE KETALS

For each molecule, four Z-matrixes corresponding to Ia, Ib, IIa, and IIb conformers were prepared as shown in Figure 1.6(a) and the energies of the optimized geometries were calculated. The optimized geometries obtained from gas phase calculations have been used as starting geometry for the solvent effect calculations. Total axial conformer percentages have been computed using a Boltzman distribution for the four conformers as described in the appendix C. The results of the isolated and the solvated molecules are given in Table 3.1 and Table 3.2 respectively. Solvation energy, E_{solv} is the difference between the energy in solution and the gas phase energy. The potential energy curves obtained from the rotamer studies of -OH, -OCH$_3$, and -NO$_2$ substituted propylene ketals are given in Figure 3.3-Figure 3.8.

Table 3.1. Computed total, E_{total}, and relative energies, ΔE, (kcal/mol); dipole moments (Debyes); total axial conformer percentages for 2-substituted cyclohexanone **propylene ketals** in the **gas phase**.

X		E_{total}	ΔE	μ	% ax
-H[a]		-43850.272		1.77	
-F	Ia	-53646.802	0.46	2.76	37.83
	IIa	-53646.453	0.81	2.16	
	Ib	-53647.262	0.00	3.16	
	IIb	-53646.275	0.99	0.19	
-Cl	Ia	-50797.973	0.00	2.58	68.84
	IIa	-50797.569	0.40	2.06	
	Ib	-50797.673	0.30	2.95	
	IIb	-50796.426	1.55	0.14	
-CN	Ia	-49940.837	0.31	4.28	48.28
	IIa	-49940.542	0.60	3.49	
	Ib	-49941.144	0.00	4.81	
	IIb	-49939.166	1.98	1.74	
-CH$_3$	Ia	-47296.177	0.75	1.72	53.05
	IIa	-47296.930	0.00	1.77	
	Ib	-47296.608	0.32	1.76	
	IIb	-47296.573	0.36	1.62	
-NO$_2$	Ia	-60709.226	0.56	5.34	35.11
	IIa	-60708.672	1.11	4.20	
	Ib	-60709.783	0.00	5.82	
	IIb	-60707.538	2.26	4.93	
-OCH$_3$	Ia	-54058.068	0.81	2.81	90.25
	IIa	-54058.879	0.00	0.87	
	Ib	-54057.460	1.42	2.66	
	IIb	-54056.963	1.92	1.50	
-OH	Ia	-50621.791	1.07	3.15	45.74
	IIa	-50622.660	0.79	0.95	
	Ib	-50622.794	0.00	3.08	
	IIb	-50621.741	1.05	1.32	

(a) E_{total} and μ values are the same for syn and anti orientations.

Table 3.2. Solvation energies, E_{solv}, (kcal/mol), relative energies, ΔE_{total}, (kcal/mol) and total axial conformer percentages of 2-substituted cyclohexanone **propylene ketals**

		$CCl_4^{(a)}$ (ε=2.24)			CD_3CN (ε=37.5)		
		E_{solv}	ΔE_{total}	%ax	E_{solv}	ΔE_{total}	%ax
-H		-0.48			-1.13		
-F	Ia	-0.99	0.65	32.11	-2.34	0.90	23.23
	IIa	-0.82	1.10		-2.09	1.51	
	Ib	-1.18	0.00		-2.78	0.00	
	IIb	-0.45	1.71		-1.05	2.72	
-Cl	Ia	-0.65	0.00	64.18	-1.53	0.07	56.21
	IIa	-0.62	0.44		-1.49	0.52	
	Ib	-0.80	0.15		-1.90	0.00	
	IIb	-0.36	1.83		-0.86	2.29	
-CN	Ia	-5.03	0.51	39.88	-7.52	1.17	18.35
	IIa	-4.97	0.87		-7.47	1.51	
	Ib	-5.23	0.00		-8.38	0.00	
	IIb	-2.91	4.30		-4.24	6.12	
-CH$_3$	Ia	-0.37	0.81	53.58	-0.88	0.87	54.92
	IIa	-0.42	0.00		-1.00	0.00	
	Ib	-0.39	0.35		-0.92	0.40	
	IIb	-0.40	0.38		-0.93	0.42	
-NO$_2$	Ia	-1.91	1.26	12.37	-6.43	2.15	2.85
	IIa	-2.00	2.41		-5.88	3.96	
	Ib	-3.30	0.00		-8.72	0.00	
	IIb	-2.76	2.79		-7.63	3.34	
-OCH$_3$	Ia	-0.22	0.55	87.36	-2.06	0.14	81.32
	IIa	-0.66	0.00		-0.68	0.00	
	Ib	-0.29	1.09		-1.52	0.59	
	IIb	-0.09	1.96		-0.59	2.01	
-OH	Ia	-0.76	0.99	35.11	-2.58	0.88	26.02
	IIa	-0.83	0.65		-1.95	1.23	
	Ib	-0.68	0.00		-2.39	0.00	
	IIb	-0.21	1.53		-1.25	2.19	

(a)-CN derivative has been calculated in $CDCl_3$ (ε=4.81) because experimental data is available only in $CDCl_3$.

Figure 3.3. Potential scans of 2-NO$_2$ cyclohexanone propylene ketals for conformers Ia and IIa. ($\triangle$ in gas phase, o in acetonitrile)

Figure 3.4. Potential scans of 2-NO$_2$ cyclohexanone propylene ketals for conformers Ib and IIb. (▲ in gas phase, o in acetonitrile)

46

Figure 3.5. Potential scans of 2-OH cyclohexanone propylene ketals for conformers Ia and IIa. (△ in gas phase, ○ in acetonitrile)

Figure 3.6. Potential scans of 2-OH cyclohexanone propylene ketals for conformers Ib and IIb. (Δ in gas phase, o in acetonitrile)

Figure 3.7. Potential scans of 2-OCH$_3$ cyclohexanone propylene ketals for conformers Ia and IIa. (Δ in gas phase, o in acetonitrile)
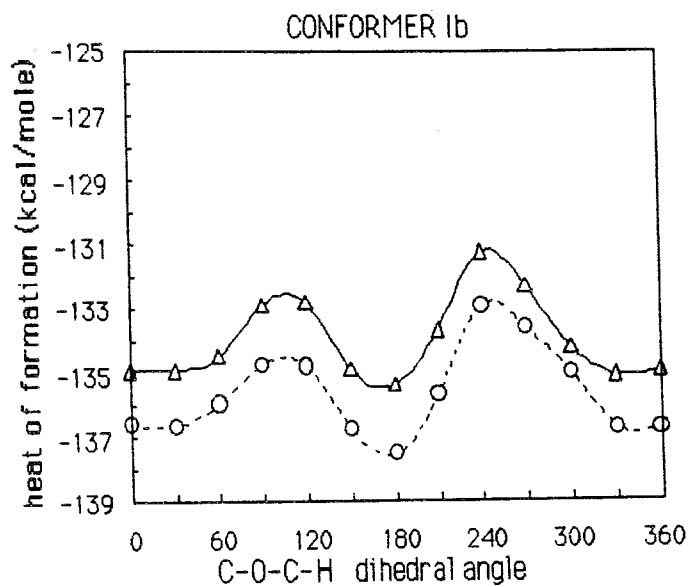
Figure 3.8. Potential scans of 2-OCH$_3$ cyclohexanone propylene ketals for conformers Ib and IIb. (▲ in gas phase, o in acetonitrile)

3.3. RESULTS FOR 2-SUBSTITUTED CYCLOHEXANONE ETHYLENE KETALS

The dioxolane ring pseudorotates as described in section 1. In order to obtain its most stable form, for unsubstituted cyclohexanone ethylene ketal, we scanned the rotation around C5-O1 and C5-O4 bonds at 5°.intervals of C6-C5-O4-C3 angle from 95°-140°. The planar structure was found to be at the transition state showing only one negative vibrational frequency in force calculations. The most stable puckered structure confirmed by force calculation has been used as the starting geometry for the substituted molecules.

The conformations of the cyclohexane and the puckered dioxolane rings are represented in Figure 1.6(b). For anti conformers Ia and Ib, the dioxolane fragment stays away from the substituent whereas for syn conformers, IIa and IIb, it is extended towards the substituent. The similar calculations described for propylene ketals were applied on ethylene ketal derivatives. The results are given in Table 3.3 and Table 3.4. Potential energy curves of -OH, $-OCH_3$, and $-NO_2$ derivatives of ethylene ketals are given in Figure 3.9-Figure 3.14

Table 3.3. Computed total, E_{total}, and relative energies, ΔE, (kcal/mol); dipole moments (Debyes); total axial conformer percentages for 2-substitued cyclohexanone **ethylene ketals** in the **gas phase**

X		E_{total}	ΔE	μ	% ax
-H[a]		-40404.545		0.89	
-F	Ia	-50200.850	1.21	2.25	14.65
	IIa	-50200.882	1.18	2.02	
	Ib	-50201.749	0.32	1.99	
	IIb	-50202.064	0.00	0.76	
-Cl	Ia	-47352.111	0.29	2.04	40.85
	IIa	-47352.009	0.39	1.84	
	Ib	-47352.149	0.25	1.75	
	IIb	-47352.396	0.00	0.72	
-CN	Ia	-46495.025	0.77	3.91	22.74
	IIa	-46495.048	0.75	3.62	
	Ib	-46495.795	0.00	3.30	
	IIb	-46495.750	0.05	2.87	
-CH$_3$	Ia	-43850.818	0.63	0.90	31.32
	IIa	-43850.983	0.47	0.95	
	Ib	-43851.299	0.15	0.83	
	IIb	-43851.449	0.00	0.84	
-NO$_2$	Ia	-57263.360	0.72	4.72	36.96
	IIa	-57263.570	0.51	4.40	
	Ib	-57264.075	0.00	4.60	
	IIb	-57263.245	0.83	3.59	
-OCH$_3$	Ia	-50612.681	0.29	1.82	57.19
	IIa	-50612.969	0.00	0.66	
	Ib	-50612.280	0.67	1.77	
	IIb	-50612.902	0.07	1.08	
-OH	Ia	-47176.226	1.18	2.18	16.06
	IIa	-47176.533	0.88	1.16	
	Ib	-47177.380	0.03	2.08	
	IIb	-47177.409	0.00	1.48	

(a) E_{total} and μ values are the same for syn and anti orientations.

Table 3.4. Solvation energies, E_{solv}, (kcal/mol), ΔE_{total}, (kcal/mol) and total axial conformer percentages of 2-substituted cyclohexanone **ethylene ketals**

		$CCl_4^{(a)}$ (ε=2.24)			CD_3CN (ε=37.5)		
		E_{solv}	ΔE_{total}	%ax	E_{solv}	ΔE_{total}	%ax
-H		-0.45			-1.06		
-F	Ia	-1.04	0.77	23.23	-2.12	0.55	35.34
	IIa	-1.03	0.76		-2.47	0.54	
	Ib	-0.91	0.03		-1.82	0.00	
	IIb	-0.60	0.00		-1.18	0.43	
-Cl	Ia	-0.66	0.13	46.47	-1.57	0.05	51.37
	IIa	-0.75	0.14		-1.68	0.04	
	Ib	-0.65	0.10		-1.58	0.00	
	IIb	-0.50	0.00		-1.17	0.16	
-CN	Ia	-5.14	0.58	71.62	-8.09	0.71	89.97
	IIa	-5.69	0.00		-8.78	0.00	
	Ib	-4.52	0.43		-6.85	1.18	
	IIb	-3.29	1.70		-4.83	3.25	
-CH$_3$	Ia	-0.47	0.90	25.58	-0.71	0.97	23.84
	IIa	-0.63	0.58		-0.89	0.63	
	Ib	-0.74	0.16		-1.04	0.16	
	IIb	-0.74	0.00		-1.05	0.00	
-NO$_2$	Ia	-3.39	0.89	29.60	-7.92	0.97	24.21
	IIa	-3.18	0.88		-7.44	1.24	
	Ib	-3.56	0.00		-8.18	0.00	
	IIb	-2.97	1.42		-6.71	2.29	
-OCH$_3$	Ia	-0.83	0.24	52.68	-1.78	0.37	42.28
	IIa	-0.71	0.07		-1.51	0.35	
	Ib	-0.92	0.55		-2.13	0.42	
	IIb	-0.75	0.00		-1.93	0.00	
-OH	Ia	-1.31	1.02	18.51	-2.98	0.85	22.03
	IIa	-1.13	0.90		-2.54	1.98	
	Ib	-1.18	0.00		-2.68	0.00	
	IIb	-1.02	0.13		-2.30	0.35	

(a)-CN derivative has been calculated in $CDCl_3$ (ε=4.81) because experimental data is available only in $CDCl_3$.
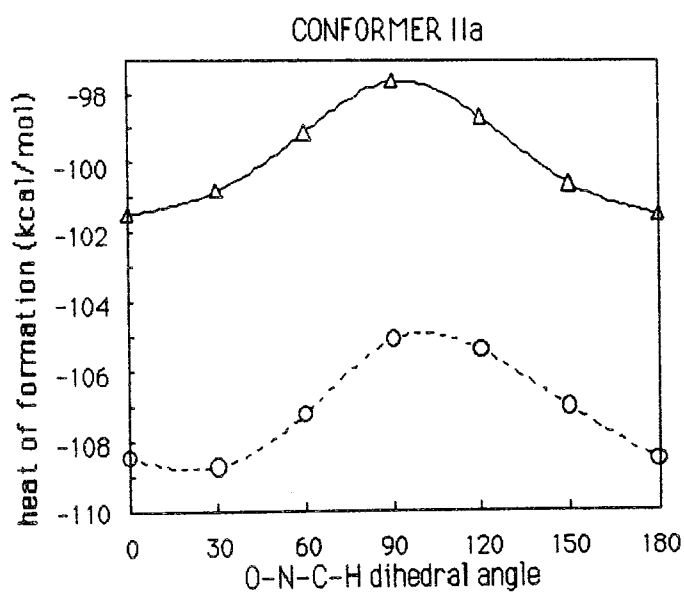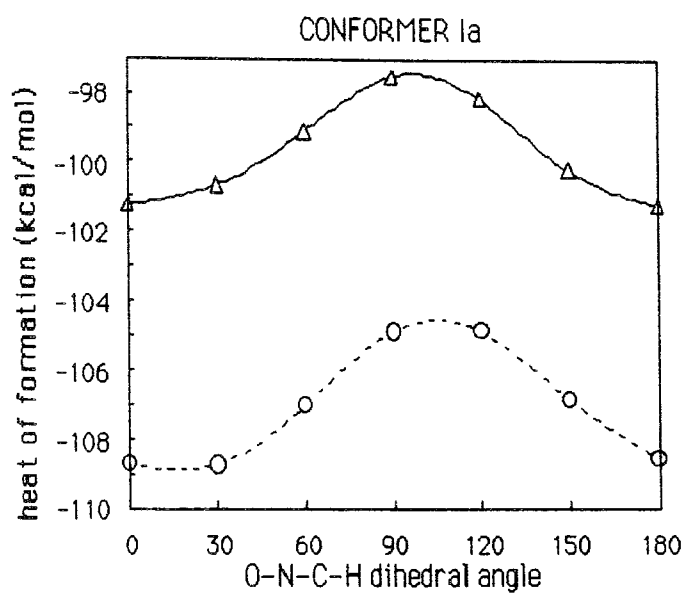
Figure 3.9. Potential scans of 2-NO$_2$ cyclohexanone ethylene ketals for conformers Ia and IIa. ($\triangle$ in gas phase, o in acetonitrile)
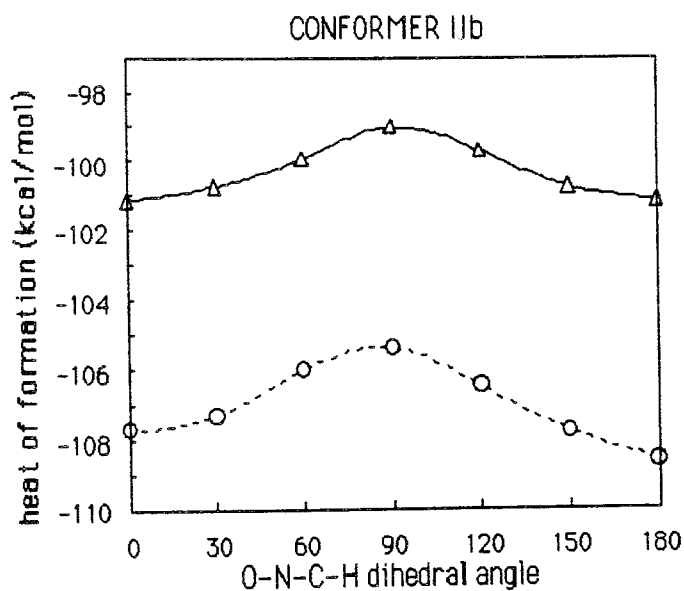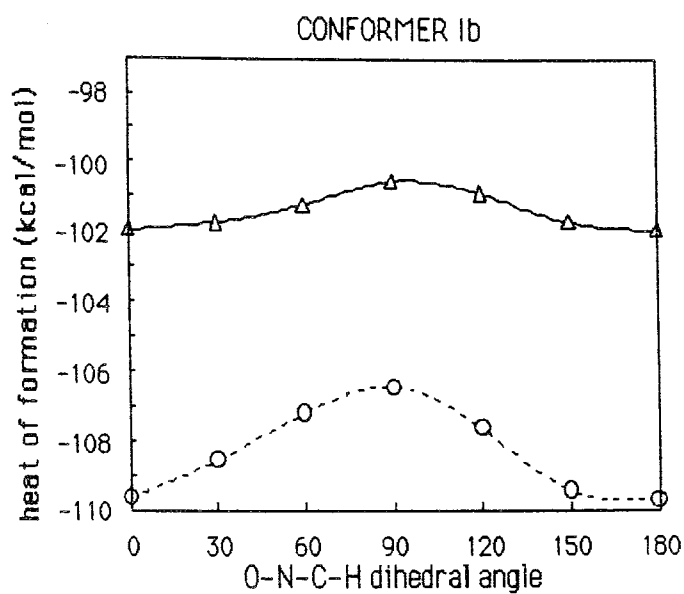
Figure 3.10. Potential scans of 2-NO$_2$ cyclohexanone ethylene ketals for conformers Ib and IIb. (△ in gas phase, o in acetonitrile)
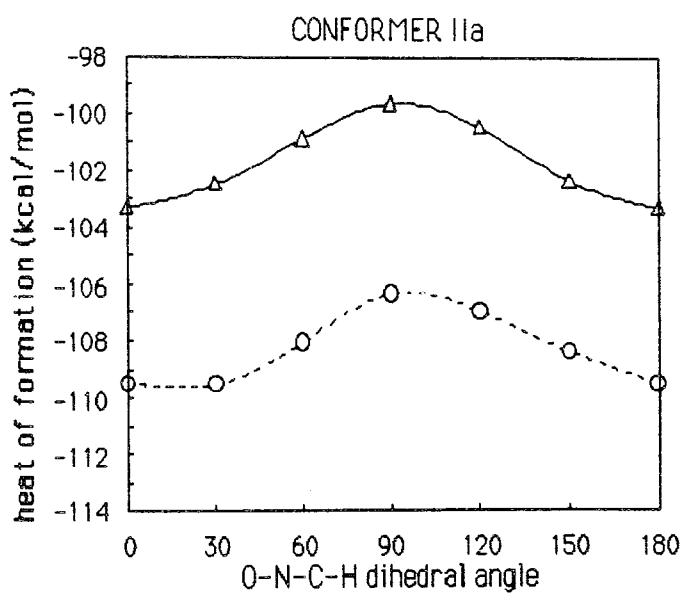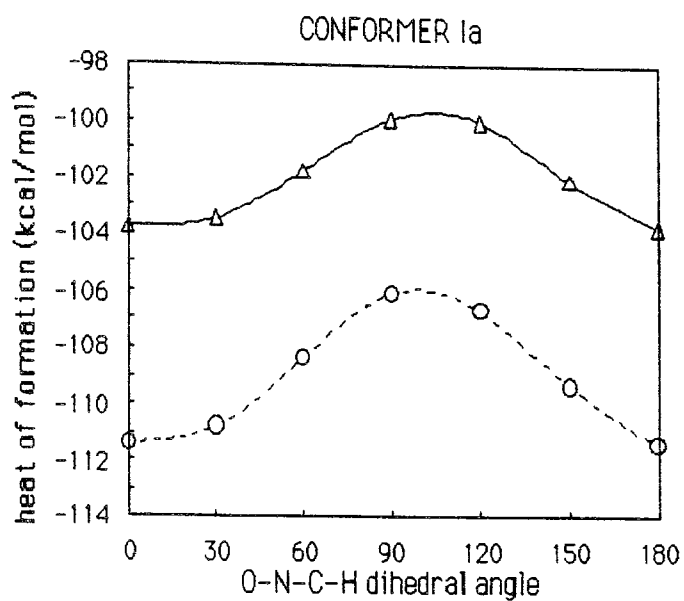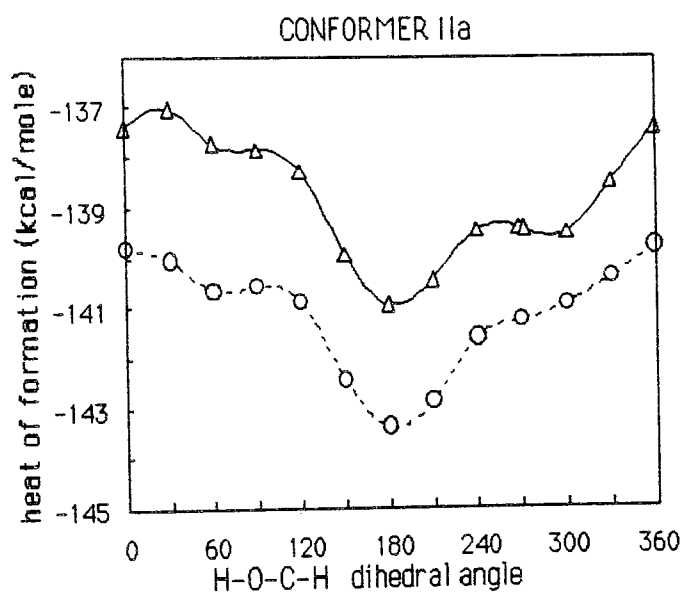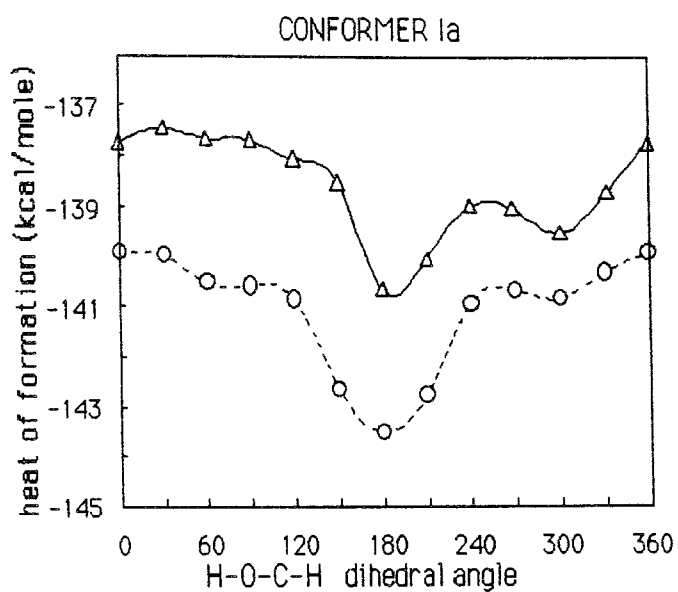
Figure 3.11. Potential scans of 2-OH cyclohexanone ethylene ketals for conformers Ia and IIa. (▲ in gas phase, o in acetonitrile)
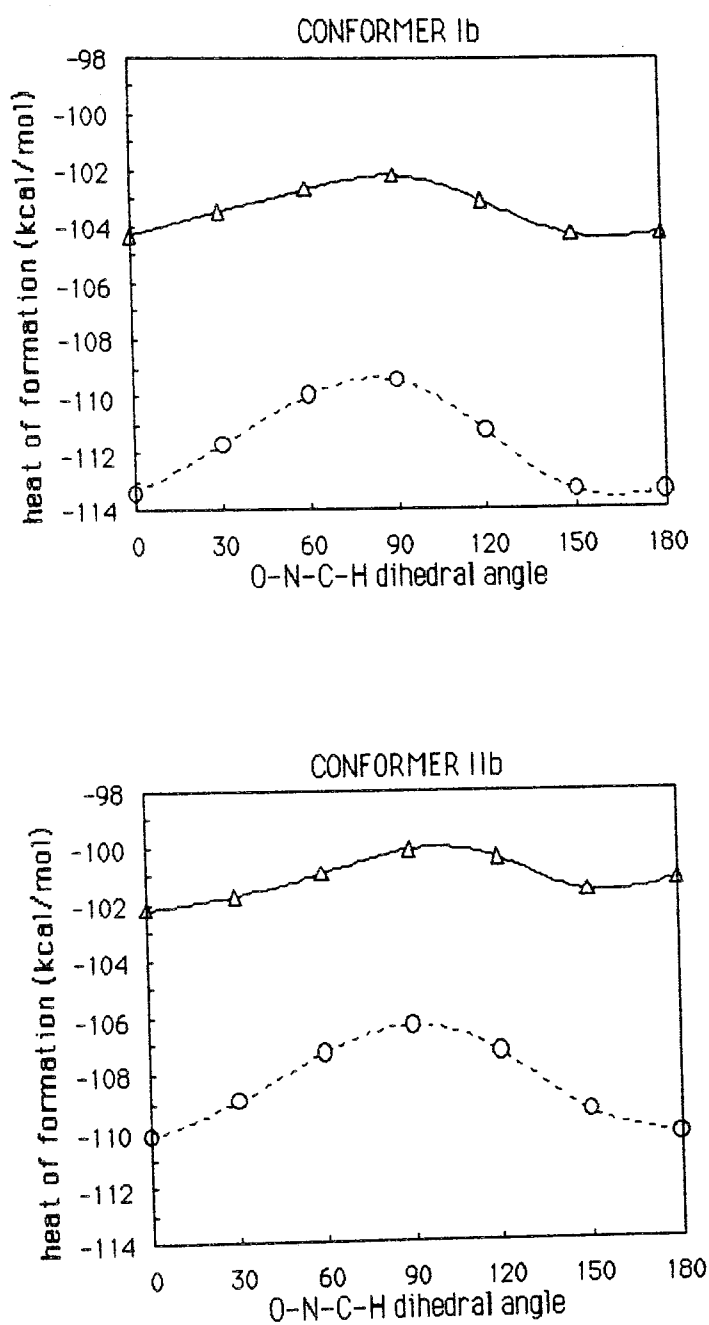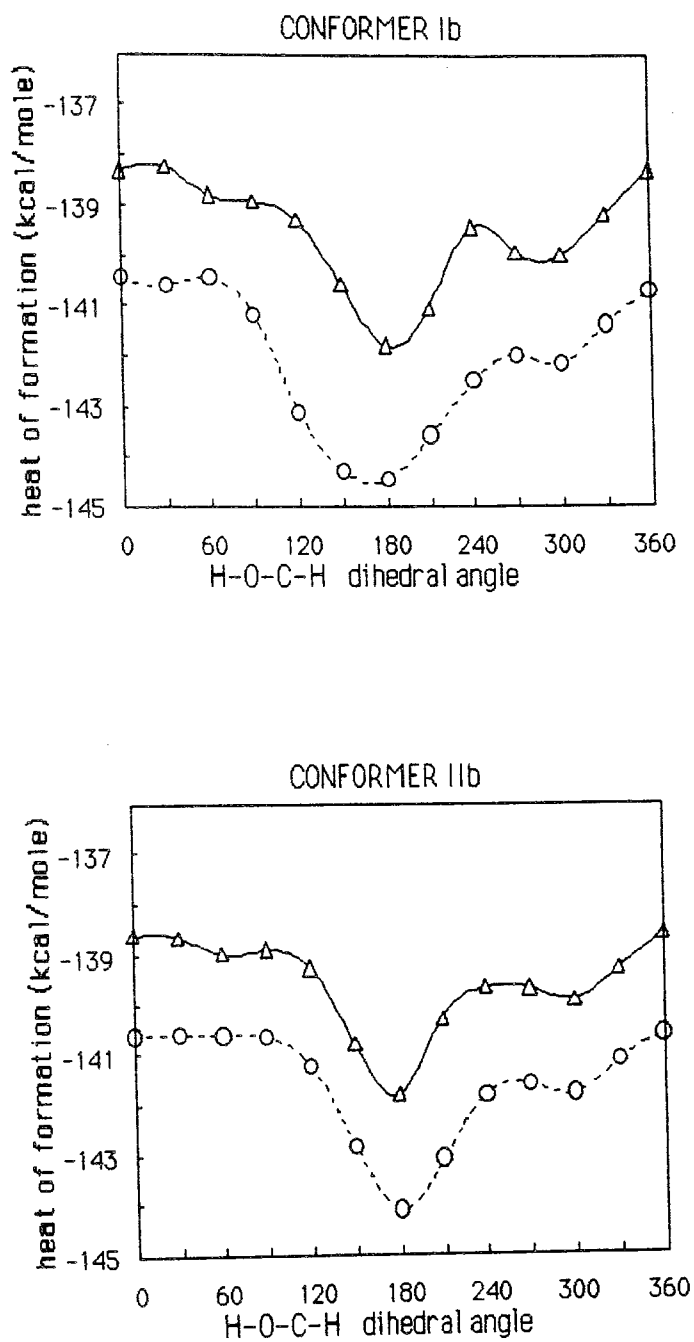
Figure 3.12. Potential scans of 2-OH cyclohexanone ethylene ketals for conformers Ib and IIb. (Δ in gas phase, o in acetonitrile)
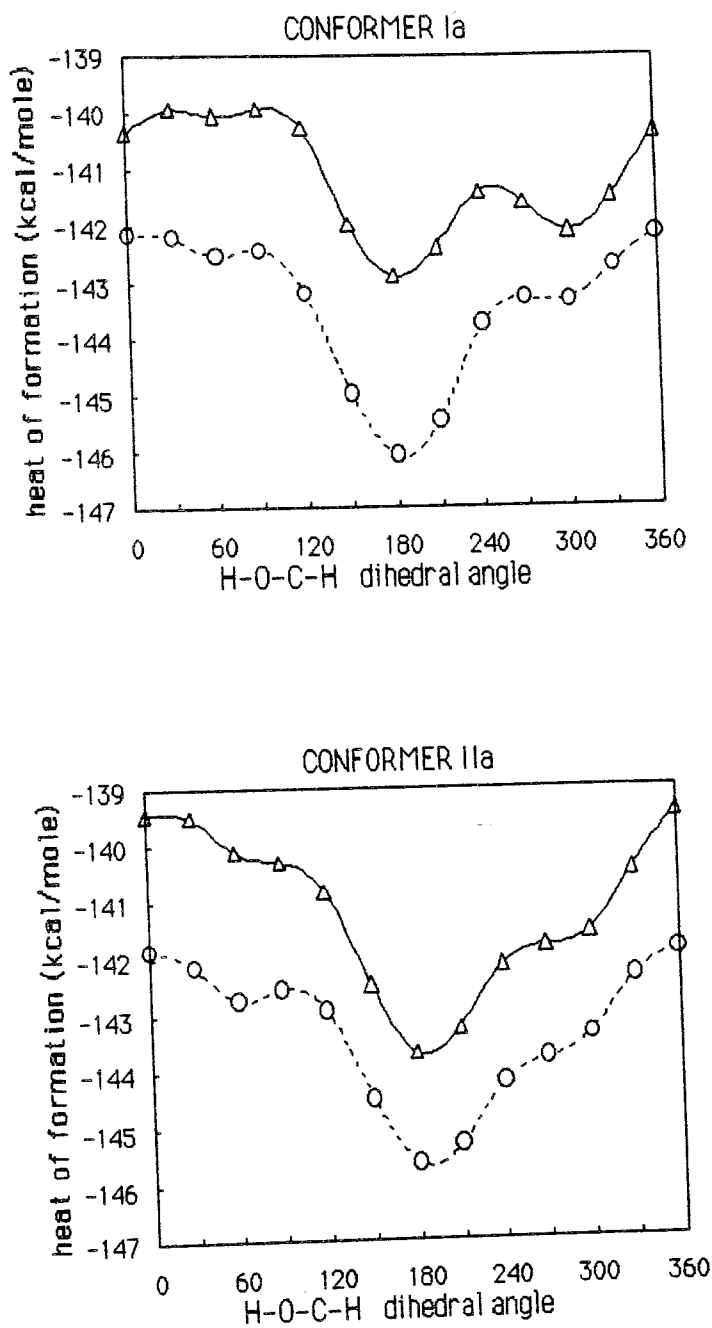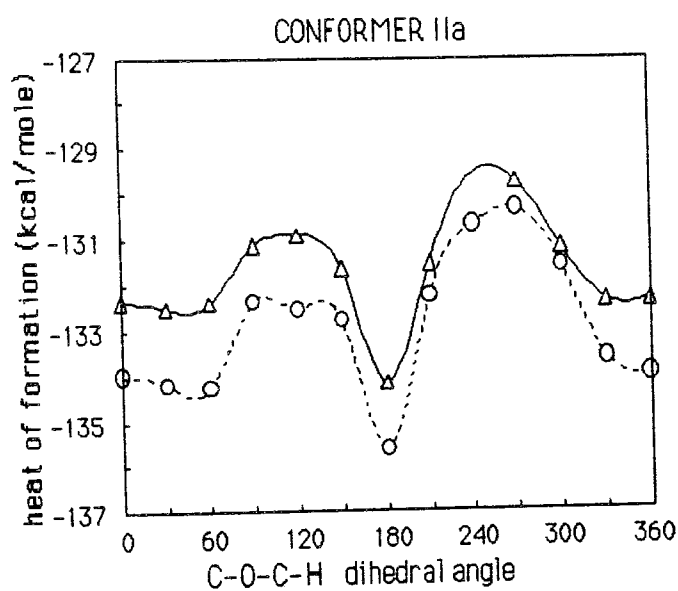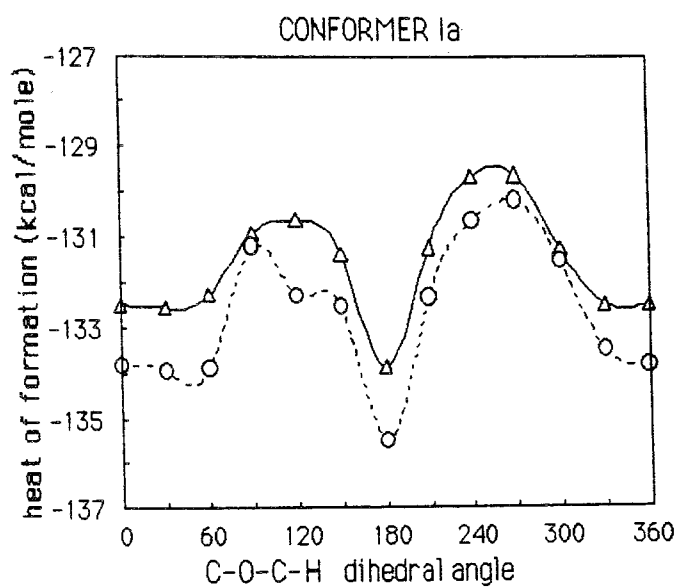
Figure 3.13. Potential scans of 2-OCH$_3$ cyclohexanone ethylene ketals for conformers Ia and IIa. (▲ in gas phase, o in acetonitrile)
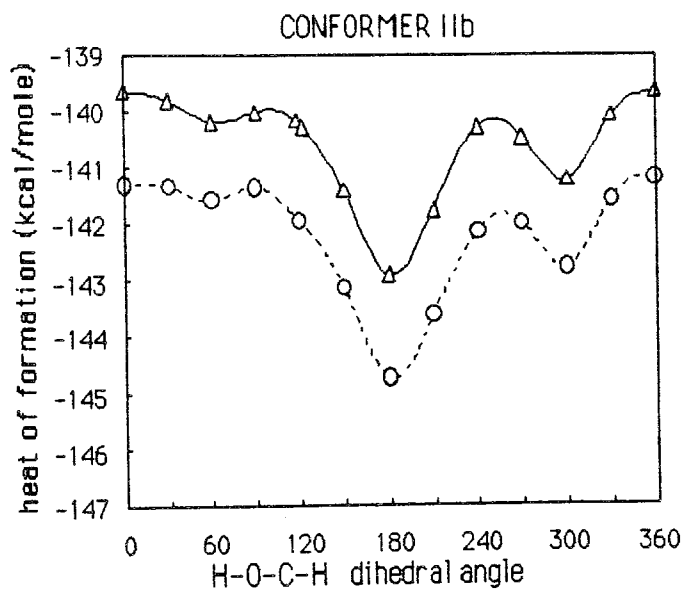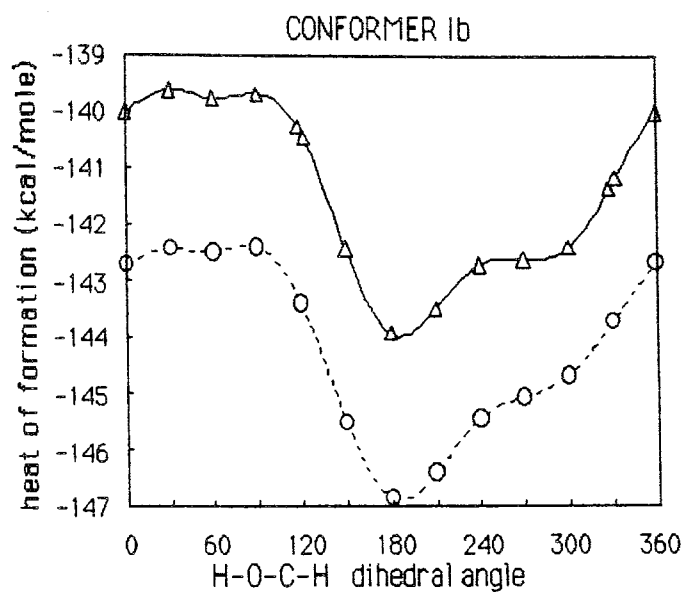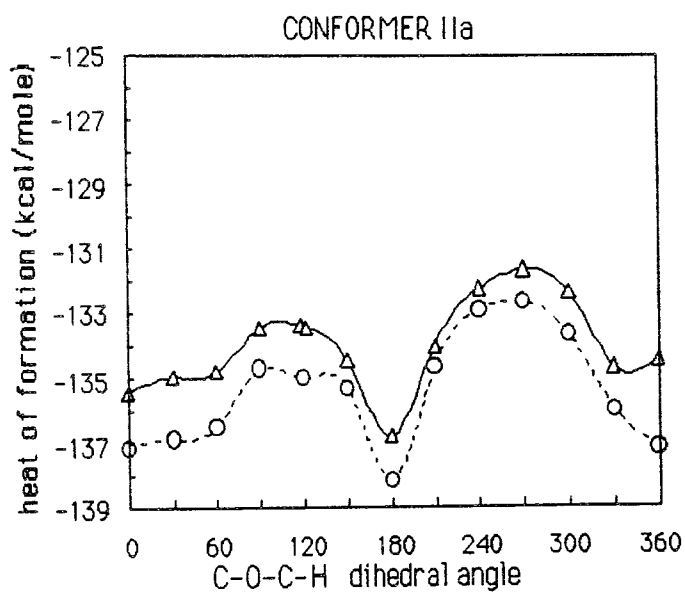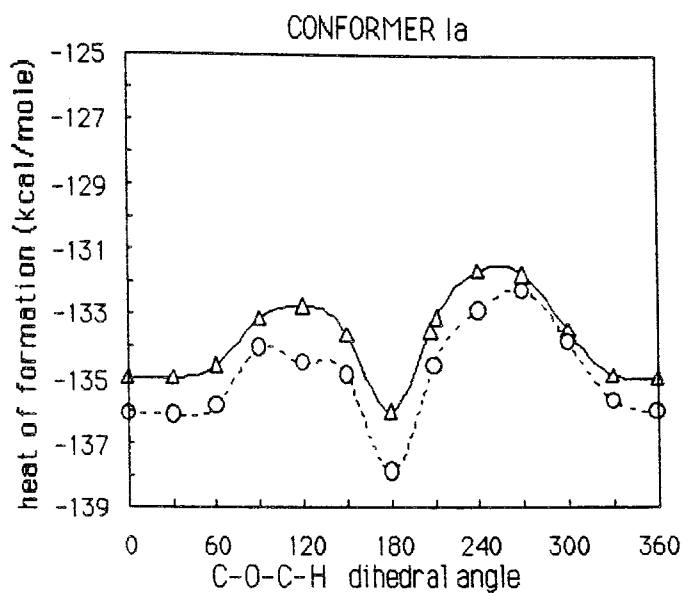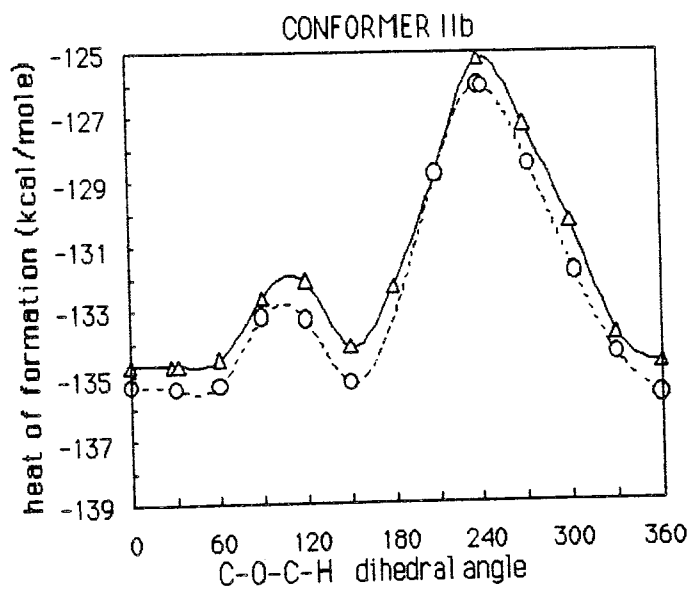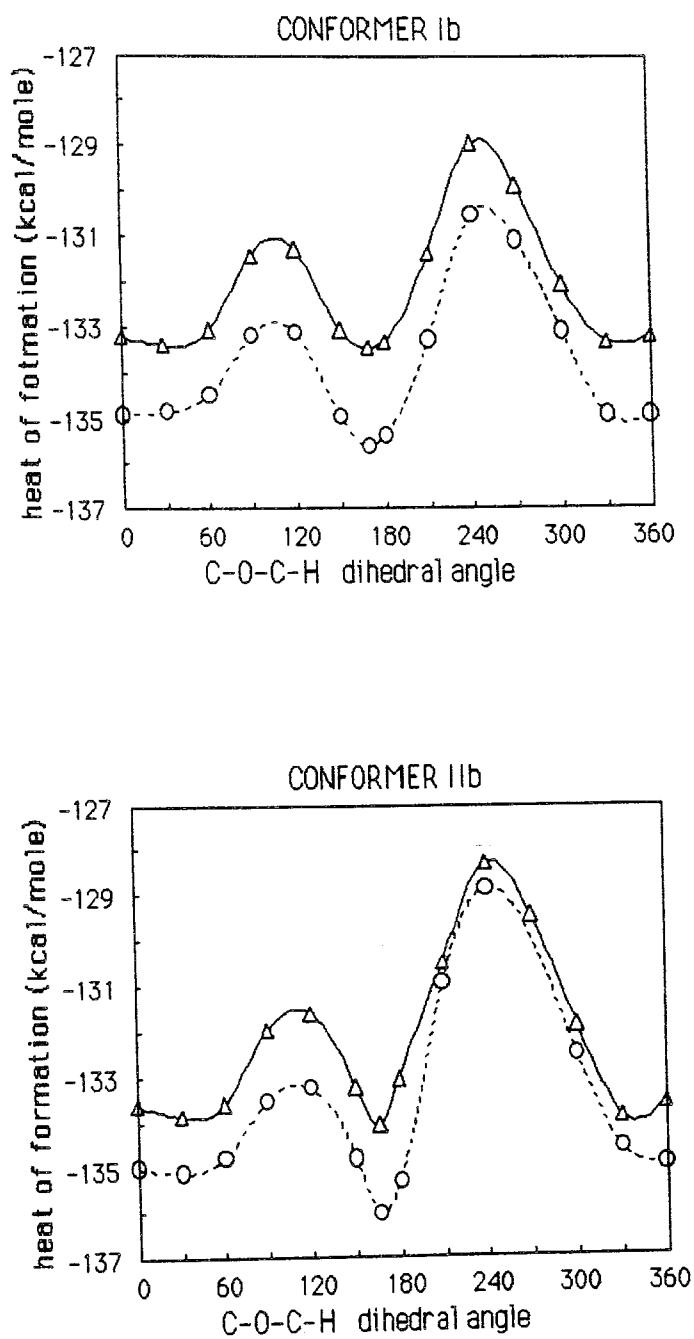
Figure 3.14. Potential scans of 2-OCH$_3$ cyclohexanone ethylene ketals for conformers Ib and IIb. ($\triangle$ in gas phase, o in acetonitrile)

3.4. RESULTS FOR 1,1,2-TRIHYDROXYETHANE

3.4.1. PM3 Calculations

First of all, semi-empirical PM3 calculations have been applied on 1,1,2-trihydroxyethane in gas phase using MOPAC 5.0.

1,1,2-trihydroxyethane has four rotatable bonds as shown in Figure 3.15. Therefore, its conformations can be described with four individual dihedral angles, each of which corresponds to a rotation about a single bond represented below:

C2-C3 bond	O8-C2-C3-O6 dihedral angle
C2-O8 bond	C3-C2-O8-H9 dihedral angle
C3-O4 bond	C2-C3-O4-H5 dihedral angle
C3-O6 bond	C2-C3-O6-H7 dihedral angle
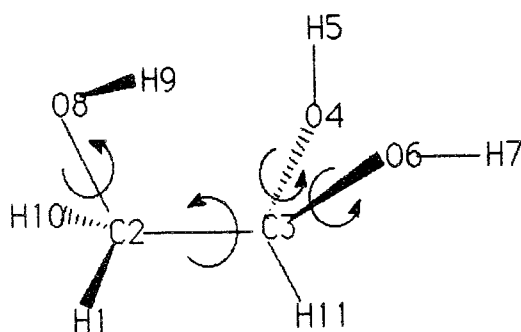
Figure 3.15. Four rotatable bonds in 1,1,2-trihydroxyethane.

In order to investigate all possible conformational minima, staggered configurations resulting from the rotation around C2-C3 and C2-O8 bonds have been considered. For each staggered configuration around C2-C3 and C2-O8 bonds, C3-O4 and C3-O6 bonds have been rotated together in a grid calculation. These possibilities are shown in Figure 3.16. Rotations have been done with 30° intervals of H7-O6-C3-C2 and H5-O4-C3-C2 torsional angles between 0° and 360°. C2-C3 and C2-O8 bonds have been fixed while all the
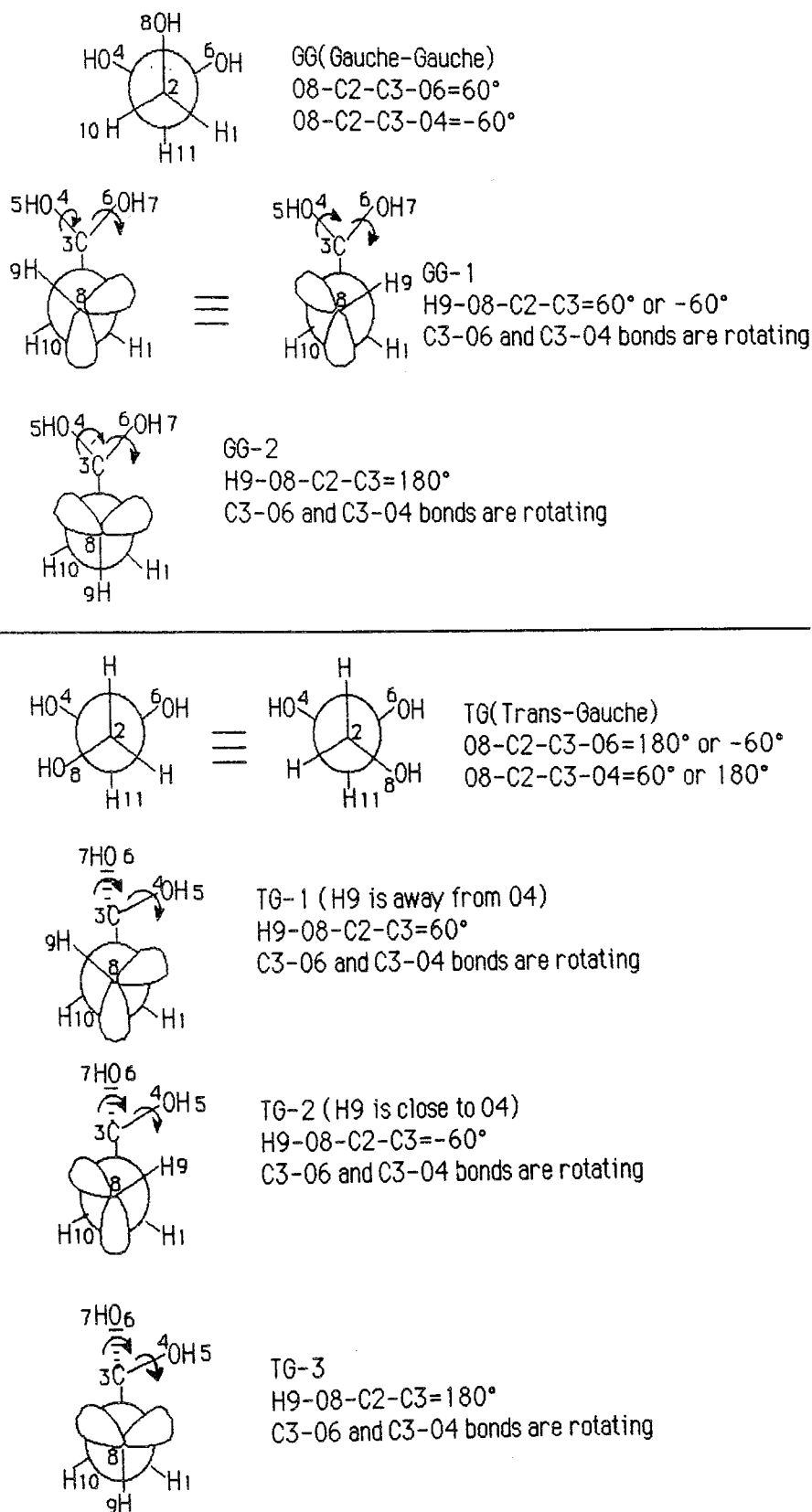
Figure 3.16. GG and TG structures of 1,1,2-trihydroxyethane.

other parameters are fully optimized. As a result, five contour maps were obtained and given in Figure 3.17-Figure 3.21, where horizontal axes represent the rotation around C3-O4 bond and the vertical axes represent the rotation around C3-O6 bond. Nine minima were obtained from contour maps. Force calculations gave positive frequencies for all nine structures after full geometry optimizations have been performed. The results obtained are given in Table 3.5.

Apart from the grid calculations corresponding to the staggered configurations shown in Figure 3.16., another configuration where C3-C2-O8-H9 angle is 0° and O8-C2-C3-O6 angle is 60° has been also applied to grid calculation. In the geometry described, intra-molecular H-bonding is checked since H9 is located in between O4 and O6. Although PM3 has predicted these geometries as minima, ab initio calculations have not located any one of them as stable geometries for all the model structures studied.

Table 3.5. The values of total energies, E_{total} (kcal/mol), relative energies, E_{rel} (kcal/mol), dipole moments, μ(Debye) of all conformers obtained from PM3 calculations.

		dihedral angles*	E_{total}	E_{rel}	μ
GG-1	A	(63°, -65°, 42°, 177°)	-27939.385	0.00	1.175
	B	(64°, -64°, -16°, -124°)	-27939.290	0.09	0.821
GG-2	C	(63°, 179°, 51°, -51°)	-27937.100	2.28	3.221
TG-1	D	(181°, 69°, -45°, -111°)	-27939.213	0.17	1.233
	E	(181°, 52°, 54°, 61°)	-27937.084	2.30	2.393
TG-2	F	(190°, -58°, 56°, 165°)	-27938.642	0.74	1.058
	G	(181°, -60°, 108°, 60°)	-27939.077	0.31	1.678
	H	(191°, -63°, 192°, -50°)	-27938.922	0.46	1.030
TG-3	I	(181°, 176°, -57°, -110°)	-27937.976	1.41	2.022

*are the following in the order written O8-C2-C3-O6, H9-O8-C2-C3, H5-O4-C3-C2, H7-O6-C3-C2
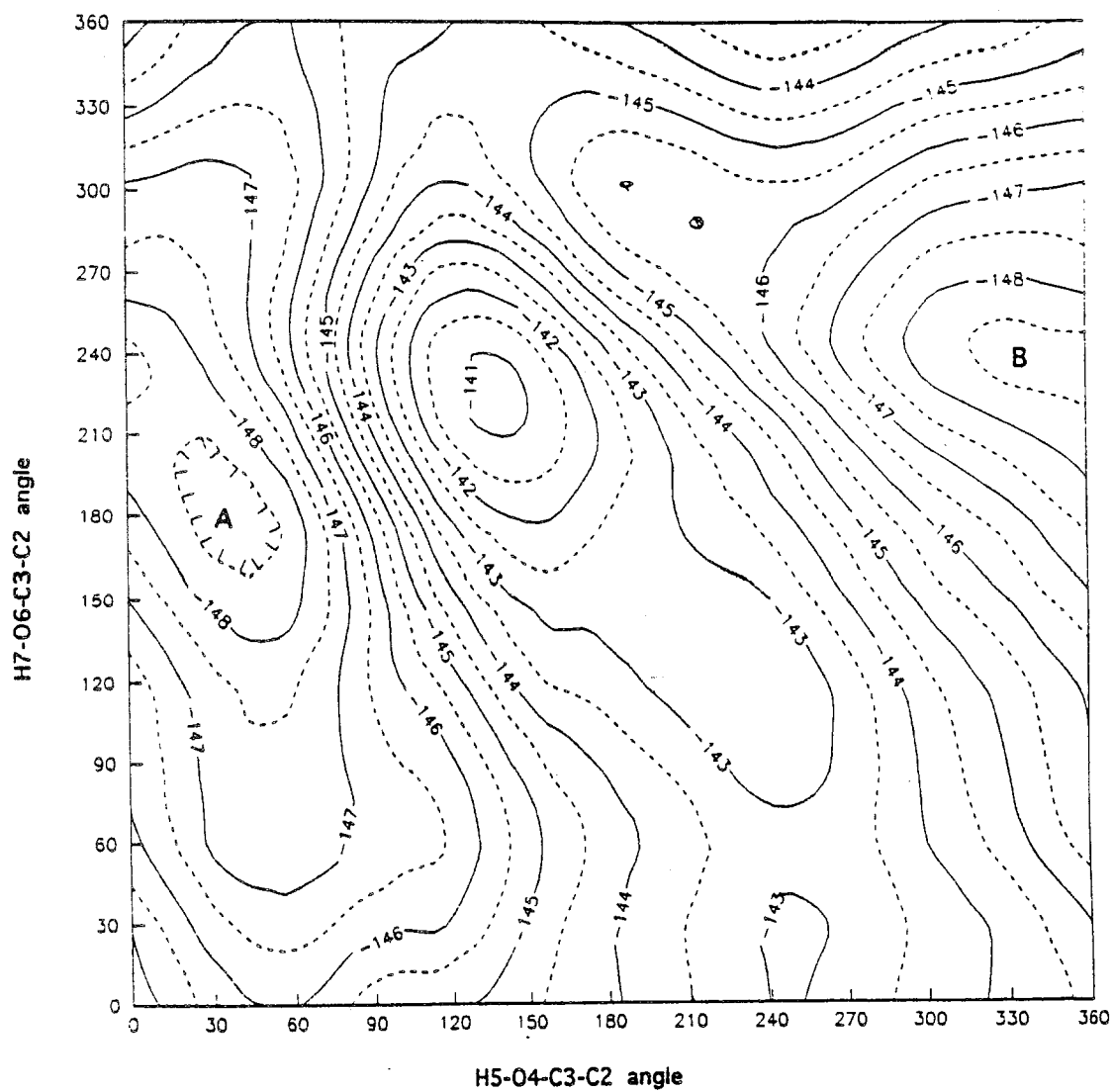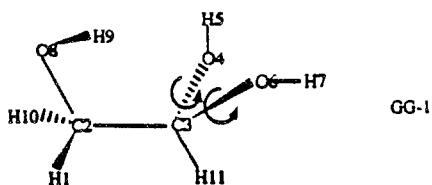
Figure 3.17. Contour map for GG-1
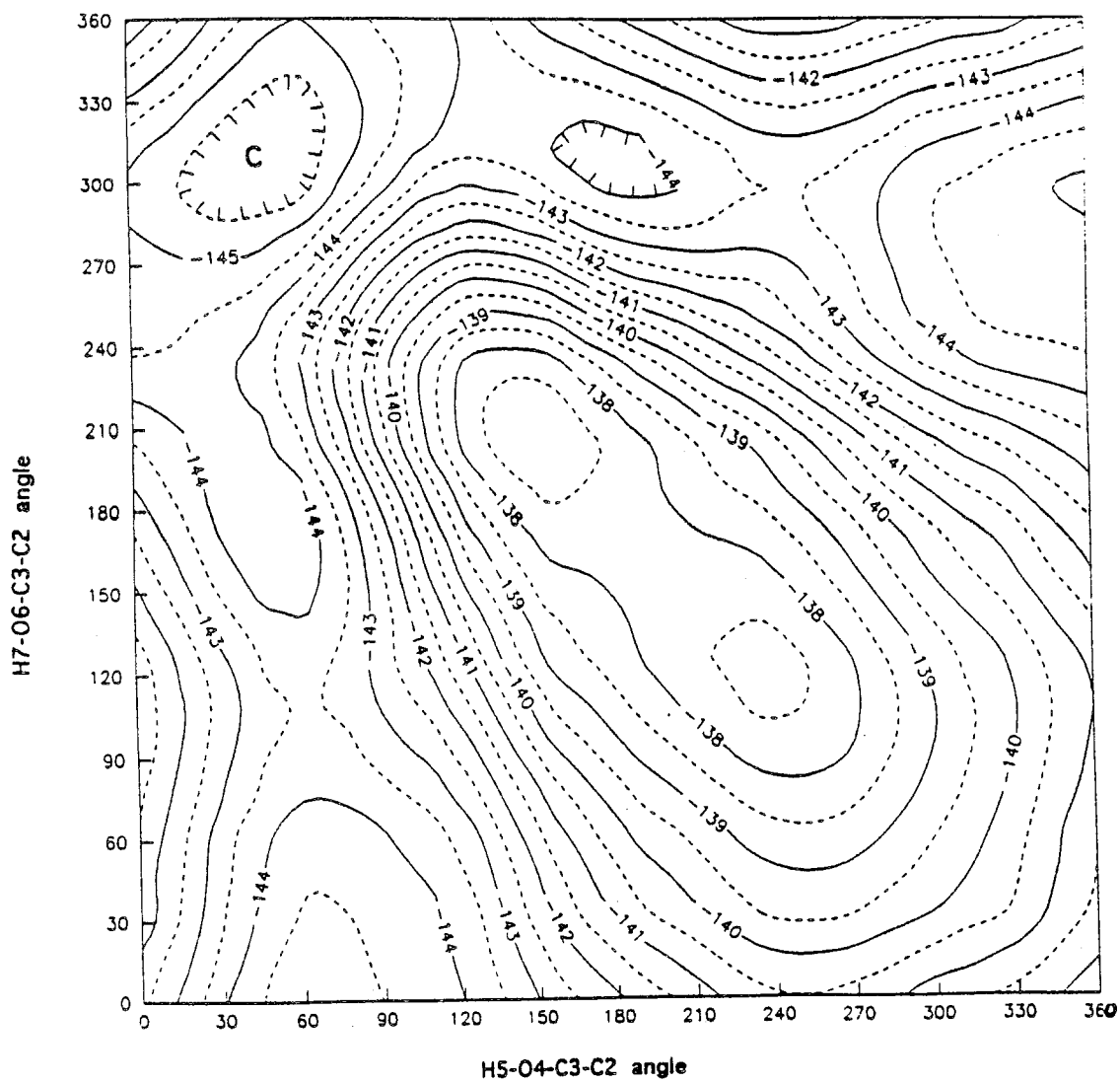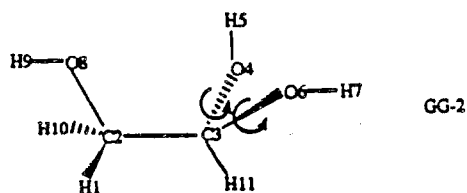
Figure 3.18. Contour map for GG-2
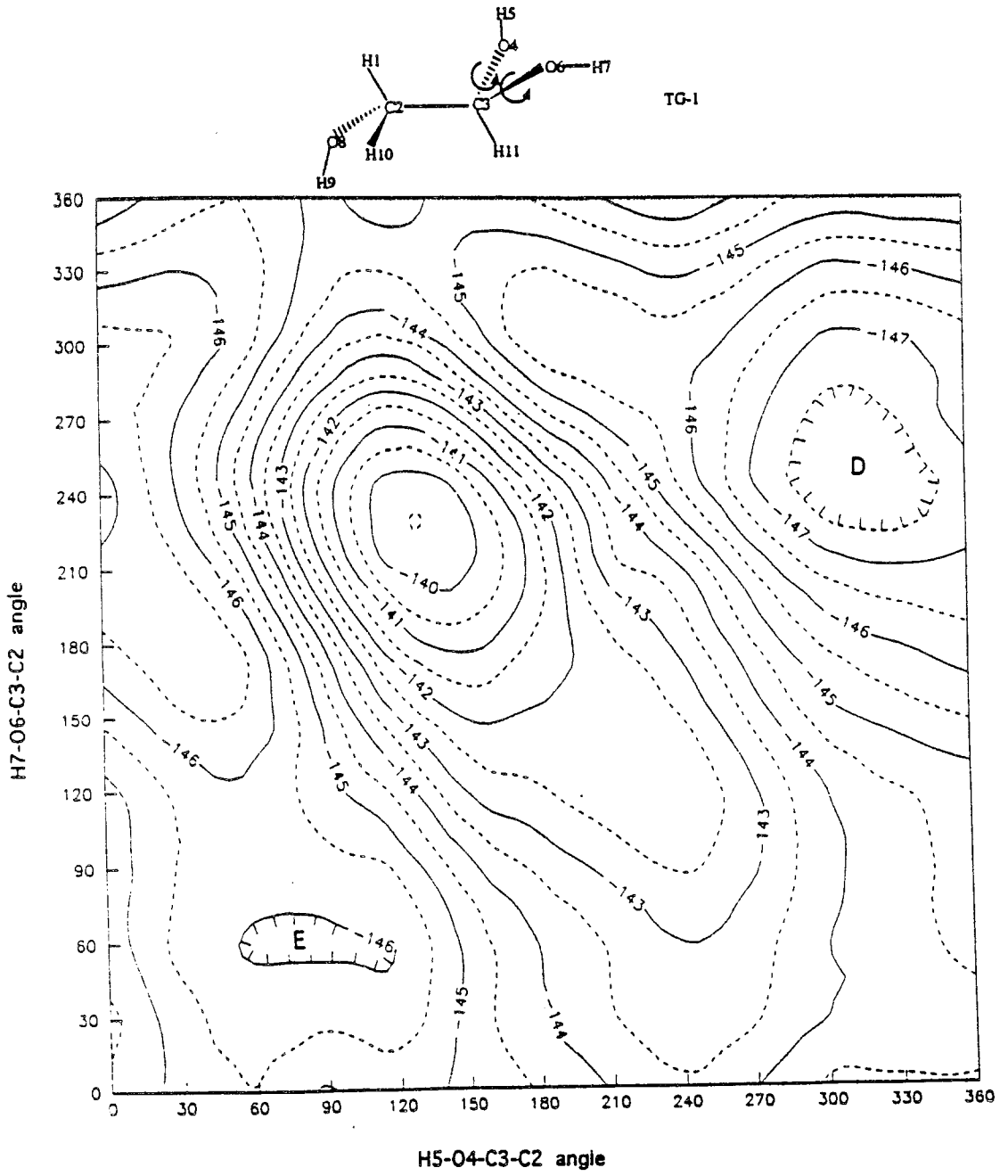
Figure 3.19. Contour map for TG-1
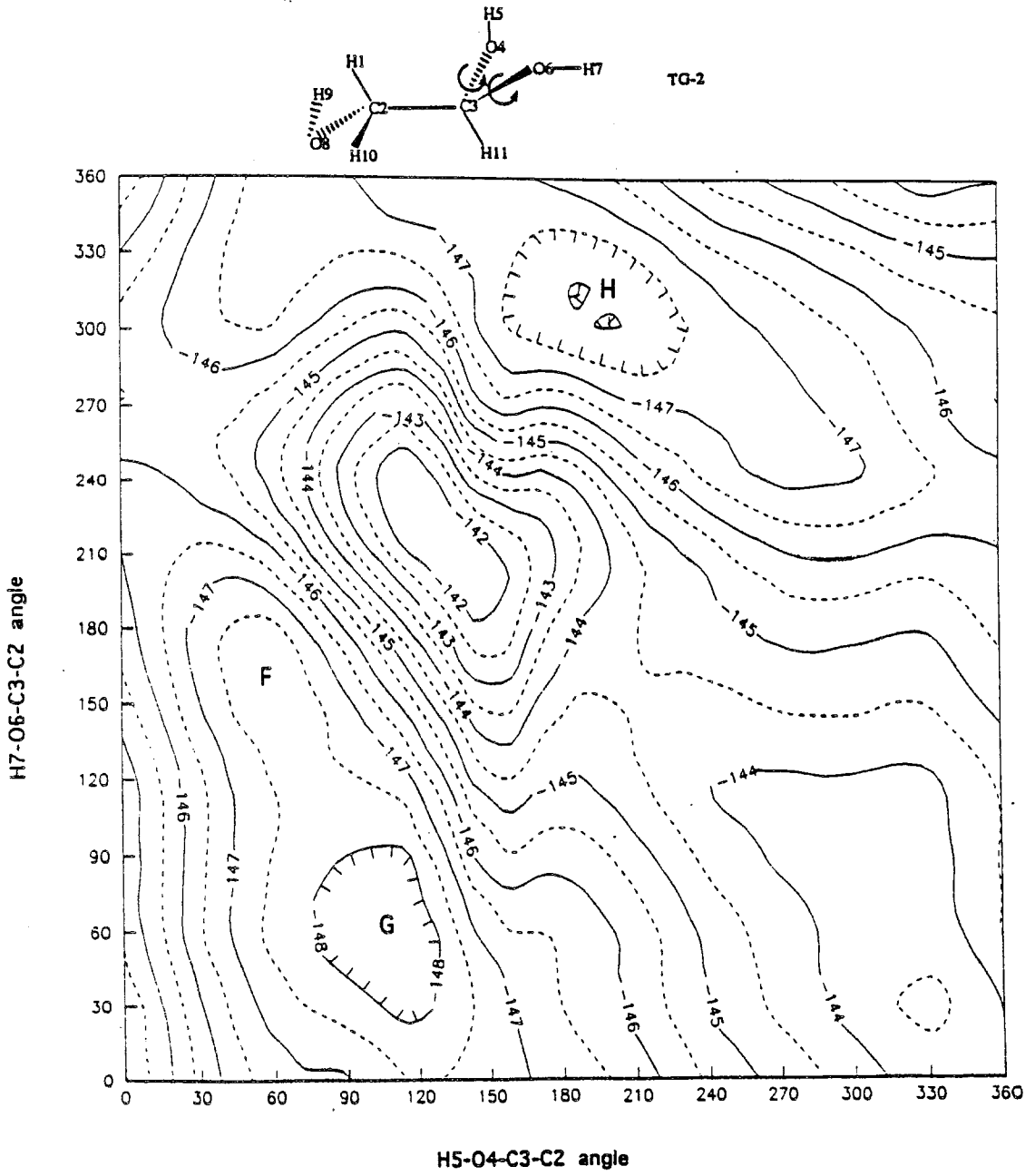
Figure 3.20. Contour map for TG-2
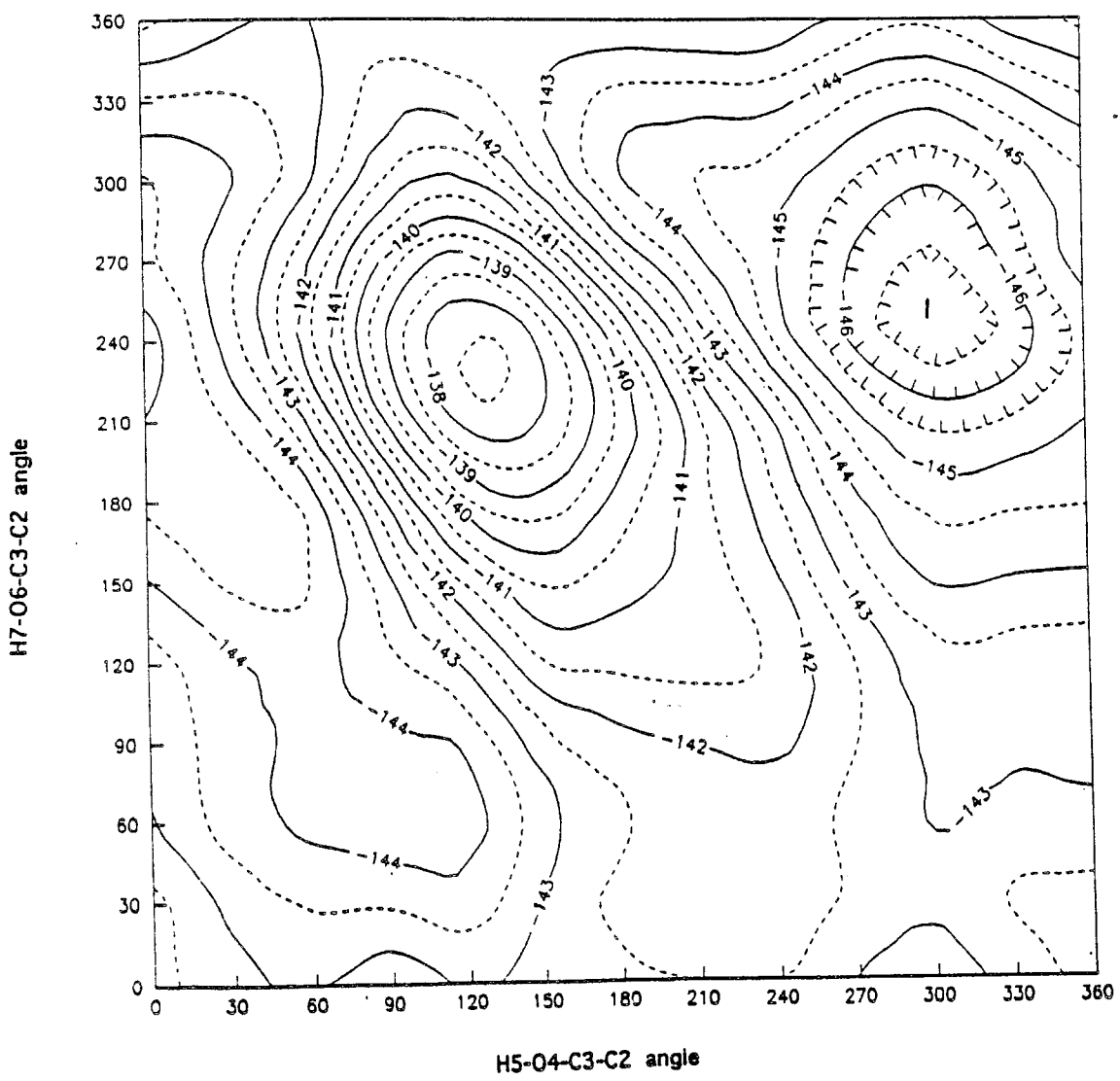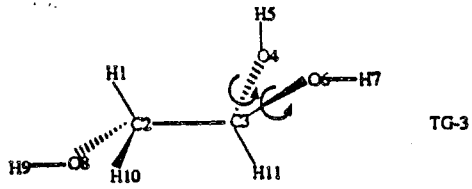
Figure 3.21. Contour map for TG-3

3.4.2. Ab Initio Calculations

Nine minima shown in Table 3.5 have been investigated with ab initio calculations. The optimized structures obtained from PM3 calculations have been used as starting geometries in RHF calculations using 6-31G basis set. Full geometry optimizations were carried out in Gaussian 92 (74). All the energy minima were further checked by force calculations. We also performed single point calculations on the optimized geometries obtained at 6-31G level, to examine the effects of electron correlation using Moller-Plesset perturbation theory at the second order (MP2) level, with the 6-31G** basis set. The results of ab initio work are given in Table 3.6. and Table 3.7.

Table 3.6. The values of total energies, E_{total}, relative energies, E_{rel}, (kcal/mol) and dipole moments, μ(Debye) of all conformers obtained from 6-31G calculations.

		dihedral angles*	E_{total}	E_{rel}	μ
GG-1	A	(64°, -68°, 40°, 188°)	-190555.8473	0.00	1.6402
	B	-	-	-	-
GG-2	C	(62°, 180°, 51°, -51°)	-190552.3295	3.52	4.6856
TG-1	D	-	-	-	-
	E	-	-	-	-
TG-2	F	(181°, -52°, 72°, 170°)	-190552.9109	2.94	2.5393
	G	(180°, -63°, 198°, 176°)	-190550.9803	4.87	3.9716
	H	(181°, -58°, 188°, -61°)	-190553.7763	2.07	2.3028
TG-3	I	(176°, 180°, -48°, -156°)	-190552.6062	3.24	2.1645

*are the following in the order written O8-C2-C3-O6, H9-O8-C2-C3, H5-O4-C3-C2, H7-O6-C3-C2

Table 3.7 . Energies, E_{total} and relative energies, E_{rel}, (kcal/mol) obtained from single point 6-31G**/MP2 calculations of trihydroxyethane.

	E_{total}		E_{rel}	
	6-31G**	MP2	6-31G**	MP2
A	-190647.4396	-191167.7843	0.00	0.00
C	-190644.1271	-191164.1577	3.31	3.63
F	-190645.2365	-191164.723	2.20	3.06
G	-190643.1207	-191162.4224	4.32	5.36
H	-190645.8716	-191165.4255	1.57	2.36
I	-190643.5531	-191162.1775	3.89	5.61

Solvent effect calculations have been performed on optimized structures obtained in the gas phase using both PM3 and ab initio method. Acetonitrile was selected as a solvent since it is used for cyclohexanone ethylene and propylene ketal derivatives. Solvent effect results are given in Table 3.8. Ab initio calculations do not locate B, D, and E as stable structures therefore, the values of these structures are not given in the table.

Table 3.8 . Solvation energies, E_{solv}, (kcal/mol), relative energies, E_{rel}, (kcal/mol) and dipole moments, μ, (debye) obtained from PM3 and 6-31G calculations of trihydroxyethane in CH_3CN.

	PM3			6-31G		
	E_{solv}	E_{rel}	μ	E_{solv}	E_{rel}	μ
A	-3.51	0.00	1.35	-9.242	0.00	1.921
B	-3.55	0.05	0.97	——	——	——
C	-4.99	0.81	3.63	-12.193	0.567	5.358
D	-3.66	0.02	1.49	——	——	——
E	-5.56	0.25	2.76	——	——	——
F	-3.97	0.28	1.22	-10.174	2.00	2.905
G	-3.54	0.28	1.97	-11.454	2.65	4.534
H	-3.84	0.13	1.21	-10.192	1.12	2.658
I	-3.25	1.67	2.27	-7.626	4.86	2.494
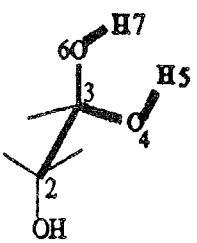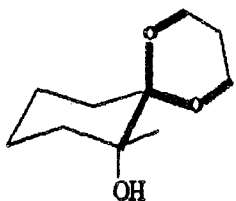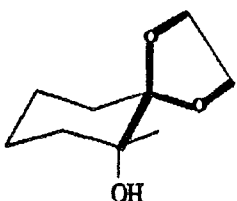
3.4.3. Modelling Cyclohexanone Ketal Derivatives
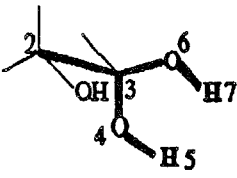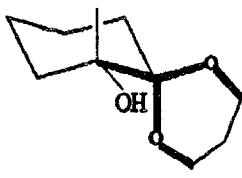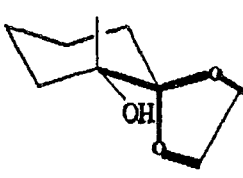
In order to make a good comparison between 2-OH cyclohexanone ketal derivatives and 1,1,2 trihydroxyethane, the contour maps in Figure 3.17-Figure 3.21 can be used. GG-1 and GG-2 maps correspond to equatorial -OH whereas TG-1, TG-2, and TG-3 correspond to axial -OH of the ketals. On these contour diagrams, we placed the dihedral angles of 2-hydroxy cyclohexanone

propylene and ethylene ketals corresponding to H5-O4-C3-C2 and H7-O6-C3-C2 angles of 1,1,2-trihydroxyethane shown in Table 3.9. The intersection point of the two dihedral angle gives us the energy level of that individual conformer (Figure 3.22.-Figure 3.26.)

The aim was to investigate these crossing points with ab initio calculations since they correspond to Ia, IIa, Ib, and IIb conformers of the ketal systems.

Table 3.9. C-O-C-C dihedral angles of 2-hydroxy cyclohexanone propylene and ethylene ketals corresponding to H7-O6-C3-C2 and H5-O4-C3-C2 dihedral angles of trihydroxyethane.

| | propylene ketal | | ethylene ketal | |
	Ia	IIa	Ia	IIa
H7-O6-C3-C2	189.3	294.2	224.8	263.8
H5-O4-C3-C2	169.9	64.3	133.8	97.8

| | propylene ketal | | ethylene ketal | |
	Ib	IIb	Ib	IIb
H7-O6-C3-C2	189.8	281.5	227.9	251.2
H5-O4-C3-C2	171.0	78.5	132.4	110.2

Figure 3.22. Contour map for GG-1
propylene ketal --> ●=Ib ◎=IIb
ethylene ketal --> ✳=Ib ❖=IIb
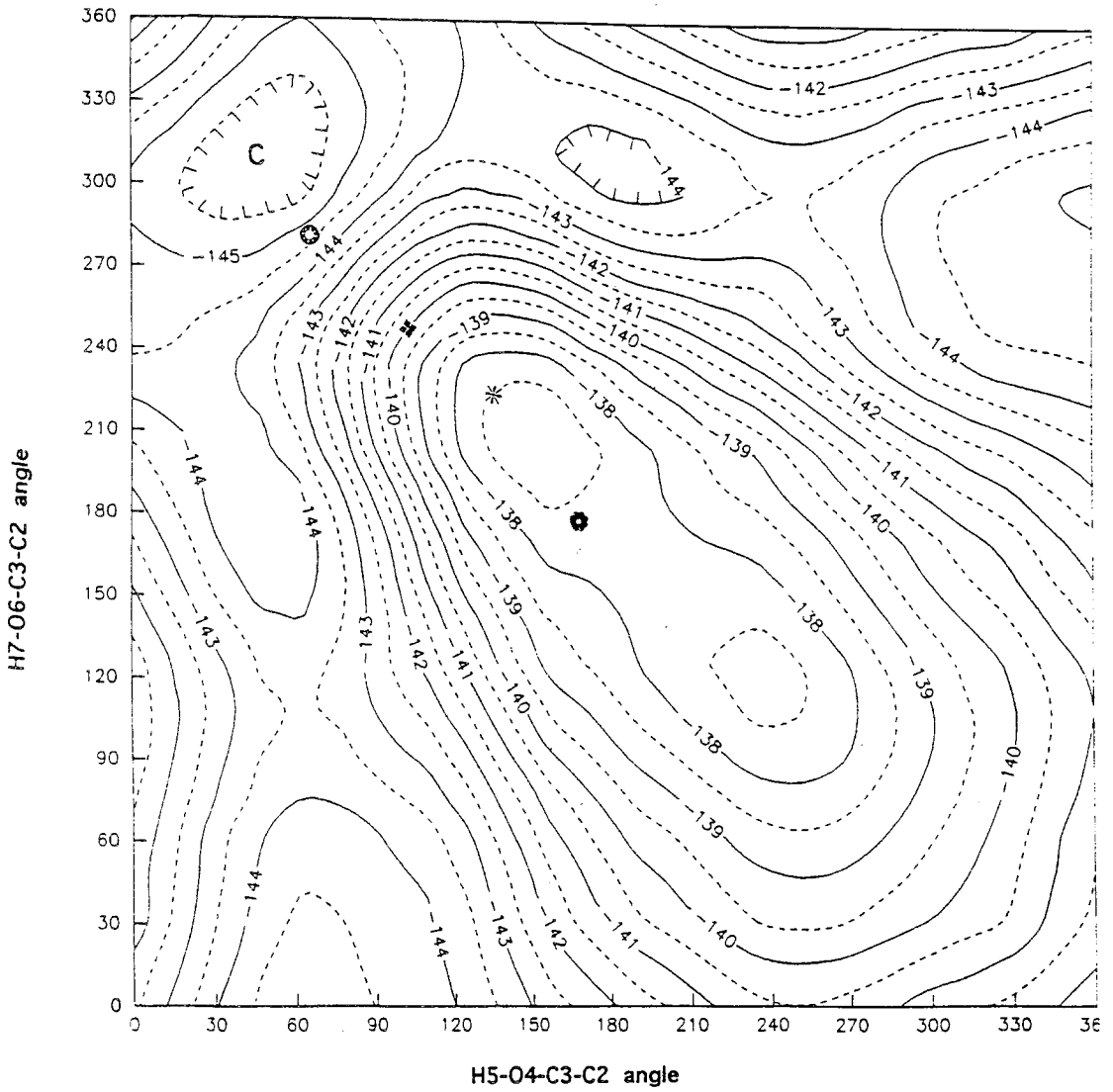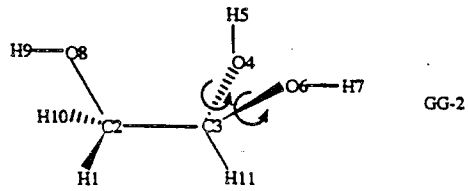
Figure 3.23. Contour map for GG-2
propylene ketal --> ●=Ib ◐=IIb
ethylene ketal   --> ✳=Ib ❖=IIb
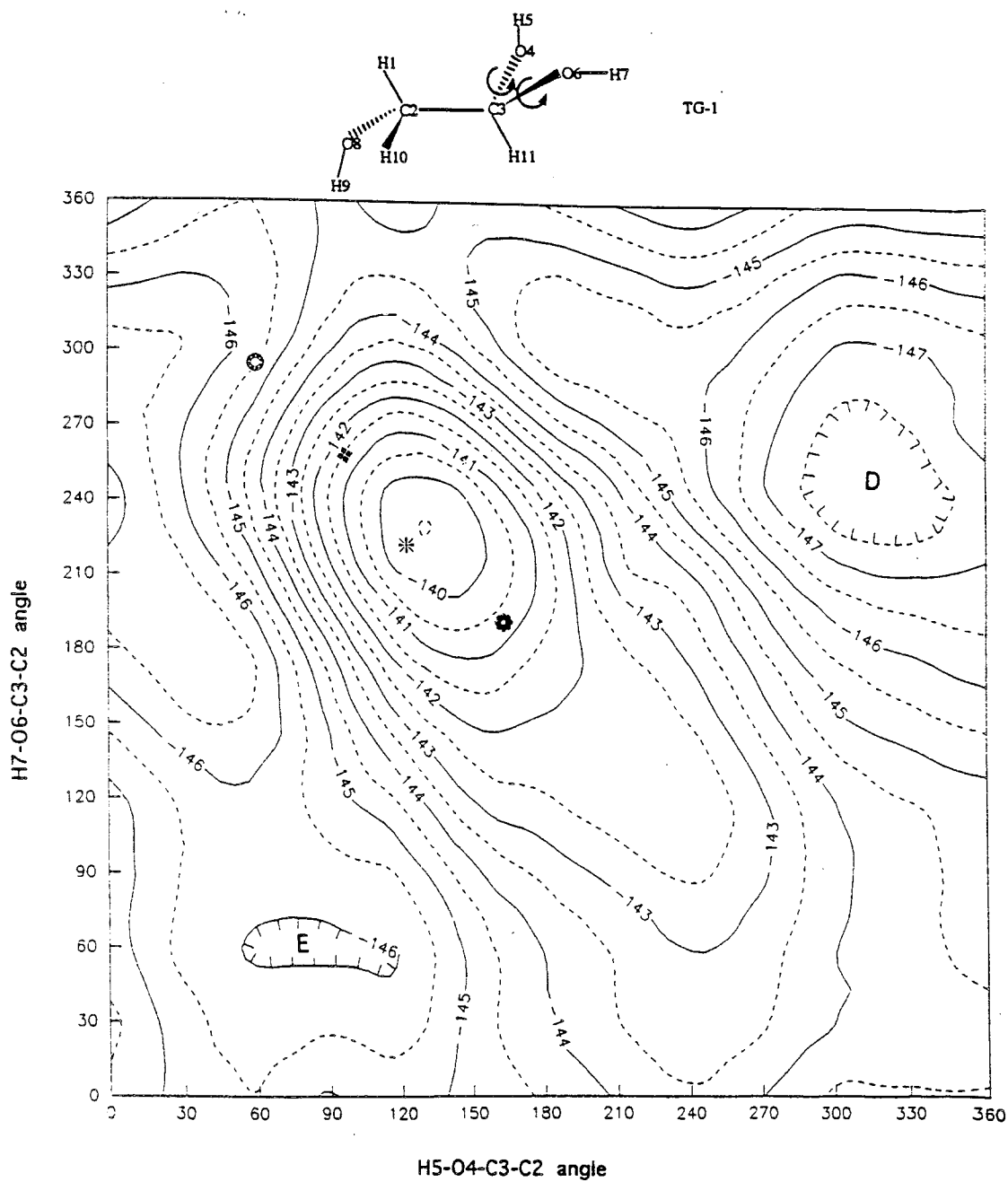
Figure 3.24. Contour map for TG-1
propylene ketal --> ⬤=Ia ◉=IIa
ethylene ketal   --> ✳=Ia ❖=IIa
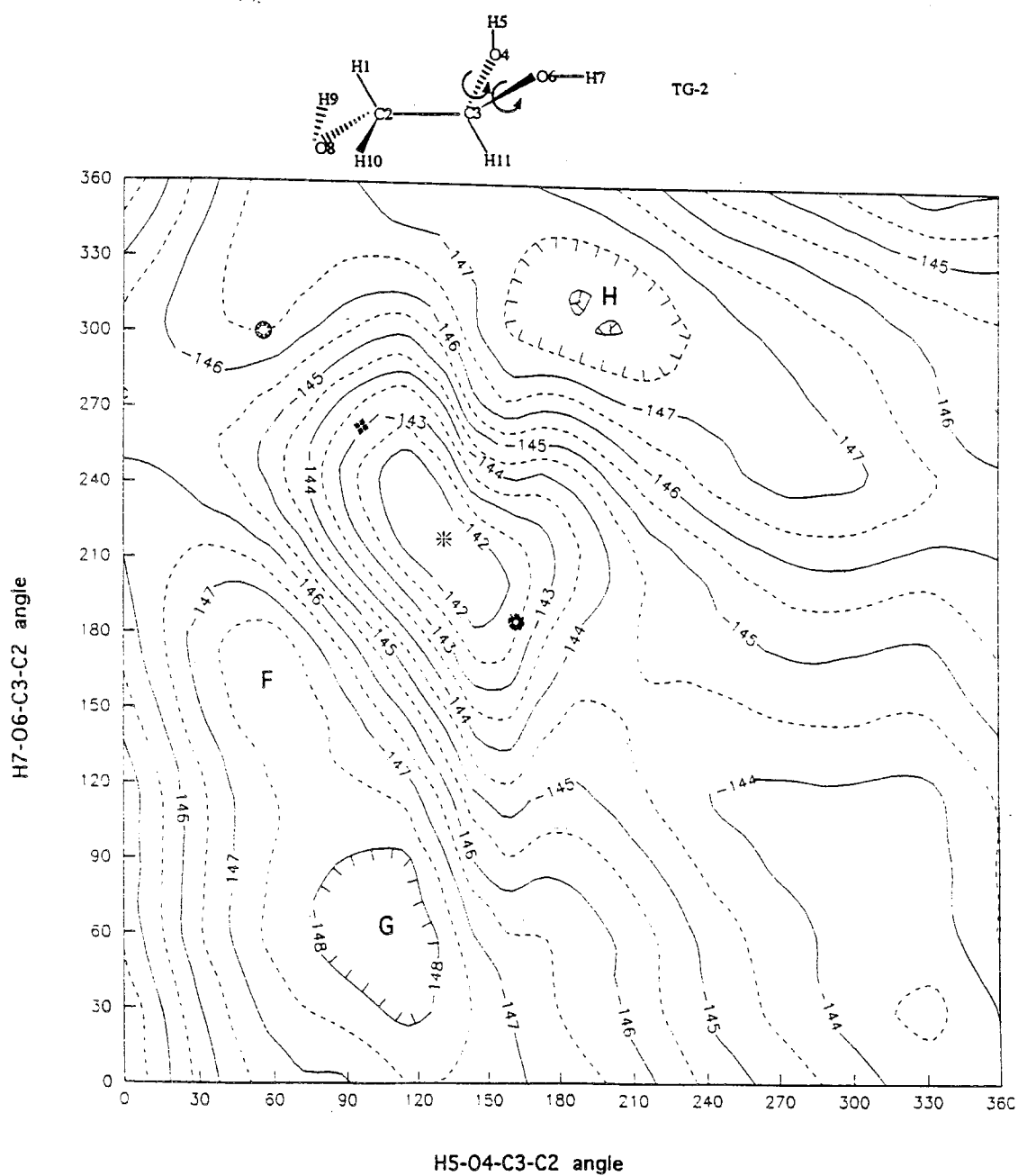
Figure 3.25. Contour map for TG-2
propylene ketal --> ❁=Ia ◉=IIa
ethylene ketal   --> ❋=Ia ❖=IIa
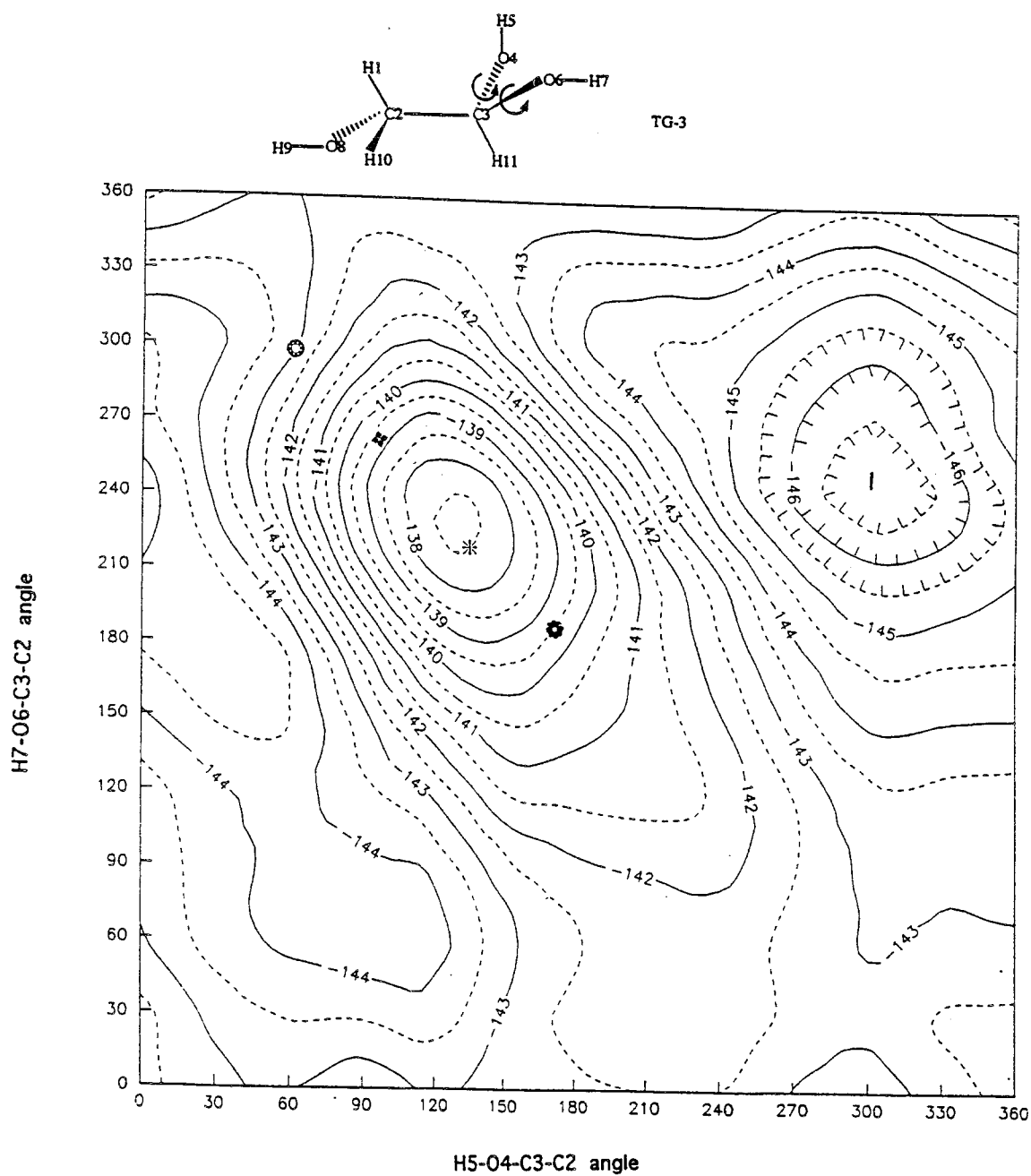
Figure 3.26. Contour map for TG-3
propylene ketal --> ✿=Ia ⊙=IIa
ethylene ketal   --> ✳=Ia ❖=IIa

We first performed PM3 calculations on 1,1,2-trihydroxyethane in order to locate these crossing points and obtain initial geometries for ab initio calculations. H5-O4-C3-C2 and H7-O6-C3-C2 angles were fixed at the corresponding angles of propylene and ethylene ketals where all the other parameters were optimized. To simplify and generalize the H5-O4-C3-C2 and H7-O6-C3-C2 angles we used the following values respectively:

To represent propylene ketal, anti conformers(Ia and Ib), 180°, -180°

To represent propylene ketal, syn conformers(IIa and IIb), 60°, -60°

To represent ethylene ketal, anti conformers(Ia and Ib), 135°, -135°

To represent ethylene ketal, syn conformers(IIa and IIb), 100°, -100°

The energies and the percentages obtained from ab initio calculations in gas phase and in acetonitrile are given in Table 3.10-Table 3.13. Some conformers that prove to be minima in PM3 method are not minima at 6-31G level.

Table 3.10. 6-31G energies in kcal/mol and percentages for the conformations of 1,1,2-trihydroxyethane corresponding to 2-OH cyclohexanone **propylene ketal** in **gas phase**.

axial	E(Ia)	%(Ia)	E(IIa)	%(IIa)
TG-1	–	–	–	–
TG-2	-190550.621	9.82	-190546.934	0.02
TG-3	–	–	-190543.646	0.00
% axial				
9.84				

equatorial	E(Ib)	%(Ib)	E(IIb)	%(IIb)
GG-1	-190547.240	0.03	–	–
GG-2	-190540.567	0.00	-190551.934	90.13
%eq				
90.16				

Table 3.11. 6-31G energies in kcal/mol and percentages for the conformations of 1,1,2-trihydroxyethane corresponding to 2-OH cyclohexanone **propylene ketal** in **acetonitrile**.

axial	E(Ia)	%(Ia)	E(IIa)	%(IIa)
TG-1	–	–	–	–
TG-2	-190556.104	6.24	-190553.594	0.09
TG-3	–	–	-190547.845	0.00
% axial				
6.33				

equatorial	E(Ib)	%(Ib)	E(IIb)	%(IIb)
GG-1	-190554.447	0.38	–	–
GG-2	-190548.806	0.00	-190557.706	93.29
%eq				
94.67				

Table 3.12. 6-31G energies in kcal/mol and percentages for the conformations of 1,1,2-trihydroxyethane corresponding to 2-OH cyclohexanone **ethylene ketal** in **gas phase**.

axial	E(Ia)	%(Ia)	E(IIa)	%(IIa)
TG-1	-190540.109	0.01	-190540.378	0.02
TG-2	-190545.156	54.71	-190544.748	27.46
TG-3	-	-	-190540.606	0.03
% axial				
82.23				

equatorial	E(Ib)	%(Ib)	E(IIb)	%(IIb)
GG-1	-190543.045	1.55	-190544.057	8.54
GG-2	-190539.265	0.00	-190543.994	7.68
%eq				
17.77				

Table 3.13. 6-31G energies in kcal/mol and percentages for the conformations of 1,1,2-trihydroxyethane corresponding to 2-OH cyclohexanone **ethylene ketal** in **acetonitrile**.

axial	E(Ia)	%(Ia)	E(IIa)	%(IIa)
TG-1	-190546.667	0.00	-190547.339	0.00
TG-2	-190550.053	0.00	-190550.581	0.00
TG-3	-	-	-190551.870	0.02
% axial				
0.02				

equatorial	E(Ib)	%(Ib)	E(IIb)	%(IIb)
GG-1	-190549.532	0.00	-190550.008	0.00
GG-2	-190545.839	0.00	-190556.924	99.98
%eq				
99.98				

4. DISCUSSION

4.1. GENERAL COMMENTS

The computed total and relative energies of cyclohexanone propylene and cyclohexanone ethylene ketal and their corresponding dipole moments in the gas phase are presented in Table 3.1.and Table 3.3. The total axial-conformer percentages, computed using a Boltzmann distribution (see appendix C) for the four conformers, are also given in Table 3.1 and Table 3.3. Table 3.1. shows that for propylene ketals, -F, -CN, $-NO_2$ and -OH substituents prefer the equatorial orientation but -Cl, $-CH_3$ and $-OCH_3$ substituents prefer the axial orientation in gas phase. In contrast, all ethylene ketal derivatives except $-OCH_3$ prefer the equatorial orientation of the substituent (Table 3.3).

The effect of the medium on conformational equilibria has been investigated in a non-polar solvent (CCl_4, ε = 2.24) and a polar solvent (CD_3CN, ε = 37.50) where ε represents the dielectric constant of the solvent. The solvation energies and the relative energies in solution are given in Table 3.2. and Table 3.4..

The common trend for all the propylene ketals studied, (except for the methyl derivative, which is not quite sensitive to the medium) is that as the dielectric constant of the medium increases, the computed axial percentage decreases, which is in agreement with the experimental data (Table 1.1.). The total % axial trends of ethylene ketal derivatives (Table 3.4.) are also

parallel to the experimental data (Table 1.1.) with the exception of the -OH derivative. For ethylene ketal derivatives, calculations of -F, -Cl, -CN and -OH substituted molecules show that the amount of the axial orientation increases with increase in the polarity of the solvent. On the other hand, -CH_3, -OCH_3 and -NO_2 derivatives show a trend in the opposite direction.

Careful analysis of the geometrical parameters for the optimized structures show that the geometries are in general not affected much by the solvent. However, it is possible to observe the effect of solvent by analyzing the electron distribution in these molecules. Table 4.1 and 4.2 give the electron population on atoms sensitive to solvent polarity. As expected, electron population on electronegative atoms increases in CD_3CN as compared to gas phase for all the molecules studied. This effect is more clearly observed in the case of -CN and -NO_2 derivatives since their dipole moments are much larger than the other derivatives (Table 3.1. and Table 3.3.).

Table 4.1. Atomic charges for the most stable axial (ax) and equatorial (eq) orientations of the 2- substituent in cyclohexanone **propylene ketals** in gas phase and in acetonitrile

Substituent	Atom	Gas Phase		CD_3CN	
		ax	eq	ax	eq
-H	O5	-0.27	-0.27	-0.28	-0.28
	O1	-0.28	-0.28	-0.29	-0.29
	H	+0.06	+0.06	+0.06	+0.06
-F	O5	-0.27	-0.26	-0.28	-0.27
	O1	-0.26	-0.27	-0.28	-0.28
	F	-0.14	-0.14	-0.16	-0.16
-Cl	O5	-0.27	-0.26	-0.27	-0.26
	O1	-0.27	-0.27	-0.28	-0.28
	Cl	-0.06	-0.04	-0.09	-0.08
-CN	O5	-0.27	-0.27	-0.28	-0.28
	O1	-0.27	-0.28	-0.29	-0.29
	C	-0.14	-0.13	+0.01	+0.04
	N	-0.07	-0.07	-0.26	-0.29
$-CH_3$	O5	-0.27	-0.26	-0.28	-0.27
	O1	-0.27	-0.28	-0.29	-0.29
$-NO_2$	O5	-0.27	-0.26	-0.28	-0.28
	O1	-0.29	-0.28	-0.31	-0.30
	N	+1.24	+1.24	+1.27	+1.28
	O	-0.58	-0.57	-0.58	-0.60
	O	-0.58	-0.59	-0.66	-0.65
$-OCH_3$	O5	-0.27	-0.27	-0.28	-0.27
	O1	-0.27	-0.27	-0.28	-0.28
	O	-0.25	-0.25	-0.26	-0.27
	C	+0.03	+0.04	+0.03	+0.05
-OH	O5	-0.27	-0.28	-0.28	-0.28
	O1	-0.27	-0.26	-0.28	-0.28
	O	-0.30	-0.30	-0.33	-0.33
	H	+0.19	+0.19	+0.20	+0.21

Table 4.2. Atomic charges for the most stable axial (ax) and equatorial (eq) orientations of the 2- substituent in cyclohexanone **ethylene ketals** in gas phase and in acetonitrile

Substituent	Atom	Gas Phase		CD_3CN	
		ax	eq	ax	eq
-H	O4	-0.28	-0.28	-0.28	-0.28
	O1	-0.28	-0.28	-0.30	-0.30
	H	+0.06	+0.06	+0.06	+0.06
-F	O4	-0.27	-0.27	-0.28	-0.28
	O1	-0.27	-0.27	-0.29	-0.29
	F	-0.14	-0.15	-0.16	-0.16
-Cl	O4	-0.28	-0.27	-0.28	-0.28
	O1	-0.27	-0.28	-0.29	-0.29
	Cl	-0.05	-0.07	-0.09	-0.08
-CN	O4	-0.28	-0.27	-0.28	-0.28
	O1	-0.28	-0.28	-0.30	-0.29
	C	-0.14	-0.14	+0.05	+0.02
	N	-0.07	-0.07	-0.29	-0.24
-CH_3	O4	-0.28	-0.28	-0.29	-0.28
	O1	-0.28	-0.29	-0.29	-0.30
-NO_2	O4	-0.27	-0.27	-0.28	-0.29
	O1	-0.28	-0.29	-0.31	-0.30
	N	+1.24	+1.24	+1.27	+1.27
	O	-0.59	-0.59	-0.59	-0.66
	O	-0.58	-0.58	-0.65	-0.59
-OCH_3	O4	-0.28	-0.28	-0.28	-0.28
	O1	-0.27	-0.28	-0.28	-0.29
	O	-0.25	-0.25	-0.26	-0.27
	C	+0.03	+0.03	+0.03	+0.04
-OH	O4	-0.28	-0.28	-0.28	-0.29
	O1	-0.27	-0.28	-0.29	-0.29
	O	-0.30	-0.30	-0.33	-0.33
	H	+0.19	+0.19	+0.20	+0.21

4.2. 2-SUBSTITUTED CYCLOHEXANONE PROPYLENE KETALS

The calculations have been performed both in gas phase and in solvated medium as described in section 3. The results are discussed below in detail

4.2.1. Gaseous Phase

On the basis of steric effects only, one could expect the conformation with axial substituent to be the most stable since the dioxane moiety and the substituent are closer when the latter occupies the equatorial position. Results illustrate that (Table 3.1) the substituent prefers axial orientation when the dioxane ring is syn. When the dioxane ring adopts "anti" form, the substituent favors equatorial position (except for -Cl and -OCH$_3$). This trend is observed on comparison of Ia & Ib's, IIa &IIb's, Ia & IIa's, and Ib & IIb's. At the PM3 level, the anti equatorial orientation, Ib, is preferred for the -F, -CN, -OH and -NO$_2$ substituents whereas the axial orientation is preferred by -CH$_3$ syn, -OCH$_3$ syn and and by -Cl anti derivatives respectively. It is clear that the preference for the axial or the equatorial position depends on the nature of the substituent as well as the orientation of the dioxane ring. This indicates that other important factors have to be considered.

Electrostatic interactions between the substituent and the oxygens of the dioxane moiety may be responsible for the equatorial preference of -CN, and -NO$_2$. The charges in gas phase and in acetonitrile for these substituents are given in Table 4.1. and Figure 4.1 illustrates the electrostatic interaction for the -NO$_2$ derivative. In equatorial orientation, the positively charged nitrogen atom is close to two negatively charged oxygens O1 and O5 of dioxane ring. The calculated inter-atomic distances for Ib, the most stable equatorial orientation, are N-O1=2.9 A° and N-O5=2.9 A°. For the most stable axial orientation, Ia, the same distances have been calculated as 2.8 A° and 3.8 A° respectively, which indicates that axial -NO$_2$ may have electrostatic attraction with only one oxygen, O1. The calculated inter-atomic distances

for -CN-substituted propylene ketal are N-O1=2.9 A° and N-O5=2.8 A° for Ib, and 2.8 A° and 3.7 A° for Ia, showing a parallel behaviour with the -NO$_2$ substituent.
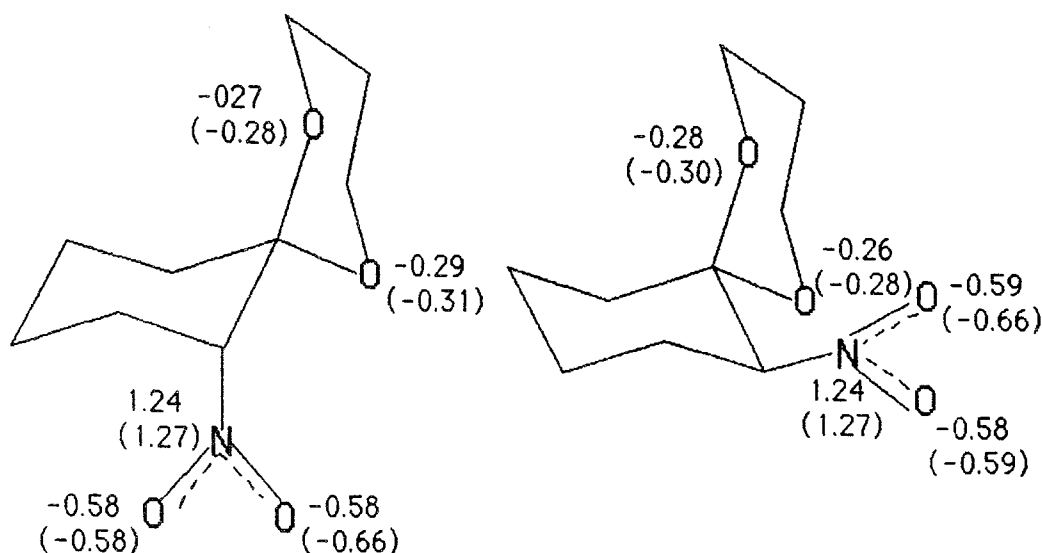
Figure 4.1. Atomic charges for 2-NO$_2$ propylene ketals in axial and equatorial orientations. The values in paranthesis represent the charges in acetonitrile.

The fluorine derivative is observed to behave in the opposite direction to that of the chlorine derivative. The unusual behaviour of fluorine with respect to the other halogen derivatives in the conformational equilibria of fluorocyclohexane derivatives (9, 27), 1,2-difluoroethane (33-35) and 5-fluoro-1,3-dioxane (42) has been observed. These results have been attributed to the attractive gauche effect and the interpretation is based on the small size of fluorine and/or lone pair interactions (104, 105).

Finally, for the hydroxyl substituent, the equatorial preference may be explained through weak O-H--O interactions since in the equatorial conformation the optimized geometry shows that the hydrogen atom of the hydroxyl is pointing towards one of the oxygens in the dioxane ring with an O--H distance of 2.48 Å (Table 4.3). Only the most stable axial and equatorial

orientations, IIa and Ib, of -OH group are given in the Table 4.3.

Table 4.3. Interatomic distances (A°) between hydrogen atom of -OH and the oxygens of dioxane ring in 2-OH **propylene ketal**.

	axial	equatorial
H-05	3.93	2.48
H-01	2.93	3.09

In general, for the propylene ketal derivatives considered, the anti conformations are more favorable than the syn conformations. This is not surprising since anti conformations are sterically less hindered than syn conformations. The steric repulsion in conformer IIb between the substituent and the two axial H atoms of dioxane ring is schematized in Figure 4.2 (IIb-syn) and in Table 4.6. X-H distances are given for reasonably uncrowded substituents.

The preference of the axial or equatorial substituents for the anti dioxane ring depends basically on the balance between the steric effects and the electrostatic repulsive forces between the dipole moments situated at the dioxane ring and C-X bond. This is illustrated for the Ib and IIb propylene ketal conformers in Figure 4.2. The dipoles are more or less parallel in the anti conformation leading to a destabilizing electrostatic interaction for the isolated species. On the other hand, this conformation is free from X--H repulsions present in syn conformation. From the results in Table 3.1 one may conclude that steric effects are the main factors in determining the syn or anti conformation for the equatorial conformers since, in all cases, Ib is substantially more stable than IIb in spite of its large dipole moment. However, for the axial conformers, where the steric interactions between the substituent and the dioxane ring are less important, electrostatic effects

play a role which is probably at the origin of the larger stability of IIa, with respect to Ia as predicted for the -OH and -OCH$_3$ derivatives.

Ib-anti
larger μ
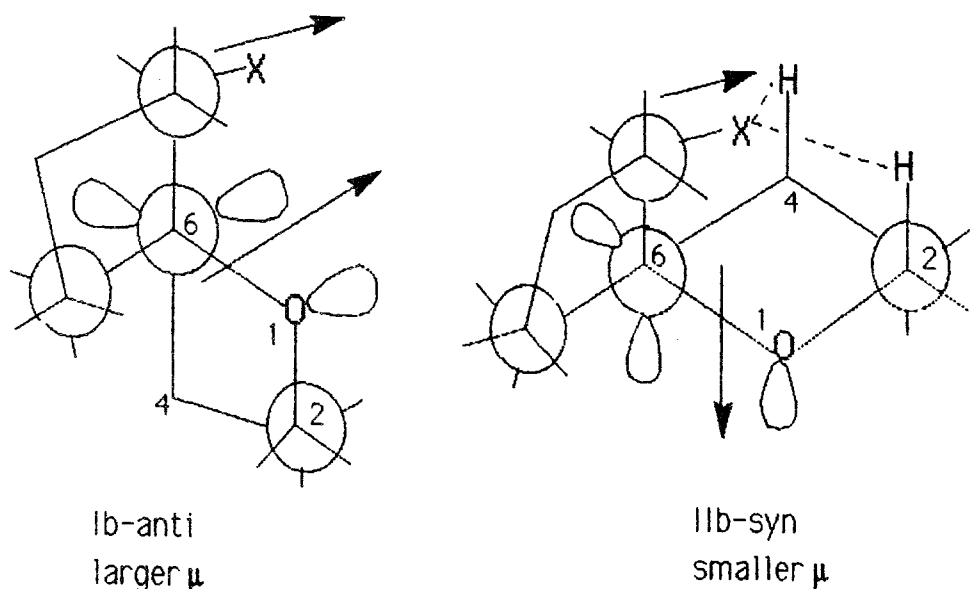
IIb-syn
smaller μ

Figure 4.2. Newman projection through C6-O5 bond for propylene ketal derivatives. (Arrows show the direction of dipoles. X--H repulsions in IIb-syn are also illustrated.)

-CH$_3$ group, which is nonpolar, exhibits almost equal axial/equatorial percentage composition. Detailed examination shows axial preference for syn dioxane fragment and a shift to equatorial orientation when dioxane moiety is anti.

For X=-NO$_2$, -OH, -OCH$_3$, contributions of stable rotamers to the total energy may be important. Therefore, rotation around C-X bond has been studied as described in section 3.1. Energy change through rotation of the substituent for -NO$_2$, -OH, -OCH$_3$ derivatives may be interpreted in general due to steric and electronic interactions between the substituent and the dioxane ring.

For -NO$_2$, we found that there is only one minimum for a geometry in which the H-C-N plane and the -NO$_2$ group are nearly coplanar and only one

maximum at 90° O-N-C-H dihedral angle. The barrier of rotation varies from 2 kcal/mol (for Ib and IIb) to 4.2 kcal/mol (for Ia) (Figure 3.3-Figure 3.4.).

Though the 0° and 180° dihedral angles are the same for $-NO_2$ substituent due to its planar symmetry, the situation is different for -OH and $-OCH_3$ substituents. Between the region 0°-180° dihedral angle, these substituents are close to the cyclohexane ring whereas in the region 180°-360° they are close to the dioxane ring.

In the case of -OH, the computed potential energy curves are represented in Figure 3.5-Figure 3.6. The absolute minimum is also a coplanar structure in which the H-C-O-H angle is close to 180°. The energy barriers are 3.5 kcal/mole (Ia and IIb) and 4.5 kcal/mole (Ib and IIa). Local minima have been also found for angles close to 300° and 60° for all 4 conformations. The three minima around 60°, 180°, and 300° correspond to the staggered configurations of the -OH group and the maxima around 0°, 120°, and 240° are the eclipsed configurations. The energy difference between the rotamers is not very large (about 1.5 kcal/mole).

Finally, for $-OCH_3$, we found two rotamers for each conformation at H-C-O-C angles 174° and -16°, 180° and -5°, 174° and -21°, 150° and 9° for Ia, IIa, Ib, IIb respectively (Figures 3.7-3.8.). Here, the energy differences between the rotamers are smaller (1 or <1 kcal/mole) than in -OH derivative results. It seems that, in 2-OCH_3 cyclohexanone propylene ketal which has a bulky substituent, steric factors affect the shape of potential energy curves especially in conformer IIb which suffers from strong X--H repulsions as illustrated in Figure 4.2 (IIb-syn). In parallel to this, the absolute minima correspond to H-C-O-C ~180° in the case of Ia, IIa and Ib but 9° in the case of IIb. The highest rotational energy barriers are around 4 kcal/mol for Ia, IIa, and Ib, but in IIb the barrier is 9 kcal/mole at 240° C-O-C-H dihedral angle. This is not surprising since at 240° the $-OCH_3$ group stays in its closest proximity to the axial hydrogens in the dioxane fragment, which destabilizes this rotamer to a larger extent than the ones in the other conformers.

4.2.2. In Solution

Generally the anti structures Ia and Ib are more stable than the syn structures IIa and IIb for propylene ketals in the gas phase. Among the anti structures, the equatorial conformer Ib exhibits the highest solvation energy (Table 3.2). Only for the -OH and -OCH$_3$ derivative the solvation energy of Ia in acetonitrile is greater than that for Ib. Although the syn structure is preferred in the axial conformation in the gas phase, the anti structure is expected to be more stable in polar solvents, since the dipole moment of anti conformations are larger than syn conformations.

The solvation energy is in general larger for the most polar conformations although there are some exceptions which are due to the fact that multipole contributions are substantial in many cases. The molecules considered may be divided in three categories according to the effect that the solvent has on their relative conformational energies.

The first group corresponds to those systems in which the substituent X has a dipole moment contribution along the C-X bond (-F, -Cl, -CN, -NO$_2$). In that case, the anti equatorial conformations Ib have always the largest total dipole moment since the C-X dipole adds to the dioxane ring dipole. The solvent stabilizes these conformations to a larger extent so that in a medium polar solvent, such as acetonitrile, they become the most stable.

The -OH and -OCH$_3$ substituted molecules represent another group: Here, the situation is different since the oxygen lone pairs of the substituent contributes to the C-X dipole moment so that its direction is not along the C-X bond. Besides, they may have several stable rotamers with close energies, the stability of which may be substantially modified through the effect of the environment. The total dipole moment is obviously quite dependent on the rotation angle. However, the rotamer study in acetonitrile showed that the locations of the minima do not change upon rotation of the substituent around C-X bond. The dipole moments of the most stable rotamer for the conformers Ia and Ib are close and larger than the ones for the

conformers IIa and IIb (Table 3.1). Therefore, the solvation energies of Ia and Ib are also larger than in IIa and IIb. This is also observed from the potential energy curves in acetonitrile for Ia and Ib. They lie in lower enrgies than IIa and IIb with respect to the gas phase curves.

Finally, the $-CH_3$ derivative which contains a nonpolar substituent may be considered. Since in this case the C-X dipole is small, the total molecular dipole moment does not change much (Table 3.1) with conformation and therefore, the solvent effect on the conformational equilibrium is small as expected.

4.3. 2-SUBSTITUTED CYCLOHEXANONE ETHYLENE KETALS

4.3.1. Gaseous Phase

Before studying the 2-substituted cyclohexanone ethylene ketals, a structural investigation of dioxolane ring has been performed as described in section 3. The structural parameters of minimum energy conformation of cyclohexanone ethylene ketal are given in Table 4.4. The values indicate an envelope form described in literature (see section 1).

Table 4.4. Structural parameters of dioxolane fragment in cyclohexanone ethylene ketal.

bond length (A°)		bond angle(°)		dihedral angle(°)	
O4-C5	1.43	O1-C5-O4	105.50	O1-C5-O4-C3	-19.53
O1-C5	1.44	C3-O4-C5	109.89	O4-C5-O1-C2	18.21
C3-O4	1.42	C2-O1-C5	110.02	C2-C3-O4-C5	13.34
C2-O1	1.42	C2-C3-O4	105.43	C3-C2-O1-O5	-10.10
C2-C3	1.53	C3-C2-O1	105.48	O1-C2-C3-O4	-1.95
				C6-C5-O4-C3	99.93
				C10-C5-O1-C2	135.85

The Newman projection of cyclohexanone ethylene ketal through C5-O4 bond is shown in Figure 4.3 for the envelope and the planar dioxolane rings. In the envelope dioxolane, the C6-C5-O4-C3 angle is about 100° but in the planar dioxolane, this angle is about 120°. Thus, according to dihedral angle C6-C5-O4-C3 there is 20° deviation from planarity. Table 4.5. compares the envelope and planar structures in terms of heat of formation values. The energy barrier which amounts to 0.142 kcal/mol is quite low. For the unsubstituted dioxolane, the energy barrier obtained from far-infrared spectra was reported in the literature as 1116 cm^{-1} (3.192 kcal/mol)(23). This quantity is incomparable with our result because unsubstituted dioxolane pseudorotates freely whereas pseudorotation of dioxolane ring in cyclohexanone ethylene ketal is hindered.
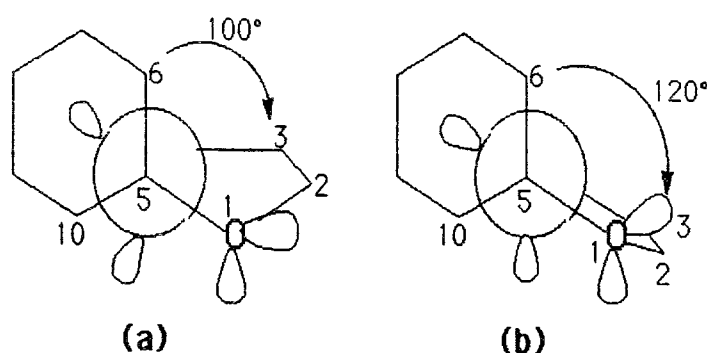
Figure 4.3. C6-C5-O4-C3 angle of cyclohexanone ethylene ketal. (a) envelope (b) planar.

Table 4.5. Heat of formation values ΔH_f (kcal/mol) and dipole moments of μ cyclohexanone ethylene ketal.

	ΔH_f	μ
envelope	-101.178	0.89
planar	-101.036	0.76

The calculations of 2-substituted cyclohexanone ethylene ketals have been performed using the envelope dioxolane fragment which may be syn or anti with respect to the substituent (Figure 1.6(b)). The results in the gas phase (Table 3.3.) show that the equatorial position is generally favored regardless with the syn and anti orientation of the dioxolane ring. This equatorial preference is in agreement with the experimental results in a nonpolar solvent CCl_4 (Table 1.1.). The gas phase calculations indicate that when the substituent is in axial position, IIa-syn is generally the prefered conformer except for -Cl derivative (Table 3.3). Similarly, when the substituent is in equatorial position, conformer IIb-syn is generally prefered except for -CN and -NO_2. IIa and IIb exhibit smaller dipole moments than Ia and Ib. Figure 4.4. illustrates directional dipoles in equatorial orientations and X-H interactions in IIb. Steric interaction observed between the substituent and the 1,3-syn axial hydrogens of the dioxane fragment is absent on the dioxolane fragment. Absence of steric interactions have left the electrostatics to play a major role in equilibria.

Ib-anti
larger μ

IIb-syn
smaller μ
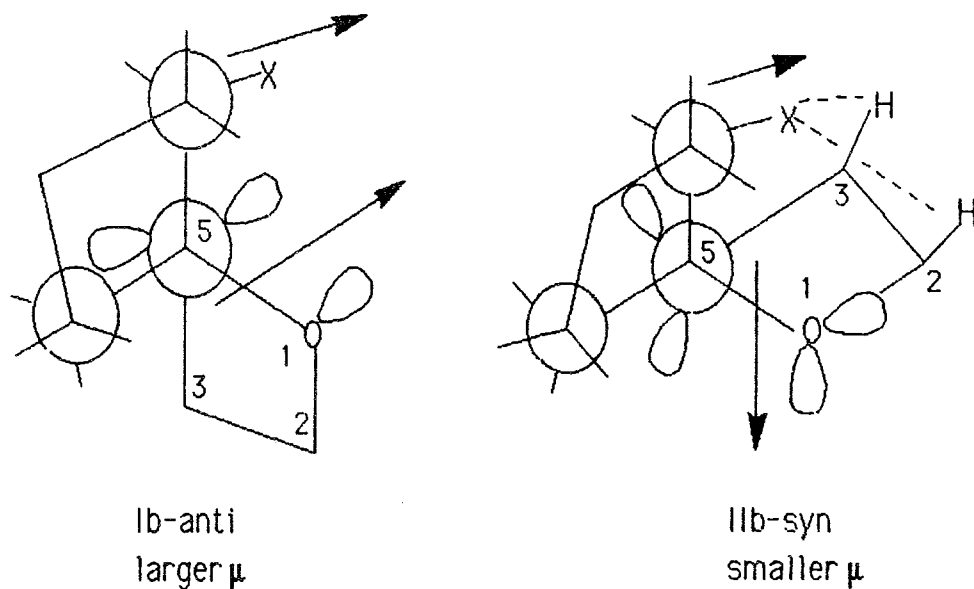
Figure 4.4. Newman projection through C5-O4 bond for ethylene ketal derivatives. (Arrows show the direction of dipoles.)

For $-NO_2$ and $-CN$ derivatives, Ib is more stable than IIb contrary to other ethylene ketals. Electrostatic forces between the substituents and the oxygens of the dioxolane fragment may be dominant similar to the case in 2-NO_2 propylene ketal. The charges on the substituents and the oxygens of dioxolane ring are given in Table 4.2. The calculated interatomic distances in the most stable axial (IIa) $-NO_2$ group are N-O1=2.8 A°, N-O5=3.8 A° and in the most stable equatorial (Ib) $-NO_2$ group are N-O1=2.9 A°, N-O5=3.0 A°. The corresponding distances in the axial and equatorial $-CN$ group have been calculated as C-O1=2.8 A°, C-O5=3.7 A° and C-O1=2.9 A°, C-O5=2.9 A°.

The rotamer studies for the potential curve of $-NO_2$ derivative (Figure 3.9-Figure 3.10) give the similar features as its propylene ketal analogue; only one minimum around 180° and one maximum around 90° dihedral angles showing a flat surface near minimum. The potential curves of $-OH$ and $-OCH_3$ derivatives (Figure 3.11-Figure 3.14) also show a very similar rotational profile as propylene ketals. The absolute minima of these molecules appear near 180° dihedral angle for Ia, IIa, Ib and IIb. Another similarity in the potential curves of the $-OCH_3$ derivatives in propylene and ethylene ketals is the very high energy barrier around 240° in conformer IIb. This is the dihedral angle where the methoxy group stays closest to the hydrogens of the heterocyclic ring causing strong steric repulsions.

Finally, when we compare the propylene and the ethylene ketal systems, the most striking difference is that, when the ketal moiety is syn, the substituent tends to be axial for propylene ketals, and the substituent tends to be equatorial for ethylene ketals. The balance between electrostatic and steric interactions are not in the same directions for propylene and ethylene ketal systems. While electrostatic interactions favor syn position of heterocyclic system, steric interaction present in propylene ketals force 2-substituent to adopt axial orientation, whereas such steric repulsions are not very effective in ethylene ketals because the 5-membered dioxolane ring is more flattened than the 6-membered dioxane ring allowing hydrogens to stay further away from the substituent (Figure 4.4). These repulsions are

dominant in propylene ketals as shown from the interatomic distances between the substituent and the hydrogens of the dioxane and dioxolane rings (Table 4.6.). This interpretation is also confirmed by potential scans around C-X bond of methoxy derivatives where the rotational barrier for IIb at 240° dihedral angle is about 9 kcal in propylene ketal but only 6 kcal in ethylene ketal.

A common feature of both systems is the stability of conformer Ib-anti over the others for -CN and $-NO_2$ derivatives despite the fact that this preference is contrary to the behavior of other derivatives in ethylene ketals.

Table 4.6. X-H distances in A° illustrated in Figures 4.2 and 4.4

Substituent	propylene ketals		ethylene ketals	
	Ib	IIb	Ib	IIb
-H	4.39	1.92	3.81	3.05
	4.41	2.36	3.79	2.92
-F	4.76	2.46	3.78	2.87
	4.79	2.47	3.68	2.97
-Cl	4.95	2.49	3.63	2.85
	5.04	2.52	3.76	3.03
-CN	4.85	2.56	3.63	3.30
	4.88	2.57	3.65	3.45
$-CH_3$	4.88	2.54	3.72	3.20
	4.95	2.58	3.70	3.29
-OH	4.54	2.54	3.77	3.24
	4.52	2.49	3.78	3.21

4.3.2. In Solution

For the ethylene ketals, the molecules can be categorized in two groups. The first group consists of -F, -Cl, -CN and -OH derivatives . In these molecules, the content of axially oriented molecule starts to increase as the solvent polarity increases. This tendency to the axial orientation is expected on the basis of solute-solvent electrostatic interactions since Ia and IIa conformers, having larger dipole moments than Ib and IIb conformers, are stabilized more in polar solvents than the conformers with the equatorially oriented substituent. Note in Table 3.4 that Ib, whose dipole moment is close to Ia and IIa is more stable than IIb in acetonitrile for -F and -Cl derivatives.

The $-CH_3$, $-NO_2$ and $-OCH_3$ substituted ethylene ketals fall in the second category. In these molecules, the tendency to equatorial position increases as the dielectric constant of the solvent increases. The tendency of $-OCH_3$ group to equatorial position in polar solvent is parallel with experimental results. There is not enough experimental data to compare our results for $-CH_3$ and $-NO_2$ derivatives, but, as expected, for $-CH_3$, the magnitude of the tendency is small because of the relatively nonpolar character of $-CH_3$ group. For the NO_2 derivative, the increase in tendency to equatorial position in polar solvent confirms the idea of electrostatic attractions disscused above. If these interactions are present, they are expected to be stronger in polar solvent.

As pointed out above, comparison with available experimental data shows that the predicted solvent effects are in general as expected, except for the -OH derivative. It is difficult to elucidate the origin of this disagreement without performing more accurate computations. Therefore, ab initio calculations were run on 1,1,2 trihydroxy ethane, modelling the 2-OH cyclohexanone ketals.

4.4. 1,1,2-TRIHYDROXYETHANE

1,1,2-Trihydroxyethane's conformational space has been studied exclusively in gaseous phase and in solution.

4.4.1. Gaseous Phase

According to the results of PM3 calculations, 1,1,2-trihydroxy ethane exhibits nine minima corresponding to staggered configurations around the C2-C3 and C2-O8 bonds as shown in Table 3.5. and in Figure 3.17-Figure 3.21. Hovewer, the ab initio calculations with 6-31G basis set have predicted no minimum for structures B, D, and E (Table 3.6). The optimized PM3 structures of B, D, and E were converted to one of the other minima in Table 3.5 by 6-31G calculations. Also, structures G and I obtained from 6-31G calculations are different than the ones obtained from PM3 in terms of the dihedral angles of H5-O4-C3-C2 and H7-O6-C3-C2.

Among the nine minima, structures A, B, and C have two gauche interactions (GG) between O8-O6 and O8-O4, whereas the other minima have one gauche and one trans (TG) interactions with the same oxygens. There are many factors effecting the stabilities of these conformers such as steric, dipolar, etc. Intramolecular H-bonding may play an important role. In order to investigate its role, the interatomic O-H distances are given in Table 4.7.

The comparison of interatomic O-H distances obtained from both methods shows that the PM3 calculations give rise to shorter O-H distances than 6-31G. In the literature, the examples of H-bonding distances calculated with PM3 method are in the order of 1.8 A° (106, 107) whereas ab initio calculations give longer distances. For instance, in the H-bonded conformer of ethylene glycol, the O-H distance varies between 2.141 A° to 2.362 A° according to ab initio and density functional theory calculations (36). The distances in Table 4.7 are in agreement with the values for similar O-H distances found in literature. Table 4.7 shows that PM3 method predicts

shorter O--H distances and thus stronger O--H interactions than 6-31G in structures B, D, G, and I. One reason for this may be the shorthening of some bonds which will allow closer contact between hydrogen and oxygen atoms. The two methods are compared in terms of C-O bond lengths and O-C-O bond angle in Table 4.8 .As expected PM3 locates minima at shorter C-O bond lengths than does 6-31G, which may explain the shorter O--H distances obtained by PM3. For PM3 structures of B, D, E, G, and I, O--H interactions are so attractive that the calculations give rise to very small O-C-O angles (about 98°) and B, D, and E are not located as stable structures with the 6-31G basis set.

Table 4.7. Interatomic H-O distances obtained from PM3 and 6-31G calculations in Angstroms.

PM3	A	B	C	D	E	F	G	H	I
H9-O6	2.579	2.650	3.776	3.907	3.862	3.875	3.883	3.941	4.316
H9-O4	3.237	3.149	3.756	3.445	3.241	2.723	2.691	2.655	3.820
H7-O8	3.765	3.300	2.544	4.117	3.907	4.313	3.926	3.912	4.065
H7-O4	2.385	1.886	2.548	1.879	2.983	2.492	2.961	2.454	1.877
H5-O8	2.529	2.651	2.523	2.687	3.291	3.357	3.785	3.736	2.655
H5-O6	2.532	2.859	2.551	2.946	2.342	2.410	1.878	2.463	2.960

6-31G	A	B	C	D	E	F	G	H	I
H9-O6	2.485	–	3.617	–	–	3.869	3.897	3.920	4.331
H9-O4	3.168	–	3.615	–	–	2.478	2.447	2.404	3.605
H7-O8	3.574	–	2.363	–	–	4.368	4.380	3.975	4.256
H7-O4	2.515	–	2.673	–	–	2.652	2.681	2.562	2.351
H5-O8	2.360	–	2.364	–	–	3.287	3.518	3.579	2.329
H5-O6	2.680	–	2.672	–	–	2.489	2.783	2.636	3.120

Table 4.8. C-O bond lengths (A°) and O-C-O bond angles obtained from PM3 and 6-31G calculations of 1,1,2-trihydroxyethane.

	C2-O8		C3-O4		C3-O6		O-C-O	
	PM3	6-31G	PM3	6-31G	PM3	6-31G	PM3	6-31G
A	1.400	1.431	1.394	1.407	1.405	1.423	105.4	110.9
B	1.400	-	1.398	-	1.400	-	98.1	-
C	1.409	1.441	1.394	1.411	1.395	1.411	106.7	112.9
D	1.400	-	1.398	-	1.394	-	97.4	-
E	1.398	-	1.386	-	1.400	-	99.9	-
F	1.400	1.424	1.398	1.424	1.400	1.409	105.4	111.0
G	1.398	1.423	1.395	1.421	1.398	1.410	97.0	112.6
H	1.398	1.421	1.404	1.420	1.396	1.411	105.3	111.3
I	1.409	1.436	1.398	1.417	1.395	1.404	97.2	107.9

When Table 3.5 and Table 3.6 are compared, it is seen that the relative stabilities of PM3 and 6-31G structures are quite different. On the other hand, the structure GG-1,A is the most stable conformer in both methods. According to 6-31G calculations, Table 4.7. indicates that some intramolecular O--H interactions are possible in A, between H9-O6, H5-O8, H7-O4, and may be H5-O6 (Figure 4.5.). These interactions may be intramolecular H-bonding of various strength. The other GG structure, C, also shows four similar interactions. However the dipole moment of C is the highest of all the structures which makes it energetically the least stable after structure G. In G, the dipole moment is also very large and the intramolecular O--H interactions are weaker. Therefore, G exhibits the highest energy.

All the TG structures are less favored than GG-1,A although they also exhibit some similar interactions. (Figure 4.5). The stability of GG-1,A is in agreement with the well-known "gauche effect" in literature (26-30, 32-38) which states that when electron pairs or polar bonds are placed on adjacent pyramidal atoms the maximum number of gauche interaction is favored". It is
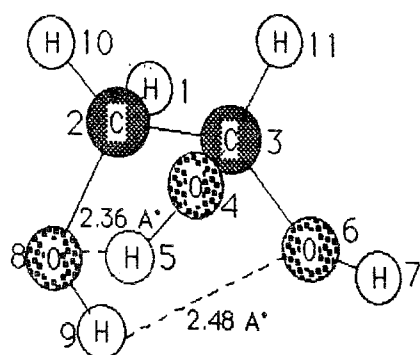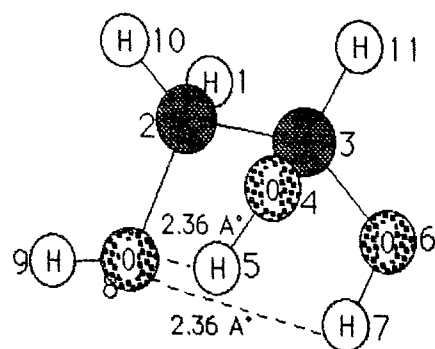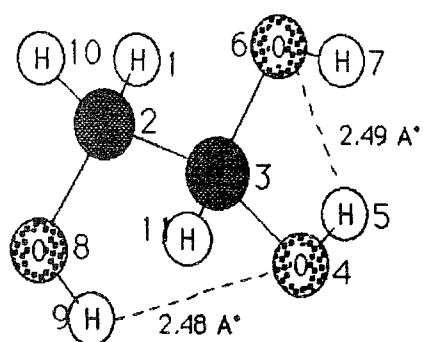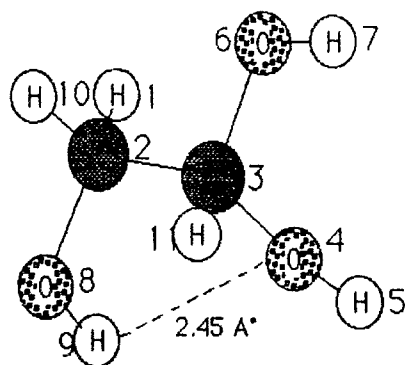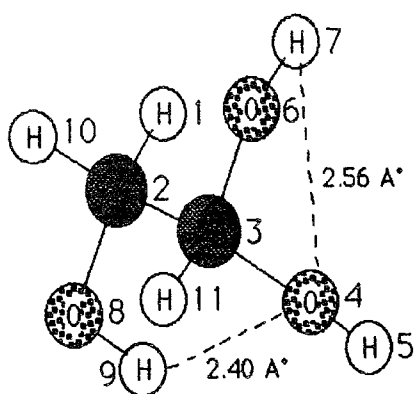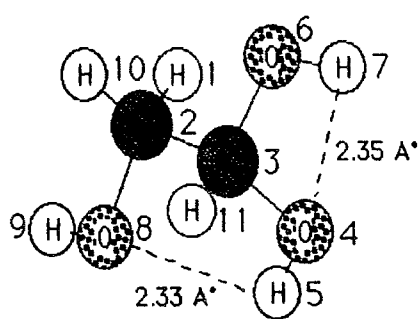
Figure 4.5. Possible forms of intra-molecular O--H interactions in structures obtained from 6-31G calculations.

important to realize that a gauche preference may result from intramolecular H-bonding. H-bonding, for instance explains the strong gauche preference seen in such molecules as 2-fluoroethanol, 2-chloroethanol, and ethylene glycol (37, 38) In other cases, however, there is no possibility of such an effect and the cause of unusual gauche preference is less clear. Examples are 1,2-difluoroethane (33, 35), 1,2-dimethoxyethane (37). These examples are contrary to the chemical intuition since in the gauche conformation the dipoles of the substituents are parallel instead of antiparallel and electronegative atoms are sterically closer than in the trans case.

The gauche effect for 1,2-difluoro ethane has been explained by Wiberg et al. using the bond path method (108) and concluded that the gauche effect is due to a destabilizing interaction in the trans rotamer, in which the C-C bond orbitals are bent in opposite directions, giving decrease overlap and thus poorer bond. On the other hand, the gauche rotamer has bond orbitals bent in roughly the same direction, giving better overlap. The same effect may be expected to be operative in 1,1,2-trihydroxyethane and also in 1,1,2-trifluoroethane which has the similar skeleton as 1,1,2-trihydroxyethane. No information on 1,1,2-trihydoxyethane is present in the literature but for 1,1,2-trifluoroethane, both experimental and theoretical studies have shown that the staggered trans configurations are favored over the gauche conformers (109). In 1,1,2-trifluoroethane, the preference to trans has been explained by steric factors (32). Gauche rotamers have three fluorines mutually cis, so repulsive interactions are greatly increased in comparison to 1,2-difluoroethane. In 1,1,2-trihydroxyethane, similar repulsive interactions are expected to operate in GG conformers. However, in our calculations, gauche-gauche conformer A has been found to be the most stable rotamer. This suggests that intramolecular O--H interactions or gauche effect dominate over the repulsions in 1,1,2-trihydroxyethane. Ethylene glycol, which contains one less -OH group than 1,1,2-trihydroxy ethane can be used for comparison. An x-ray diffraction structure of ethylene

glycol has determined the O-C-C-O torsion angle to be 74°, i.e., the gauche form (36). An infrared spectrum of ethylene glycol has demonstrated only the presence of gauche form. Also a combined ab initio and isotopic-labeled infrared spectrum predicted the gauche form to be more stable than the trans form by about 3.5 kcal/mole (36). Our results, which predict the stability of gauche-gauche form (GG-1,A) over trans-gauche forms (TG structures), are in agreement with these findings. Our calculations have shown that structure A is 2.07 to 4.87 kcal/mole more stable than TG structures in 6-31G level as seen in Table 3.6.

In Table 3.7, total and relative energies obtained from high level RHF and electron correlation calculations are given. The results show that the relative energies have increased by about 1 kcal in TG conformers when electron correlation has been included in 6-31G** calculations while the increase in relative energy of the GG type conformer is only about 0.3 kcal. In other words, GG-1,A becomes even more stable when the electron correlation is included in calculations. Although the presence of real H-bonding is not definite in the structures studied, we can say that gauche conformer of 1,1,2-trihydroxyethane is stabilized at least by attractive nonbonded interactions. It is known that electron correlation treatments are better in taking into account such interactions than HF procedure alone because the complete description of correlation energy between the motions of electrons is included in configuration interaction treatment.

4.4.2. In Solution

The PM3 and 6-31G results of solvent effect calculations are given in Table 3.8. The dipole moments of the conformers change drastically because the direction of oxygen lone pairs are different in each conformer. As a result, it is expected that a polar solvent will affect the relative stability of these conformers. In principle, PM3 and 6-31G calculations are in agreement. It is known that the compounds with large dipole moments are stabilized

more in polar solvents due to the dipole-dipole interactions between the solvent and the solute. In parallel to this, the relative energies of the more polar conformers decrease in comparison to their gas phase values in Table 3.5 and Table 3.6. Also their solvation energies have larger negative values. As a result, they are stabilized in a moderately polar solvent, acetonitrile.

Another important feature of Table 3.8 is that "A" is still the most stable conformer in solution according to the results of both semiempirical and ab initio methods although its dipole moment is the smallest in 6-31G calculations. This is also an evidence for the dominance of intra-molecular O--H interactions.

4.4.3. Modelling Cyclohexanone Ketal Derivatives

As it is described in section 3, the contour diagrams (Figure 3.22-Figure 3.26) can be used to locate the conformers corresponding to axial and equatorial orientations of -OH substituent in 2-OH cyclohexanone ketals. The contour maps are useful in a way that one can see all the critical points altogether and compare them. A common feature is that the points which belong to ethylene ketal correspond to higher energy levels in all the contour maps. This can be explained in terms of higher strain in the dioxolane fragment of ethylene ketal than the dioxane ring of propylene ketal. Another common feature is that syn structures (IIa and IIb) fall in lower energy levels and therefore are favored with respect to anti structures (Ia and Ib). This is in agreement with the results in Table 3.1. and Table 3.3 with the exception that 2-OH propylene ketal prefers Ib over IIb. The reason is that 1,1,2-trihydroxyethane does not represent the X--H repulsions discussed in section 4.2 (Figure 4.2) which play an important role in propylene ketal derivatives.

The contour maps obtained can also be used in modelling many other compounds which have the same skeletal structure. Such compounds are generally related to carbohydrates. Therefore the information can be gained

for many sugar structures and similar compounds in a short and simple way using the contour diagrams appropriately.

According to the experimental results in Table 1.1, for both 2-OH cyclohexanone propylene and 2-OH cyclohexanone ethylene ketals, preference for the axial orientation decreases as the solvent polarity increases. The results of 6-31G calculations for the model structures (Table 3.10-Table 3.13) show good agreement with these experimental findings. Total axial percentage of the model structures representing both ketal systems have shown a decrease as going from gas phase to acetonitrile with the available data. Thus, one can say that 1,1,2-trihydroxy ethane mimics 2-OH cyclohexanone ketal systems in consideration of solute-solvent interactions. Steric interactions between the -OH substituent and the axial hydrogens of the dioxane fragment (Figure 4.2.) is not represented in this model. Therefore, 1,1,2-trihydroxyethane does not mimic steric interactions. The shift produced in going from gas phase to solvated medium is mainly due to the electrostatic interactions between the solute and the solvent. PM3 calculations have predicted the equatorial shift for both syn and anti ethylene ketal. For the propylene ketal, axial shift is produced for the syn and equatorial shift is produced for the anti corresponding structures. One needs to differentiate between the syn and anti corresponding structures due to the fact that they are of crucial importance in the 6-membered ketal fragment.

In the models of 2-OH cyclohexanone propylene ketal, Table 3.10. and Table 3.11. show that the main contributions to the total energy in gas phase come from Ia and IIb. In acetonitrile, contribution of IIb increases as Ia decreases which results in an overall decrease in axial percentage. To clearify this result, the solvation energies and the dipole moments are given in Table 4.9.

When the solvation energies of Ia and IIb are compared, it is seen that Ia is stabilized slightly less than IIb in acetonitrile which is the reason of the decrease in axial percentage. Although IIa and Ib structures are stabilized to a larger extent than Ia and IIb in acetonitrile, they have almost

no effect on the overall result since their contributions are negligible.

Another feature of these compounds is that the solvation energies are dependent on higher moments as well as dipole moments. In other words, the highest solvation energy does not correspond to the largest dipole moment or vice versa because, multipole contributions to the solvation energy play an important role as seen in Table 4.10. The third and fourth terms also contribute to the energy.

In the model structures of 2-OH cyclohexanone ethylene ketal, Table 3.12 shows that Ia and IIa structures contribute to the total energy more than Ib and IIb in the gas phase. However, in acetonitrile, the percentage of all the structures becomes zero except GG-2 (IIb), the percentage of which increases to 100%. As a result, a sharp drop of the total axial percentage is observed in acetonitrile. The reason for this can be seen from Table 4.11. GG-2 (IIb) exhibits an extremely large solvation energy in comparing to the other structures in spite of its small dipole moment. This is again because of the contribution of higher multipole terms to the solvation energy. Table 4.12 shows that in GG-2(IIb), the first five term all contribute to a considerable extent whereas in the other structures the higher terms are not as effective as in GG-2(IIb).

Table 4.9. Solvation energies E_{solv} (kcal/mol) in acetonitrile from 6-31G calculations and gas phase dipole moments, μ,(Debye) of 1,1,2-trihydroxyethane for the models corresponding the conformers of 2-OH cyclohexanone **propylene ketal**

	E_{solv}(Ia)	μ(Ia)	E_{solv}(IIa)	μ(IIa)
TG-1	–	–	–	–
TG-2	-5.4835	4.129	-6.6609	3.434
TG-3	–	–	-8.2245	4.933
	E_{solv}(Ib)	μ(Ib)	E_{solv}(IIb)	μ(IIb)
GG-1	-7.2069	5.228	–	–
GG-2	-8.2390	3.448	-5.7722	4.214

Table 4.10. Multipole contributions to the solvation energy of 1,1,2-trihydroxyethane for the models corresponding the conformers of 2-OH cyclohexanone **propylene ketal**

	1	2	3	4	5	6
TG-1(Ia)	–	–	–	–	–	–
(IIa)	–	–	–	–	–	–
TG-2(Ia)	-2.589	-1.361	-0.589	-0.728	-0.410	-0.093
(IIa)	-2.853	-2.396	-1.063	-0.568	-0.132	-0.063
TG-3(Ia)	–	–	–	–	–	–
(IIa)	-5.320	-1.701	-0.741	-0.711	-0.272	-0.071
GG-1(Ib)	-4.739	-1.277	-0.372	-0.844	-0.407	-0.083
(IIb)	–	–	–	–	–	–
GG-2(Ib)	-2.511	-3.845	-1.149	-0.809	-0.298	-0.072
(IIb)	-2.842	-1.141	-0.822	-0.935	-0.291	-0.060

Table 4.11. Solvation energies E_{solv} (kcal/mol) in acetonitrile from 6-31G calculations and gas phase dipole moments, μ,(Debye) of 1,1,2-trihydroxyethane for the models corresponding the conformers of 2-OH cyclohexanone **ethylene ketal**

	$E_{solv}(Ia)$	$\mu(Ia)$	$E_{solv}(IIa)$	$\mu(IIa)$
TG-1	-6.5574	3.236	-6.9616	2.238
TG-2	-4.8966	4.165	-5.8329	3.976
TG-3	-	-	-7.2386	3.896
	$E_{solv}(Ib)$	$\mu(Ib)$	$E_{solv}(IIb)$	$\mu(IIb)$
GG-1	-6.4875	3.355	-5.9516	1.733
GG-2	-6.5736	0.748	-12.9302	1.695

Table 4.12. Multipole contributions to the solvation energy of 1,1,2-trihydroxyethane for the models corresponding the conformers of 2-OH cyclohexanone **ethylene ketal**

	1	2	3	4	5	6
TG-1(Ia)	-1.608	-3.999	-0.326	-0.442	-0.384	-0.078
(IIa)	-0.738	-5.212	-0.513	-0.449	-0.237	-0.079
TG-2(Ia)	-2.631	-0.464	-1.063	-0.454	-0.459	-0.074
(IIa)	-3.088	-1.071	-1.205	-0.410	-0.337	-0.062
TG-3(Ia)	-	-	-	-	-	-
(IIa)	-3.617	-2.274	-0.779	-0.529	-0.412	-0.066
GG-1(Ib)	-1.914	-2.987	-1.001	-0.495	-0.347	-0.064
(IIb)	-0.590	-3.259	-1.585	-0.449	-0.230	-0.052
GG-2(Ib)	-0.109	-4.003	-1.378	-0.908	-0.375	-0.023
(IIb)	-0.782	-5.685	-3.329	-2.821	-1.087	-0.117

5. CONCLUSION

From the results of PM3 calculations, detailed information has been obtained about the conformational equilibria of the molecules studied. Gas phase calculations of propylene and ethylene ketal derivatives show different tendencies in the following aspects:

In propylene ketals, the substituents prefer equatorial position if the dioxane moety is anti and they prefer axial position when the dioxane ring is syn. On the other hand, in ethylene ketals, the substituents tend to be equatorial for both syn and anti orientations of the ketal fragment. In propylene ketals, steric interactions force the substituent to stay in axial position. However, such interactions are not effective in ethylene ketals, instead electrostatic interactions are effective which fovor syn position of the dioxolane ring.

Propylene ketals, except some special substituents, tend to have 50 or more than 50% total axial preference. However, ethylene ketals give less than 50% total axial preference except X=-OCH$_3$ in which the size of the substituent is effective.

There are also some common features in both systems:

When X=-F, -CN, -NO$_2$, -OH both systems favor equatorial substituents. This has been attributed to some attractive interactions between the substituents and the oxygens of the ketal fragment.

Dipole moments of -OH and -OCH$_3$ substituents in conformers Ia, IIa, Ib, and IIb exhibit different relative tendency than the other substituents in

both systems because the oxygen lone pairs of -OH and $-OCH_3$ groups also contribute to the overall dipole of the molecule.

The rotamer studies proved to be necessary in predicting the global minimum for the conformers for X=-OH, $-NO_2$, $-OCH_3$. In both systems, the rotamer corresponding to 180° dihedral angle is the most stable except 2-OCH_3 propylene ketal, conformer IIb which suffers from strong steric repulsions due to the axial hydrogens in dioxane ring. Therefore in IIb, 9° is the most stable rotamer

Calculations in solution showed that the conformational equilibria of the compounds have been considerably effected by the solvent except X=$-CH_3$ case which is a nonpolar substituent.

The rotamer studies showed that the internal rotation around C-X bond is not effected strongly by the solvent. The location of the global minimum in gas phase does not change in solution.

In propylene ketals preference for axial orientation decreases as the dielectric constant of the solvent increases. On the other hand, ethylene ketals show a tendency in opposite direction except X=$-NO_2$ and $-OCH_3$. These tendencies show agreement with available experimental results of both systems except 2-OH ethylene ketal.

Molecular orbital quantum chemical calculations have been proved to be very useful in understanding many chemical phenomena for isolated and solvated species. Among them, semi-empirical PM3 method in general gave qualitatively parallel results with experiments for all the molecules used in this research with the only exception of 2-OH cyclohexanone ethylene ketal. Thus, this method seems to be appropriate to predict the interactions governing the conformational equilibria of complex systems in solution. However, in some cases, higher level ab initio calculations may be required. For this purpose, several important chemical phenomena of complex systems, for which ab initio calculations are quite challenging, can be investigated using their small models. In this research, ab initio calculations on 1. 1,1,2-trihydroxyethane has provided a suitable model for 2-OH cyclohexanone ketal

derivatives to study the electrostatics and the effect of the solvent on the balance of electrostatic interactions although it does not mimic the steric interactions present in the ketals.

The cavity model and the SCRF approach appear to be appropriate in describing the solute-solvent interactions for conformational equilibria in solution. In general ellipsoidal cavity shape fits for the molecules studied especially for 1,1,2-trihydroxyethane.

The role of multipole contributions to the solvation energy is also very important. The results can be improved as the higher order terms are included in the calculations.

APPENDIX A

MOPAC KEYWORDS USED:

When no keyword is specified, by default, the program runs a SCF calculation with maximum 200 SCF iteration using MNDO as the semiempirical method and BFGS routine for the geometry optimization.

AIGOUT: (Ab initio geometry output). The Z-matrix of the optimized geometry obtained from MOPAC output is converted to the input format of GAUSSIAN using this keyword.

FORCE: It is used for force calculations. The Hessian, that is the matrix of second derivatives of the energy with respect to displacements of all pairs of atoms in x, y, and z directions, is calculated. On diagonalization, this gives the force constants for the molecule. The force matrix is then used for calculating the vibrational frequencies. The system can be characterized as a minimum if all the vibrational frequencies are positive and as a transition state if only one vibrational frequency is negative and the rest are positive.

GNORM=n.nn: It specifies the termination criteria for the geometry optimization in both gradient minimization and energy minimization. In this thesis, GNORM=0.1 has been used which is good enough for high precision work. It means the optimization terminates as soon as the gradient norm drops below 0.1. The default for this keyword is GNORM=1.

PARASOK X Y Z: In order to perform the internal rotations around C-X bond in GEOMOS, one needs to define the dihedral angles H-O-C-H, C-O-C-H, and O-N-C-H in Figure 3.2. because of the different definition of the Z-matrix in MOPAC and GEOMOS. In MOPAC, one can define the dihedral angles in any order

as long as the atoms have been previously used in Z-matrix. However, in GEOMOS, the order of atoms in the definition of dihedral angle should be the same as the sequence in Z-matrix. Therefore, the order of atoms in Z-matrix described above has been changed in such a way that the numbering starts from the atoms of the substituent. The cartesian coordinates in this order have been given as an input and converted to the desired Z-matrix output using PARASOK X Y Z keyword.

PM3: The default for this keyword is MNDO. It specifies the semi-empirical method (Parametrized Method 3) to be used. It has been used together with the keywords PRECISE and GNORM=0.1.

PRECISE: It can be used when more precise results are wanted. The criteria for terminating all optimizations are increased by 100 times.

POINT1=n POINT2=n: In the grid calculations, the number of points to be calculated for the first parameter is given by POINT1=n and the ones for the second parameter is given by POINT2=n. For 1,1,2-trihydroxyethane, n=12 has been used in this thesis.

STEP1=n STEP2=n: In the grid calculations, the step size in degrees or in A° for the first parameter is given by STEP1=n and for the second parameter by STEP2=n. n=30 has been used in this thesis.

TS: It is used to optimize a transition state.

APPENDIX B   EXAMPLES OF INPUT DATA

1. EXAMPLE OF A MOPAC INPUT

```
PM3 PRECISE GNORM=0.1
2-OH cyclohexanone ethylene ketal IIa

 XX        0.00000  0      0.00000  0     0.00000  0   0   0   0
 XX        0.51000  0      0.00000  0     0.00000  0   1   0   0
 C         1.51944  1     85.53211  1     0.00000  0   2   1   0
 C         1.51935  1     85.60073  1   111.78764  1   2   1   3
 C         1.38801  1     87.88939  1  -122.26834  1   2   1   3
 C         1.43107  1     88.92740  1  -172.80128  1   1   2   3
 C         1.41720  1     91.01069  1    59.65352  1   1   2   3
 C         1.54271  1     94.34129  1   -55.90991  1   1   2   3
 H         1.10910  1     90.95243  1   177.99682  1   3   2   1
 H         1.10933  1     91.57379  1  -177.75338  1   4   2   1
 O         1.40483  1     98.83529  1   178.80630  1   5   2   1
 H         1.10795  1     95.06217  1   177.75326  1   7   1   2
 H         1.10833  1     95.13933  1   179.98270  1   8   1   2
 H         1.10721  1    163.21025  1   -14.06616  1   3   2   1
 H         1.10780  1    162.26289  1    14.85492  1   4   2   1
 H         1.11499  1    159.90807  1    -2.69933  1   5   2   1
 H         1.10770  1    158.67515  1     6.14264  1   7   1   2
 H         1.10727  1    159.06324  1    -0.78205  1   8   1   2
 O         1.43237  1     99.10283  1  -178.31290  1   6   1   2
 O         1.43112  1    155.76351  1    -0.74392  1   6   1   2
 C         1.42005  1    109.65366  1   156.98874  1  19   6   1
 C         1.41909  1    109.68211  1  -154.77490  1  20   6   1
 H         1.10125  1    105.93330  1   134.80853  1  21  19   6
 H         1.10340  1    108.50935  1  -108.99228  1  21  19   6
 H         1.10344  1    108.79261  1   107.23436  1  22  20   6
 H         1.10117  1    105.79884  1  -136.45387  1  22  20   6
 H         0.95010  1    107.46055  1   180.00000  1  11   5  16
```

1st line: The keywords

2nd line: The title of the job

4th line and the rest: Z-matrix

        Z-matrix:

1st column: Symbols of atoms

2nd, 4th and 6th columns: Bond lengths, bond angles, and dihedral angles

3rd, 5th, and 7th columns: Specifies the parameter in the previous column to be optimized (1) or not optimized (0)

8th, 9th, 10th columns: Show the connectivity order of the atoms

2. EXAMPLE OF A GEOMOS INPUT

```
2-F cyclohexanone propylene ketal(IIa) in CCL4
mndo3clsd        00.000 1 fltc0.1000D-074000.0000D+000.0000D+00 0 00   0
   27    0    1   -1    0    0    0    0    0    1    0    0    0    0    0    0    0    0    0
   29
 0
 0    1  5.10000D-01                                          0
 6    2  1.45000D+00  8.98000D+01                             0
 6    2  1.47000D+00  8.93000D+01                             0
 6    2  1.48000D+00  8.74000D+01  1.18700D+02 0
 6    1  1.49000D+00  8.79000D+01  2.40400D+02 0
 6    1  1.44000D+00  9.02000D+01  1.81600D+02 0
 6    1  1.46000D+00  8.94000D+01  5.93000D+01 0
 1    3  1.10800D+00  9.16000D+01 -5.93000D+01 0
 1    4  1.10900D+00  9.30000D+01  1.81000D+02 0
 9    5  1.36500D+00  9.74000D+01  1.80000D+02 0
 1    7  1.10700D+00  9.22000D+01  1.79000D+02 0
 1    8  1.10800D+00  9.29000D+01  1.80500D+02 0
 1    3  1.10700D+00  1.62400D+02 -0.62000D+00 0
 1    4  1.10800D+00  1.61000D+02  0.74000D+00 0
 1    5  1.11200D+00  1.57000D+02 -1.42000D+00 0
 1    7  1.10700D+00  1.61200D+02  2.70000D+00 0
 1    8  1.10700D+00  1.61000D+02 -0.55000D+00 0
 8    6  1.43000D+00  9.67800D+01  1.77000D+02 0
 8    6  1.43000D+00  1.55000D+02  6.90000D+00 0
 6   19  1.41000D+00  1.14000D+02  1.25000D+02 0
 6   21  1.52000D+00  1.11400D+02  5.87000D+01 0
 6   20  1.41350D+00  1.15800D+02 -1.34000D+02 0
 1   21  1.10100D+00  1.02500D+02  1.80000D+02 0
 1   21  1.11100D+00  1.09300D+02 -6.40000D+01 0
 1   22  1.10500D+00  1.10600D+02  1.89100D+02 0
 1   22  1.10700D+00  1.10376D+02  7.16330D+01 0
 1   23  1.10240D+00  1.10180D+02  1.85900D+02 0
 1   23  1.10740D+00  1.09820D+02  7.14140D+01 0
  80
   41    42    43    51    52    53    61    62    63    71    72    73    81
   82    83    91    92    93   101   102   103   111   112   113   121   122
  123   131   132   133   141   142   143   151   152   153   161   162   163
  171   172   173   181   182   183   191   192   193    31    32   201   202
  203   211   212   213   221   222   223   231   232   233   241   242   243
  251   252   253   261   262   263   271   272   273   281   282   283   291
  292   293
   4     2.240    2.000    1.000    000.0                         3
end
```

2nd line:mndo3: PM3 method will be used

    1: the geometry will be optimized w.r.t internal coordinates.

    fltc: geometry will be optimized according to Fletcher's method.

    0.1D-07: precision (default is 10^{-5})

    400: maximum number of optimization iterations (default is 20)

3rd line:27: total number of atoms

    0: charge of the molecule

    1: spin multiplicity of the molecule

    -1: to print a short output

    1: computes the energy resulting from reaction field (solvent)

4th line:29: total number of atoms including dummies

Z-matrix:

80: total number of parameters to be optimized. These parameters are specified just below 80.

The last line:4: multipole moment contributions will be included up to the 4th term.

    2.24: dielectric const. of the solvent

    2.00: dielectric const. of the solvent at infinite frequency

    1.00: dielectric const. of the evacuated cavity

    000.0: molecular volume is deduced from the molecular polarizability
computed by variational method.

    3: cavity shape code, general ellipsoid

3. EXAMPLE OF A GAUSSIAN INPUT IN THE GAS PHASE

```
$ RunGauss
# HF/6-31G opt scf=direct

1,1,2 trihydroxyethane  PM3 Heat of formation -148.493 kcal/mol

0,1
  H
  C      1    r21
  C      2    r32        1    a321
  O      3    r43        2    a432        1    d4321        0
  H      4    r54        3    a543        2    d5432        0
  O      3    r63        2    a632        1    d6321        0
  H      6    r76        3    a763        2    d7632        0
  O      2    r82        3    a823        6    d8236        0
  H      8    r98        2    a982        3    d9823        0
  H      2    r102       3    a1023       4    d10234       0
  H      3    r113       2    a1132       1    d11321       0

    r21              1.0798
    r32              1.5138
    r43              1.4113
    r54              0.9708
    r63              1.4324
    r76              0.9668
    r82              1.4451
    r98              0.9689
    r102             1.0769
    r113             1.0763
    a321           110.6496
    a432           109.806
    a543           107.8523
    a632           103.7967
    a763           110.3225
    a823           106.2018
    a982           107.3031
    a1023          110.6251
    a1132          113.3501
    d4321         -177.0382
    d5432           36.5289
    d6321          -58.4214
    d7632          194.5092
    d8236           63.359
    d9823          -62.2073
    d10234          60.2667
    d11321          62.9023
```

$: run command

#: keyword line

HF/6-31G: Hartree-Fock calculations will be done (default is RHF) with 6-31G basis set.

opt: optimize the geometry (default is no optimization).

scf=direct: requests a direct SCF calculation in which the two-electron integrals are recomputed as needed.

0, 1:   charge and multiplicity of the molecule.

the rest: Z-matrix

4. EXAMPLE OF A GAUSSIAN INPUT IN THE SOLUTION

```
$ RunGauss
# rhf/6-31g scf=direct solvent=cavity

1,1,2 trihydroxyethane Gauss (PM3 H -148.493kcal/mol) route standard

0,1
    H
    C    1    r21
    C    2    r32        1    a321
    O    3    r43        2    a432        1    d4321      0
    H    4    r54        3    a543        2    d5432      0
    O    3    r63        2    a632        1    d6321      0
    H    6    r76        3    a763        2    d7632      0
    O    2    r82        3    a823        6    d8236      0
    H    8    r98        2    a982        3    d9823      0
    H    2    r102       3    a1023       4    d10234     0
    H    3    r113       2    a1132       1    d11321     0

        r21             1.0806
        r32             1.5097
        r43             1.4071
        r54             0.955
        r63             1.4226
        r76             0.9518
        r82             1.4307
        r98             0.9527
        r102            1.0771
        r113            1.0775
        a321          110.2697
        a432          111.4752
        a543          111.8102
        a632          105.3803
        a763          113.1053
        a823          108.8568
        a982          111.6548
        a1023         110.365
        a1132         112.4104
        d4321        -179.2161
        d5432          39.7584
        d6321         -58.8373
        d7632         188.3285
        d8236          63.5977
        d9823         -67.6916
        d10234         59.5517
        d11321         61.8621

LPMAX=6 EPSO=37.5 EPSI=2.5 EPSC=1.0 ELLIP=VDW
```

the last line represents the same information given in the last row of the geomos input.

APPENDIX C

CALCULATIONS OF PERCENTAGES OF THE CONFORMERS USING BOLTZMAN DISTRIBUTION

P_{Ia}= population of conformer Ia

P_{IIa}= population of conformer IIa

P_{Ib}= population of conformer Ib

P_{IIb}= population of conformer IIb

E_{Ia}= energy of conformer Ia

E_{IIa}= energy of conformer IIa

E_{Ib}= energy of conformer Ib

E_{IIb}= energy of conformer IIb

% Ia = percentage of conformer Ia

% IIa = percentage of conformer IIa

% Ib = percentage of conformer Ib

% IIb = percentage of conformer IIb

T= temperature = 303K

R = gas constant = 1.9872 cal. K^{-1}. mol^{-1}

$$P_{Ia} = \frac{e^{-E_{Ia}/RT}}{e^{-E_{Ia}/RT} + e^{-E_{IIa}/RT} + e^{-E_{Ib}/RT} + e^{-E_{IIb}/RT}}$$

$$\frac{1}{P_{Ia}} = \frac{e^{-E_{Ia}/RT} + e^{-E_{IIa}/RT} + e^{-E_{Ib}/RT} + e^{-E_{IIb}/RT}}{e^{-E_{Ia}/RT}}$$

$$\frac{1}{P_{Ia}} = 1 + e^{(E_{Ia}-E_{IIa})/RT} + e^{(E_{Ia}-E_{Ib})/RT} + e^{(E_{Ia}-E_{IIb})/RT}$$

$$P_{Ia} = \frac{1}{1 + e^{(E_{Ia}-E_{IIa})/RT} + e^{(E_{Ia}-E_{Ib})/RT} + e^{(E_{Ia}-E_{IIb})/RT}}$$

$$P_{IIa} = \frac{1}{e^{(E_{IIa}-E_{Ia})/RT} + 1 + e^{(E_{IIa}-E_{Ib})/RT} + e^{(E_{IIa}-E_{IIb})/RT}}$$

$$P_{Ib} = \frac{1}{e^{(E_{Ib}-E_{Ia})/RT} + e^{(E_{Ib}-E_{IIa})/RT} + 1 + e^{(E_{Ib}-E_{IIb})/RT}}$$

$$P_{IIb} = \frac{1}{e^{(E_{IIb}-E_{Ia})/RT} + e^{(E_{IIb}-E_{IIa})/RT} + e^{(E_{IIb}-E_{Ib})/RT} + 1}$$

% Ia = 100xP_{Ia}

% IIa = 100xP_{IIa}

% Ib = 100xP_{Ib}

% IIb = 100xP_{IIb}

% axial = % Ia + % IIa

REFERENCES

1. Riddel, F. G., *The conformational Analysis of Heterocyclic Compounds*, Academic Press, London, p.1, 1980.

2. Ref. 1, p. 2.

3. Jurasti, E., *Introduction to Stereochemistry and ConformationalAnalysis*, John Wiley, p.244, 1991.

4. Ref. 3, pp. 245-246.

5. Ref. 3, p. 249.

6. Ref. 3, pp. 271-272.

7. Hendrickson, J. B., "Molecular Geometry: Machine Computation of the Common Rings," *J. Am. Chem. Soc*, Vol. 83, pp. 4537-4547, 1961.

8. Zefirov, N. S., "Stereochemical Investigations IX. Conformational Investigation of trans-1-RS-2-Chlorocyclohexanes," *Zh. Org. Khim.*, Vol.6, No.9, pp. 1761-1765, 1970.

9. Zefirov, N. S., Shashkov, A. S., Krimer, M. Z., Vorob'eva, E. A., "Stereochemical Studies-XX. Conformations of 1,2-trans-disubstituted Cyclohexanes," *Tetrahedron*, Vol.32, pp. 1211-1219, 1976.

10. Abraham, R. J., Rosetti, Z. L., "Rotational Isomerism. Part XV. The Solvent Dependence of the Conformational Equilibria in trans-1,4 Dihalogeno Cyclohexanes," *J. Chem. Soc., Perkin II*, pp. 582-587, 1973.

11. Mosquera, R. A., Pereiras, A. J., Rios, M. A., "Ab initio Conformational Studies of Peroxides Part 2. A 6-31G* Study of Various Cyclic Peroxides," *J. Mol. Struc.(Theochem)*, Vol. 235, pp.25-37, 1991.

12. Ferguson, D. M., Gould, I. R., Glauser, W. A., Schroeder, S., Kollman, P. A., "Comparison of Ab initio, Semiempirical, and Molecular Mechanics Calculations for the Conformational Analysis of Ring Systems," *J. Comp. Chem.*, Vol. 13, No. 4, pp. 525-532, 1992.

13. Zheng, Y., Le Grand, S. M., Merz Jr, K. M., "Conformational Preferences for Hydroxyl Groups in Substituted Tetrahydropyrans," *J.Comp. Chem.*, Vol. 13, No. 6, pp. 772-791, 1992.

14. Dobado, J. A., Molina, J., Espinosa, M. R., "A Comparative Molecular Mechanics, Semiempirical and Ab initio Study of Saturated Five-membered Rings," *J. Mol. Struc.,(Theochem)*, Vol. 303, pp. 205-212, 1994.

15. Eliel, E. L. and Willy, W. E., "Configurational Equilibria in 2,4,5-Trisubstituted 1,3-Dioxolanes, *Tetrahedron Letters* No.22, pp. 1775-1778, 1969.

16. Ref. 3, p. 273.

17. Eliel, E., "Conformational Analysis in Saturated Heterocyclic Compounds," *Acc. Chem. Res.*, Vol. 3, pp. 1-8, 1970.

18. Juaristi, E., "Conformational Analysis of Six-membered, Sulfur-Containing Saturated Heterocycles," *Acc. Chem. Res.*, Vol. 22, pp. 357-364, 1989.

19. Greenberg, A., and Laszio, P., "Spiro bis(1,3-Dioxanes). Mutual Influence of the Attached Rings on the Inversion Rate," *Tetrahedron Letters*, No. 30, pp. 2641-2644, 1970.

20. Apaydin, G., Varnali, T., Aviyente, V., Ruiz-Lopez, M. F., "Conformational Equilibria of 5-Substituted-1,3-Dioxanes. Study of Solvent Effects," *J. Mol. Struc. (Theochem)*, Vol. 287, pp. 185-191, 1993.

21. Greenhouse, J. A., Strauss, H. L., "Spectroscopic Evidence for Pseudorotation. II. The Far-Infrared Spectra of Tetrahydrofuran and 1,3-Dioxolane," *J. Chem. Phys.*, Vol. 50, No. 1, pp. 124-134, 1969.

22. Baron, P. A., Harris, D. O., "Ring Puckering in Five Membered Rings. The Microwave Spectrum, Dipole Moment and Barrier to Pseudorotation in 1,3-Dioxolane," *J. Mol. Spectroscopy*, Vol. 49, pp. 70-81, 1974.

23. Davidson, R. and Warsop, P. A., "Energy Levels for Pseudorotation and Their Application to Cyclopentane, Tetrahydrofuran and 1,3-Dioxolane," *J. Chem. Soc. Faraday Trans.* 2, Vol. 68, pp.1875-1889, 1972.

24. Fuchs, B., "Conformations of Five-Membered Rings," *Top. Stereochem.*, Vol. 10, pp.1-87, 1978.

25. Legon, A. C., "Equilibrium Conformations of Four- and Five-Membered Cyclic Molecules in the Gas Phase. Determination and Classification," *Chem. Rev.*, Vol. 80, pp. 231-262, 1980.

26. Wolfe, S., Tel, L. M., Csizmadia, I. G., " The Gauche Effect. A Theoretical Study of the Topomerization and Tautomerization of Methoxide Ion Tautomer," *Can. J. Chem.*, Vol. 51, pp. 2423-2432, 1973.

27. Zefirov, N. S., Samoshin, V. V., Subbotin, O. A., Baranenkov, V. I., Wolfe, S., "The Gauche Effect. On The Nature of the Interaction Between Electronegative Substituents in Trans-1,2-Disubstituted Cyclohexanes," *Tetrahedron*, Vol. 34, pp. 2953-2959, 1978.

28. Mursakulov, I. G., Guseinov, M. M., Kasumov, N. K., Zefirov, N. S., Samoshin, V. V., Chalenko, E. G., "Stereochemical Studies-XXVI. Conformational Equilibria of Ketals of 2-Substituted Cyclohexanones," *Tetrahedron*, Vol. 38, pp. 2213-220, 1982.

29. Zefirov, N. S., "The Problem of Conformational Effects," *Tetrahedron*, Vol. 33, pp. 3193-3202, 1977.

30. Wiberg, K. B., Murcko, M. A., Laidig, K. E., MacDougall, P. J., "Origin of the Gauche Effect in Substituted Ethanes and Ethenes," *J. Phys. Chem.*, Vol. 94, pp. 6956-6959, 1990.

31. Wolfe, S., Rauk, A., Tel, L. M., Csizmadia, I. G., "A Theoretical Study of the Edward-Lemieux Effect (Anomeric Effect). The Stereochemical Requirements of Adjacent Electron Pairs and Polar Bonds," *J. Chem. Soc. (B)*, pp.136-145, 1971.

32. Martell, J. M., Boyd, R. J., "An Ab initio Study of the Series $C_2H_nF_{6-n}$ (n=0-6). Geometries, Total Energies, and C-C Bond Dissociation Energies," *J. Phys. Chem.*, Vol. 96, pp. 6287-6290, 1992.

33. Dixon, D. A., Matsuzawa, N., Walker, S. C., "Conformational Analysis of 1,2-Dihaloethanes. A Comparison of Theoretical Methods," *J. Phys. Chem.*, Vol. 96, pp. 10740-10746, 1992.

34. Wiberg, K. B., Murcko, M. A., "Rotational Barriers. 1. 1,2-Dihaloethanes," *J. Phys. Chem.*, Vol. 91, pp. 3616-3620, 1987.

35. Little, T. S., Liu, J., Durig, J. R., "Conformational Analysis, Barriers to Internal Rotation, Vibrational Assignment, and ab Initio Calculations of 1,2-Difluoroethane," *J. Phys. Chem.*, Vol. 96, pp. 8224-8233, 1992.

36. Oie, T., Topol, I. A., Burt, S. K., "Ab Initio and Density Functional Calculations on Ethylene Glycol," *J. Phys. Chem.*, Vol. 98, pp. 1121-1128, 1994.

37. Murcko, M. A., DiPaola, R. A., "Ab Initio Molecular Orbital Conformational Analysis of Prototypical Organic Systems. 1. Ethylene Glycol and 1,2-Dimethoxyethane," *J. Am. Chem. Soc.*, Vol. 114, pp. 10010-10018, 1992.

38. Nagy, P. I., Dunn III, W. J., Alagona, G., Ghio, C., "Theoretical Calculations on 1,2-Ethanediol. Gauche-Trans Equilibrium in Gas Phase and Aqueous Solution," *J. Am. Chem. Soc.*, Vol. 113, pp. 6719-6729, 1991.

39. Ref. 3, pp. 305-311.

40. Ref. 3, pp. 286-298.

41. Carey, F. A. and Sundberg, R. J., *Advanced Organic Chemistry Part A: Structure and Mechanisms*, Plenum Press, New York, pp. 130-133, 1984.

42. Apaydın, G., Conformational Equilibria of 5-Substituted 1,3-Dioxanes," M.S. Thesis, Boğaziçi University, 1993.

43. Varnalı, T., Aviyente, V., Terryn, B., Ruiz-Lopez, M.F., "Conformational Equilibria of α-Substituted Carbonyl Compounds. Study of Solvent Effects," *J. Mol. Struc. (Theochem)*, Vol. 280, pp. 169-179, 1993.

44. Perron, F. and Albizati, K. F., "Chemistry of Spiroketals," *Chem. Rev.*, Vol. 89, pp. 1617-1661, 1989.

45. Mursakulov, I. G., Ramazanov, E. A., Guseinov, M. M., Zefirov, N. S., Samoshin, V. V., Eliel, E. L., "Stereochemical Studies-XXV. Conformational Equilibria of 2-Substituted 1,1-Dialkylcyclohexanes," *Tetrahedron*, Vol. 36, pp. 1885-1889, 1980.

46. Dodziuk, H., Sitkowski, J., Stefaniak, L., Mursakulov, I. G., Gasanov, I. G., Kurbanov, V. A., "Conformational Analysis of Spiranes. Part III. Manifestation of Chirality in the NMR Spectra of Spirobisdioxanes at Low Temperatures," *Structural Chemistry*, Vol. 3, No. 4, pp. 269-276, 1992.

47. Dodziuk, H., "Conformational Analysis of Spiranes on the Basis of Force Field Method. Part II. Heats of Formation of Small-ring Spiranes from Spiro[2.2]pentane to Spiro[5.5]undecane," *Bulletin of the Polish Academy of Sciences, Chemistry*, Vol. 34, No. 1-2, pp.49-51, 1986.

48. Dodziuk, H., "Conformational Analysis of Spiranes by the Force-field Method. Part I. Chirality and Diastereoisomerism of Spiro-compounds: Spiro[5.5] undecane and Derivatives," *J. Chem. Soc. Perkin Trans. II*, pp. 249-251, 1986.

49. Iratcabal, P. and Liotard, D., "Conformational Dynamics of 9,9-Dimethyl-1,5-Dihetero-Spiro[5.5]undecanes by Molecular Mechanics Calculations: A Three-Dimensional Topological Approach," *J. Comp. Chem.*, Vol. 7, No. 4, pp. 482-493, 1986.

50. Deslongchamps, P., Rowan, D. D., Pothier, N., Sauve, T., Saunders, J. K., "1,7-Dioxaspiro[5.5]undecanes. An Excellent System for the Study of Stereoelectronic Effects (Anomeric and exo-anomeric effects) in Acetals," *Can. J. Chem.*, Vol. 59, pp. 1105-1121, 1980.

51. Deslongchamps, P., Rowan, D. D., Pothier, N., Saunders, J. K., "1,7-Dithia and 1-oxa-7-thiaspiro[5.5]undecanes. Excellent Systems for the Study of Stereoelectronic Effects (Anomeric and exo-anomeric Effects) in the Monothio and the Dithioacetal Functions," *Can. J. Chem.*, Vol. 59, pp. 1122-1131, 1980.

52.. Pothier, N., Rowan, D. D., Deslongchamps, P., Saunders, J. K., "^{13}C Chemical Shift Data for 1,7-Dioxaspiro[5.5]undecanes and Related Compounds," *Can. J. Chem.*, Vol. 59, pp. 1132-1139, 1980.

53. Wolff, J. J., Frenking, G., Harms, K., "The Conformational Behaviour of 10-Substituted Spiro[4.5]decanes," *Chem. Ber.*, Vol. 124, pp. 551-161, 1991.

54. Varnalı, T., Özbal, H., Çetin, E., "Conformational Equilibria of Ketals of 2-Substituted Cyclohexanones," *Turkish Journal of Chemistry*, Vol. 16, pp. 177-180, 1992.

55. Varnalı, T., "Molecular Mechanics Application to 1,1,2-Trisubstituted Cyclohexanes," *J. Mol. Struc.*, Vol. 268, pp. 181-190, 1992.

56. Mursakulov, I. G., Samoshin, V. V., Binnatov, R. V., Kasumov, N. K., Povolotskii, M. I., Zefirov, N. S., "Stereochemical Investigations. XXXI. Effect of the Structure of the Ketal Group on the Conformational Equilibrium in the Ketals of 2-Substituted Cyclohexanones," *Zh. Org. Khim.*, Vol.19, No. 12, pp. 2527-2538, 1983.

57. Zefirov, N. S., Chalenko, E. G., Mursakulov, I. G., Guseinov, M. M., Kasumov, N. K., Ramazanov, E. L., "Conformational Effects in Geminal Systems of the Cyclohexane Series," *Zh. Org. Khim.*, Vol. 14, No.7, pp. 1560-1561, 1978.

58. Varnalı, T., "Conformational Analysis of 2-Substituted Cyclohexanone Ketal Derivatives by Molecular Mechanics and NMR," Ph.D. Dissertation, Boğaziçi University, 1986.

59. Wolfe, S., Pinto, B. M., Varma, V., Leung, R. Y. N., "The Perlin Effect| Bond Lengths, Bond Strength, and the Origins of Stereoelectronic Effects Upon one-bond C-H Coupling Constants," *Can. J. Chem.*, Vol. 68, pp. 1051-1062, 1990.

60. Woods, R. J., Szarek, W. A., Smith, Jr. V. H., "A Comparison of Semiempirical and Ab Initio Methods for the Study of Structural Features of Relevance in Carbohydrate Chemistry." *J. Chem. Soc.*, Chem. Comm., pp. 334-337, 1991.

61. Clark, T., *A Handbook of Computational Chemistry*, John Wiley and Sons, Canada, p. 2, 1985.

62. Levine, I. N., *Quantum Chemistry*, Prentice-Hall, New Jersey, p. 584, 1991.

63. Burkert, U., Allinger, N. L., *Molecular Mechanics, ACS Monograph 177*, Am. Chem. Soc., Washington, D.C., 1982.

64. McQuarrie, D. A., *Quantum Chemistry*, University Science Books, California, p. 47, 1983.

65. Ref. 64, pp. 49-63.

66. Ref. 62, p. 342-345.

67. Ref. 62, p. 190.

68. Ref. 64, pp. 266-269.

69. Ref. 62. p. 285.

70. Hehre, W. J., Radom, L., Schleyer, P. R., Pople, J. A., *Ab Initio Molecular Orbital Theory*, John Willey and Sons, New York, pp. 17-24, 1986.

71. Ref. 70, p. 65-67.

72. Ref. 70, p. 8.

73. Ref. 70, p. 72-89.

74. GAUSSIAN 92 Revision B and G.1; Frisch, M. J., Trucks, G. W., Head-Gordon, M., Gill, P. M. W., Wong, M. W., Foresman, J. W., Johnson, B. G., Schlegel, H. B., Robb, M. A., Replogle, E. S., Gomberts, R., Andres, J. L., Raghavachari, K., Binkley, J. S., Gonzales, C., Martin, R. L., Fox, D. J., Defrees, D. J., Baker, J., Stewart, J. J. P., Pople, J. A., Gaussian Inc. Pittsburgh, PA, 1992 and 1993.

75. Lowe, J. P., *Quantum Chemistry*, Academic Press, New York, pp. 316-318, 1978.

76. Ref. 62, pp. 545-575.

77. Ref. 62, pp. 579-582.

78. Thiel, W., "Semiempirical Methods: Current Status and Perspectives," *Tetrahedron*, Vol.44, No.24, pp. 7393-7408, 1988.

79. Dewar, M. J. S., Zoebisch, E. G., Healy, E. F., and Stewart J. J. P., "AM1: A New General Purpose Quantum Mechanical Molecular Model," *J. Am. Chem. Soc.*, Vol. 107, pp. 3902-3909, 1985.

80. Stewart, J. J. P., "Optimization of Parameters for Semiempirical Methods, "*J. Comp. Chem.*, Vol. 10, No. 2, pp. 209-220, 1989.

81. Jurema, M .W., and Shields, G. C., "Ability of the PM3 Quantum-Mechanical Method to Model Intermolecular Hydrogen Bonding between Neutral Molecules," *J. Comp. Chem.*, Vol. 14, No. 1, pp. 89-104, 1993.

82. Ref 61, pp. 102-111.

83. Beveridge, D. L., and Schnuelle G. W., "Free Energy of a Charge Distribution in Concentric Dielectric Continua," *J. Phys. Chem.*, Vol. 79, No. 23, pp. 2562-2565, 1975.

84. Tomasi, J., Bonaccorsi, R., Cammi, R., and Olivares del Valle, F. J., "Theoretical Chemistry in Solution. Some Results and Perspectives of the Continuum methods and in Particular of the Polarizable Continuum Model," *J. Mol. Struc. (Theochem)*, Vol. 234, pp. 401-424, 1991.

85. Harrison, S. W., Nolte, H. J., and Beveridge, D. L., "Free Energy of a Charge Distiribution in a Spheroidal Cavity in a Polarizable Dielectric Continuum," *J. Phys. Chem.*, Vol. 80, No. 23, pp. 2580-2585, 1976.

86. Cramer, C. J., Truhlar, D. G., "PM3-SM3: A General Parameterization fro Including Aqueous Solvation Effects in the PM3 Molecular Orbital Model," *J. Comp. Chem.*, Vol. 13, No. 9, pp. 1089-1097, 1992.

87. Cramer, C. J., and Truhlar, D. G., "An SCF Solvation Model for the Hydrophobic Effect and Absolute Free Energies of Aqueous Solvation," *Science*, Vol. 256, pp. 213-217, 1992.

88. Still, W .C., Tempczyk, A., Hawley, R. C., and Hendrickson, T., "Semianalytical Treatment of Solvation for Molecular Mechanics and Dynamics," *J. Am. Chem. Soc.*, Vol. 112, pp. 6127-6129, 1990.

89. Severance, D. L., Jorgensen, W .L., "Effects of Hydration on the Claisen Rearrangement of Allyl Vinyl Ether from Computer Simulations," *J. Am. Chem. Soc.*, Vol. 114, pp. 10966-10968, 1992.

90. Pranata, J., Jorgensen, W. L., "Computational Studies on FK506: Conformational Search and Molecular Dynamics Simulation in Water," *J. Am. Chem. Soc.*, Vol. 113, pp. 9483-9493, 1991.

91. Szafran, M., Karelson, M. M., Karitzky, A. R., Koput, J., and Zerner, M. C., "Reconsideration of Solvent Effects Calculated by Semiempirical Quantum Chemical Methods," *J. Comp. Chem.*, Vol. 14, No. 3, pp. 371-377, 1993.

92. Ford, G. P., Wang, B., "The Optimized Ellipsoidal Cavity and Its Application to the Self-Consistent Reaction Field Calculation of Hydration Energies of Cations and Neutral Molecules," *J. Comp. Chem.*, Vol. 13, No. 2, pp. 229-239, 1992.

93. Beveridge, D. L., Kelly, M. M., and Radna, R. J, "A Theoretical Study of Solvent Effect on the Conformational Stability of Acetylcholine," *J. Am. Chem. Soc.*, Vol. 96, No. 12, pp. 3769-3778, 1974.

94. Urban, J. J., Cramer, C. J., and Famini, G. R., "A Computational Study of Solvent Effects on the Conformation of Dopamine," *J. Am. Chem. Soc.*, Vol. 114, pp. 8226-8231, 1992.

95. Pappalardo, R. R., and Marcos, E. S., "Theoretical Study of Simple Push-Pull Ethylenes in Solution," *J. Phys. Org. Chem.*, Vol. 4, pp. 141-148, 1991.

96. Cativiela, C., Garcia, J. I., Mayoral, J. A., Royo, A. J., and Salvatella, L., "Experimental and Theoretical Study of the Influence of the Solvent on Asymmetric Diels-Alder Reactions," *J. Phys. Org. Chem.*, Vol. 5, pp. 230-238, 1992.

97. Rivail, J. L., Terryn, B., Rinaldi, D., and Ruiz-Lopez, M. F., "Liquid State Quantum Chemistry: A Cavity Model," *J. Mol. Struct. (Theochem)*, Vol., 120, pp. 387-400, 1985.

98. Onsager, L., "Electric Moments of Molecules in Liquids," *J. Am. Chem. Soc.*, Vol. 58, pp. 1486-1493, 1936.

99. Rivail, J. L., and Rinaldi, D., "A Quantum Chemical Approach to Dielectric Solvent Effects in Molecular Liquids," *Chem. Phys.*, Vol. 18, pp. 233-242, 1976.

100. Rivail, J. L., "Electrostatic Solvent Effect on some Molecular Spectroscopic Properties," *Proceedings of an International Conference and Workshop on Current Aspects of Quantum Chemistry*, Barselona-Spain, 28 September - 3 October 1981, Vol. 21, pp. 389-405, Amsterdam, Elsevier, 1982.

101. Rinaldi, D., Ruiz-Lopez, M. F., and Rivail, J. L., "Ab Initio SCF Calculations on Electrostatically Solvated Molecules Using a Deformable Three Axes Ellipsoidal Cavity," *J. Chem. Phys.*, Vol. 78, No. 2, pp. 834-838, 1983.

102. Stewart, J. J. P, MOPAC, QCPE Program 455, Bloomington, IN, 1990.

103. Rinaldi, D., Hoggan, P. E., Cartier, A., GEOMOS, QCPE Program 584, Bloomington. IN, 1989.

104. Eisenstein, O., Anh, N. T., Jean, Y., Devaquet, A., Cantacuzene, J., and Salem, L., "Lone Pairs in Organic Molecules: Energetic and Orientational Non-Equivalence. Stereochemical Consequences," *Tetrahedron*, Vol. 30, pp. 1717-1723, 1974.

105. Ref. 3, pp. 300-304.

106. Rios, M. A., and Rodriguez, J., "Semiemprical Study of Compounds with O-H--O Intramolecular Hydrogen Bond," *J. Comp. Chem.*, Vol. 13, No. 7, pp. 860-866, 1992.

107. Rodriguez, J., "Semiemprical Study of Compounds with Intramolecular O-H--O Hydrogen Bonds. II. Further Verification of a Modified MNDO Method," *J. Comp. Chem.*, Vol. 15, No. 2, pp. 183-189, 1994.

108. Wiberg, K. B., and Murcko, M. A., "Bond Bending and Hybridization," *J. Mol. Struct. (Theochem)*, Vol. 169, pp. 355-365, 1988.

109. Chen, Y., Paddison, S. J., Tschuikow-Roux, E., "An ab Initio Study of the Structures, Barriers for Internal Rotation, Vibrational Frequencies, and Thermodynamic Functions of 1,1,2-Trifluoroethane and 1,1,2,2-Tetrafluoroethane," *J. Phys. Chem.*, Vol. 98, pp. 1100-1108, 1994.